ESTTA Tracking number: **ESTTA493824**
Filing date: **09/11/2012**

IN THE UNITED STATES PATENT AND TRADEMARK OFFICE
BEFORE THE TRADEMARK TRIAL AND APPEAL BOARD

Notice of Opposition

Notice is hereby given that the following parties oppose registration of the indicated application.

Opposers Information

Name	Roche Diagnostics GmbH
Granted to Date of previous extension	09/12/2012
Address	Sandhofer Strasse 116 D-68305 Mannheim, GERMANY

Name	Roche Diagnostics Operations, Inc.
Granted to Date of previous extension	09/12/2012
Address	9115 Hague Road Indianapolis, IN 46250 UNITED STATES

Attorney information	Jonathan G. Polak Taft Stettinius & Hollister One Indiana Square Indianapolis, IN 46204 UNITED STATES EFStrademarks@taftlaw.com, zgordon@taftlaw.com, cwittenmeier@taftlaw.com Phone:3177133500

Applicant Information

Application No	85074797	Publication date	05/15/2012
Opposition Filing Date	09/11/2012	Opposition Period Ends	09/12/2012
Applicant	MiniPumps, LLC 3579 E Foothill Blvd. #521 Pasadena, CA 91107 UNITED STATES		

Goods/Services Affected by Opposition

Class 010. All goods and services in the class are opposed, namely: Medical apparatus, namely, pump, infusion and injection devices for administering drugs, and accessories used therewith, namely, drug refill consoles, drug refill kits for refilling infusion and injection devices, calibration kits for calibrating infusion and injection devices, programming units, programming consoles, lancet systems consisting primarily of needles and lancets, catheters, drug vials; intraocular and subcutaneous pumps for medical use

Grounds for Opposition

The mark is merely descriptive	Trademark Act section 2(e)(1)
Genericness	Trademark Act section 23

Attachments	LEGALDM-#266483-v1-Roche_v__Minipump_re_MICROPUMP_Notice_of_Opposition_9_11_2012_draft.pdf (5 pages)(16628 bytes) Micropump Exhibit A.pdf (7 pages)(232766 bytes) Micropump Exhibit B.pdf (31 pages)(2662994 bytes) Micropump Exhibit C.pdf (3 pages)(128772 bytes) Micropump Exhibit D.pdf (3 pages)(93659 bytes) Micropump Exhibit E.pdf (6 pages)(600272 bytes) Micropump Exhibit F.pdf (3 pages)(152624 bytes) Micropump Exhibit G.pdf (14 pages)(2280492 bytes) Micropump Exhibit H.pdf (3 pages)(104874 bytes) Micropump Exhibit I.pdf (11 pages)(1276635 bytes) Micropump Exhibit J & K.pdf (3 pages)(108244 bytes) Replenish Inc.pdf (1 page)(101767 bytes)

Certificate of Service

The undersigned hereby certifies that a copy of this paper has been served upon all parties, at their address record by First Class Mail on this date.

Signature	/Jonathan G. Polak/
Name	Jonathan G. Polak
Date	09/11/2012

IN THE UNITED STATES PATENT AND TRADEMARK OFFICE
BEFORE THE TRADEMARK TRIAL AND APPEAL BOARD

Roche Diagnostics GmbH and Roche Diagnostics Operations, Inc. Opposerss, MiniPumps, LLC (formerly Replenish Pumps, LLC, Applicant.	)))))))))))	Opposition No. ________ Mark:MICROPUMP Serial No.: 85-074,797 Published: 05/15/2012

<u>NOTICE OF OPPOSITION</u>

U.S. Patent and Trademark Office
P.O. Box 1451
Alexandria, VA 22313-1451

In the matter of MiniPumps, LLC's ("Applicant") application for trademark registration of the term MICROPUMP (Application Serial No. 85-074797, filed on June 30, 2010 by Replenish Pumps, LLC now known as MiniPumps, LLC and published for opposition in the Official Gazette of the United States Patent and Trademark Office on May 15, 2012 (the "'797 Application")).

Roche Diagnostics GmbH, Sandhofer Strasse 116, D-68305 Mannheim, Germany, a limited liability company, organized under the laws of Germany ("RDG") and Roche Diagnostics Operations, Inc., 9115 Hague Road, Indianapolis, IN 46250, United States, a corporation organized under the laws of Delaware ("RDO") (collectively "Opposers"), believe that they would be damaged by the registration of the term MICROPUMP shown in the "'797 Application" (Exhibit A) and hereby oppose the registration of such term as a trademark.

As grounds for opposition, it is alleged that:

1. The term MICROPUMP is generic, and/or merely descriptive, for small pumps, this includes when used in connection with Applicant’s goods listed in the ‘797 Application. (Exhibit A)

2. Applicant’s intended use of the term MICROPUMP as a trademark is consistent with the generally accepted generic, and/or merely descriptive, use of the MICROPUMP term for small pumps.

3. MICROPUMP is a generic, and/or merely descriptive, term for small pumps in the national marketplace. (Exhibit B-J).

4. Applicant uses the term MICROPUMP in connection with small pumps in the same generic, and/or merely descriptive, way that Opposers and others have used the term. (Exhibit K).

5. On June 30, 2010, Applicant filed the ‘797 Application based on its intent to use the term MICROPUMP under Section 1(b). Applicant’s published application indicates that Applicant intends to use the term MICROPUMP for “Medical apparatus, namely, pump, infusion and injection devices for administering drugs, and accessories used therewith, namely, drug refill consoles, drug refill kits for refilling infusion and injection devices, calibration kits for calibrating infusion and injection devices, programming units, programming consoles, lancet systems consisting primarily of needles and lancets, catheters, drug vials; intraocular and subcutaneous pumps for medical use.”

6. The marketplace in general, has made extensive generic, and/or merely descriptive, use of the term MICROPUMP for small pumps. (Exhibit B & E).

.

7. Opposers are leading worldwide providers of diabetes care products and services, including insulin pump products. Opposers are well-known for their offerings in the diabetes care field, including insulin pump products. Opposers' primary website may be located at http://www.roche.com/index.htm. Opposers are developing small insulin delivery systems for use in the diabetes care field which they generically and/or descriptively refer to as MICROPUMPS. An affiliate of Opposers has used the term MICROPUMP for small insulin delivery systems since at least as early as December 2007, which is well before the filing date of the '797 Application. Opposers and their affiliate describe their goods using this generic term MICROPUMP. MICROPUMP has the same generic meaning when used in the diabetes care field.

8. Therefore, Opposers would be damaged by Applicant's registration of the term MICROPUMP as a trademark. Accordingly, the grant of a registration to Applicant for the term MICROPUMP should be denied on the grounds of genericness, and/or mere descriptiveness.

9. Opposers believe that the term MICROPUMP is inherently descriptive and without secondary meaning. As such, the grant of a registration to Applicant for the term MICROPUMP should be denied and the '797 Application should not proceed to registration.

10. Registration of the term MICROPUMP damages Opposers because Opposers and their affiliate are using the term MICROPUMP to describe their small insulin delivery systems. Registration of the term MICROPUMP would interfere with Opposers' and their affiliate's continuing use of the term to accurately describe the generic aspects of their goods

WHEREFORE, Opposers file this Notice of Opposition and pray that the '797

Application of Applicant, be rejected; that no registration be issued thereon to Applicant; and that this opposition be sustained in favor of Opposers.

Respectfully submitted,

DATE: September 11, 2012

/s/ *Jonathan G. Polak*

Jonathan G. Polak
James A. Coles
M. Zach Gordon
TAFT STETTINIUS & HOLLISTER LLP
One Indiana Square, Suite 3500
Indianapolis, Indiana 46204-2023
Email: zgordon@taftlaw.com

Attorney for Opposers,
Roche Diagnostics GmbH and
Roche Diagnostics Operations, Inc.

CERTIFICATE OF SERVICE

I hereby certify that on September 11, 2012 a true and correct copy of the foregoing was sent to the following parties by First Class U.S. Mail in a sealed, postage prepaid, envelope which was deposited with the United States Postal Service.

David O. Johanson
BINGHAM MCCUTCHEN LLP
ONE FEDERAL STREET
BOSTON, MA 02110
Phone Number: 617-951-8000
Fax Number: 617-951-8736

/s/_*M. Zach Gordon*_______
M. Zach Gordon
TAFT STETTINIUS & HOLLISTER LLP
One Indiana Square, Suite 3500
Indianapolis, Indiana 46204-2023
Telephone: 317-713-3500
Facsimile: 317-713-3699

EXHIBIT A

PTO Form 1478 (Rev 9/2006)
OMB No. 0651-0009 (Exp 12/31/2011)

Trademark/Service Mark Application, Principal Register

Serial Number: 85074797
Filing Date: 06/30/2010

The table below presents the data as entered.

Input Field	Entered
SERIAL NUMBER	85074797
MARK INFORMATION	
***MARK**	Micropump
STANDARD CHARACTERS	YES
USPTO-GENERATED IMAGE	YES
LITERAL ELEMENT	Micropump
MARK STATEMENT	The mark consists of standard characters, without claim to any particular font, style, size, or color.
REGISTER	Principal
APPLICANT INFORMATION	
***OWNER OF MARK**	Replenish Pumps, LLC
***STREET**	319 30th St
***CITY**	Manhattan Beach
***STATE (Required for U.S. applicants)**	California
***COUNTRY**	United States
***ZIP/POSTAL CODE (Required for U.S. applicants only)**	90266
PHONE	3105317091
FAX	3105317091
EMAIL ADDRESS	sean@minipumpsllc.com
AUTHORIZED TO COMMUNICATE VIA EMAIL	Yes
LEGAL ENTITY INFORMATION	
TYPE	limited liability company

STATE/COUNTRY WHERE LEGALLY ORGANIZED	California
GOODS AND/OR SERVICES AND BASIS INFORMATION	
INTERNATIONAL CLASS	010
***IDENTIFICATION**	Medical apparatus, namely, pump, infusion and injection devices for administering drugs, and accessories used therewith; intraocular and subcutaneous pumps for medical use
FILING BASIS	SECTION 1(b)
CORRESPONDENCE INFORMATION	
NAME	Replenish Pumps, LLC
FIRM NAME	Replenish Pumps, LLC
STREET	319 30th St
CITY	Manhattan Beach
STATE	California
COUNTRY	United States
ZIP/POSTAL CODE	90266
PHONE	310.531.7091
FAX	310.531.7091
EMAIL ADDRESS	sean@minipumpsllc.com
AUTHORIZED TO COMMUNICATE VIA EMAIL	Yes
FEE INFORMATION	
NUMBER OF CLASSES	1
FEE PER CLASS	325
***TOTAL FEE DUE**	325
***TOTAL FEE PAID**	325
SIGNATURE INFORMATION	
SIGNATURE	/Sean Caffey/
SIGNATORY'S NAME	Sean Caffey
SIGNATORY'S POSITION	CEO
DATE SIGNED	06/30/2010

Trademark/Service Mark Application, Principal Register

Serial Number: 85074797
Filing Date: 06/30/2010

To the Commissioner for Trademarks:

MARK: Micropump (Standard Characters, see mark)
The literal element of the mark consists of Micropump.
The mark consists of standard characters, without claim to any particular font, style, size, or color.

The applicant, Replenish Pumps, LLC, a limited liability company legally organized under the laws of California, having an address of
319 30th St
Manhattan Beach, California 90266
United States
requests registration of the trademark/service mark identified above in the United States Patent and Trademark Office on the Principal Register established by the Act of July 5, 1946 (15 U.S.C. Section 1051 et seq.), as amended, for the following:

International Class 010: Medical apparatus, namely, pump, infusion and injection devices for administering drugs, and accessories used therewith; intraocular and subcutaneous pumps for medical use
Intent to Use: The applicant has a bona fide intention to use or use through the applicant's related company or licensee the mark in commerce on or in connection with the identified goods and/or services. (15 U.S.C. Section 1051(b)).

The applicant's current Correspondence Information:
Replenish Pumps, LLC
Replenish Pumps, LLC
319 30th St
Manhattan Beach, California 90266
310.531.7091(phone)
310.531.7091(fax)
sean@minipumpsllc.com (authorized)

A fee payment in the amount of $325 has been submitted with the application, representing payment for 1 class(es).

Declaration

The undersigned, being hereby warned that willful false statements and the like so made are punishable by fine or imprisonment, or both, under 18 U.S.C. Section 1001, and that such willful false statements, and the like, may jeopardize the validity of the application or any resulting registration, declares that he/she is properly authorized to execute this application on behalf of the applicant; he/she believes the applicant to be the owner of the trademark/service mark sought to be registered, or, if the application is being filed under 15 U.S.C. Section 1051(b), he/she believes applicant to be entitled to use such mark in commerce; to the best of his/her knowledge and belief no other person, firm, corporation, or association has the right to use the mark in commerce, either in the identical form thereof or in such near resemblance thereto as to be likely, when used on or in connection with the goods/services of such other person, to cause confusion, or to cause mistake, or to deceive; and that all statements made of his/her own knowledge are true; and that all statements made on information and belief are believed to be true.

Signature: /Sean Caffey/ Date Signed: 06/30/2010
Signatory's Name: Sean Caffey
Signatory's Position: CEO

RAM Sale Number: 87
RAM Accounting Date: 07/01/2010

Serial Number: 85074797
Internet Transmission Date: Wed Jun 30 13:52:01 EDT 2010
TEAS Stamp: USPTO/BAS-99.96.67.197-20100630135201343
281-85074797-460bfe55c3f294fb12ce233cf28
034305d-CC-87-20100630130804677013

Micropump

Micropump

EXHIBIT B

INSTITUTE OF PHYSICS PUBLISHING JOURNAL OF MICROMECHANICS AND MICROENGINEERING

J. Micromech. Microeng. **14** (2004) R35–R64 PII: S0960-1317(04)06813-5

TOPICAL REVIEW

A review of micropumps

D J Laser and J G Santiago

Department of Mechanical Engineering, Stanford University, Stanford, CA 94305, USA

E-mail: juan.santiago@stanford.edu

Received 30 September 2003
Published 19 April 2004
Online at stacks.iop.org/JMM/14/R35 (DOI: 10.1088/0960-1317/14/6/R01)

Abstract
We survey progress over the past 25 years in the development of microscale devices for pumping fluids. We attempt to provide both a reference for micropump researchers and a resource for those outside the field who wish to identify the best micropump for a particular application. Reciprocating displacement micropumps have been the subject of extensive research in both academia and the private sector and have been produced with a wide range of actuators, valve configurations and materials. Aperiodic displacement micropumps based on mechanisms such as localized phase change have been shown to be suitable for specialized applications. Electroosmotic micropumps exhibit favorable scaling and are promising for a variety of applications requiring high flow rates and pressures. Dynamic micropumps based on electrohydrodynamic and magnetohydrodynamic effects have also been developed. Much progress has been made, but with micropumps suitable for important applications still not available, this remains a fertile area for future research.

Nomenclature

A_d	diaphragm area
a	pore/capillary/channel radius
B	magnetic flux density
C	capacitance
D_d	hydraulic diameter
d_d	diaphragm diameter
E	electric field
E_y	material Young's modulus
e	electron charge
ε	permittivity
ε_C	compression ratio
ζ	zeta potential
η	thermodynamic efficiency
η_{est}	estimated thermodynamic efficiency
F	electrostatic force
f_{sp}	self-pumping frequency
f_r	diaphragm resonant frequency
f	operating frequency
J	current density
k	Boltzmann constant
κ	compressibility
l	pore/capillary/channel length
λ_D	Debye shielding length
μ	viscosity
N	number of pores/capillaries/channels
n_i	number density of species i
ν	material Poisson ratio
P	power
p_a	applied driver pressure
Δp	pressure differential
Δp_{max}	maximum pressure differential
Q	volumetric flow rate
Q_{max}	maximum volumetric flow rate
q	charge density
ρ	density
Re	Reynolds number
S_p	package size
s	electrode separation distance
Sr	Strouhal number
σ	stress
σ_y	material yield stress
T	temperature
t_d	diaphragm thickness
U	flow velocity
V	electrical potential difference
V_0	dead volume

ΔV stroke volume
y_0 diaphragm centerline displacement
z_i valence number of species i

1. Introduction

From biology and medicine to space exploration and microelectronics cooling, fluid volumes, on the order of a milliliter—the volume contained in a cube 1 cm on a side—and below figure prominently in an increasing number of engineering systems. The small fluid volumes in these systems are often pumped, controlled or otherwise manipulated during operation. For example, biological samples must be moved through the components of miniature assay systems [1–4], and coolant must be forced through micro heat exchangers [5–7]. Microfluidic transport requirements such as these can sometimes be met by taking advantage of passive mechanisms, most notably surface tension [8–11]. For other applications, macroscale pumps, pressure/vacuum chambers and valves provide adequate microfluidic transport capabilities [12–15]. Yet for many microfluidic systems, a self-contained, active pump, the package size of which is comparable to the volume of fluid to be pumped, is necessary or highly desirable. In this introduction, we consider a few applications briefly to gain insight into design parameters relevant to micropumps.

Dispensing therapeutic agents into the body has long been a goal of micropump designers. Among the first micropumps, those developed by Jan Smits in the early 1980s were intended for use in controlled insulin delivery systems for maintaining diabetics' blood sugar levels without frequent needle injections [16]. Micropumps might also be used to dispense engineered macromolecules into tumors or the bloodstream [17, 18]. High volumetric flow rates are not likely to be required of implanted micropumps (the amount of insulin required by a diabetic per day, for example, is less than a milliliter) but precise metering is of great importance [17, 19–21]. The pressure generation requirements for implantable micropumps are not insignificant, as the back pressure encountered *in vivo* can be as high as 25 kPa. Reliability, power consumption, cost and biocompatibility are critical [17, 20, 22]. To date, deficiencies in these areas have precluded widespread implantantion of micropumps. For example, currently available implanted insulin delivery systems employ static pressure reservoirs metered by solenoid-driven valves and are over 50 cm^3 in size [15, 22, 23].

A number of researchers have sought to develop micropumps for use in single- or two-phase cooling of microelectronic devices [5–7]. Microelectronics cooling is highly demanding with respect to flow rate. For instance, Tuckerman and Pease's seminal paper on liquid-phase chip cooling contemplated flow rates of several hundred milliliters per minute [7]. Recent studies indicate that two-phase convective cooling of a 100 W microchip will require flow rates of order 10 ml min^{-1} or more [5, 24, 25]. The fundamental scaling associated with pressure-driven flow dictates that high pressures (100 kPa or greater) will be required to force such high flow rates through microchannels and/or jet structures found in micro heat sinks. In the laminar regime, an order-of-magnitude decrease in the hydraulic diameter of a channel (the channel cross-sectional area multiplied by four and divided by its perimeter) increases by two orders of magnitude the pressure difference required to maintain a constant average flow velocity. Cost and power consumption are also important considerations, the latter especially for mobile units. Micropumps might also be built directly into integrated circuits to cool transient hot spots, and so fabrication methods and temporal response characteristics may be particularly important [26]. Insensitivity to gas bubbles is also important as bubbles are present in and detrimental to many microfluidic systems.

Much attention has been focused recently on miniature systems for chemical and biological analysis [1–4, 27–30]. Miniaturization of chemical assays systems can reduce the quantities of sample and reagents required and often allows assays to be performed more quickly and with less manual intervention. Miniaturization also enables portability as in the case of a portable chemical analysis system under development at Sandia National Labs [31]. Miniaturization sometimes offers the further advantage of enabling use of inexpensive disposable substrates. Although fluids (typically liquids) must typically be introduced into, and transported within, these micro total analysis systems (μTAS) during operation, micropumps are found in very few current-generation systems. Liquid transport is instead often accomplished through manual pipetting, with external pneumatic sources, or by inducing electroosmotic flow. The limited use of micropumps in μTAS may be partly due to the lack of available micropumps with the necessary combination of cost and performance.

Compatibility with the range of fluid volumes of interest will be necessary if micropumps are to become more widely used in μTAS. Monitoring single cells may require manipulation of fluid volumes on the order of 1 pl—the volume contained in a cube 10 μm on a side [32–34]. Microchip-based systems used in drug discovery amplify DNA, separate species through capillary electrophoresis, and/or interface with mass spectrometers with sample volumes ranging from hundreds of picoliters to hundreds of microliters [1–3, 35–37]. Patient pain considerations have prompted manufacturers of *in vitro* blood glucose monitors for diabetics to minimize sample size requirements; current systems need a sample volume of only one-third of a microliter [38]. Detecting microbes in human body liquids often requires somewhat larger sample volumes; for example, a common immunoassay-based blood test for malaria uses a sample volume of 10 μl [39, 40]. Other parameters important for μTAS include working fluid properties such as pH, viscosity, viscoelesticity and temperature, as well as the presence of particles (e.g., cells or dust) which may disrupt operation of pumps and valves. Secondary effects associated with reliability and corrosion include the impact of mechanically shearing the sample, chemical reactions, adsorption of analytes and wear of moving parts.

Space exploration is another exciting area for micropump technologies. Miniature roughing pumps are needed for use in mass spectrometer systems to be transported on lightweight spacecraft [41]. Such a pump would likely be required to achieve a vacuum of approximately 0.1 Pa, the level at which high vacuum pumps typically become effective [42]. Miniature roughing pumps have been sought

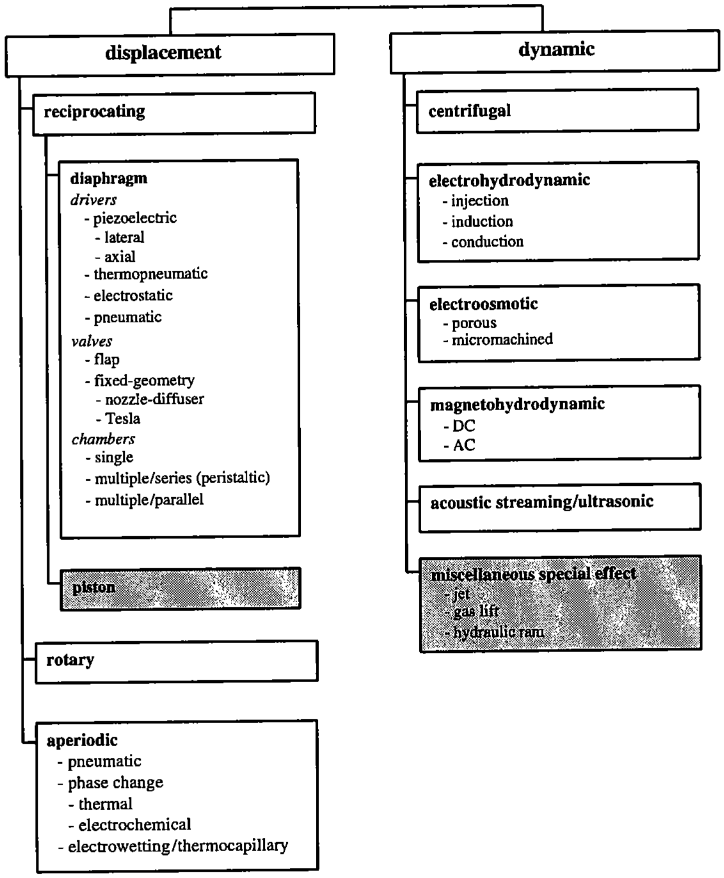

Figure 1. Classification of pumps and micropumps; after Krutzch and Cooper [46]. Unshaded boxes are pump categories reviewed here of which operational micropumps have been reported.

for other applications as well [43]. Micropropulsion is another potential application of micropumps in space. For example, ion-based propulsion systems proposed for future 1–5 kg 'microspacecraft' may require delivery of compressed gases at 1 ml min^{-1} flow rates [44, 45]. Larger stroke volumes are generally required for pumping gases than for pumping liquids, making these space exploration applications particularly challenging.

Inspired by this wide range of applications, over 200 archival journal papers reporting new micropumps or analyzing micropump operation have been published since Smits' micropump was first developed in the 1980s. A robust, coherent system of categorization is helpful for making sense of the diverse set of devices that have been reported. In this review, we categorize micropumps according to the manner and means by which they produce fluid flow and pressure. Our system of micropump classification, illustrated in figure 1, is applicable to pumps generally and is essentially an extension of the system set forth by Krutzch and Cooper for traditional pumps [46]. Pumps generally fall into one of two major categories: (1) *displacement pumps*, which exert pressure forces on the working fluid through one or more moving boundaries and (2) *dynamic pumps*, which continuously add energy to the working fluid in a manner that increases either its momentum (as in the case of centrifugal pumps) or its pressure directly (as in the case of electroosmotic and electrohydrodynamic pumps). Momentum added to the fluid in a displacement pump is subsequently converted into pressure by the action of an external fluidic resistance. Many displacement pumps operate in a periodic manner, incorporating some means of rectifying periodic fluid motion to produce net flow. Such periodic displacement pumps can be further broken down into pumps that are based on reciprocating motion, as of a piston or a diaphragm, and pumps that are based on rotary elements such as gears or vanes. The majority of reported micropumps are reciprocating displacement pumps in which the moving surface is a diaphragm. These are sometimes called membrane pumps or diaphragm pumps. Another subcategory of displacement pumps are aperiodic displacement pumps, the operation of which does not inherently depend on periodic movement of the pressure-exerting boundary. Aperiodic displacement pumps typically pump only a limited volume of working fluid; a syringe pump is a common macroscale example. Dynamic pumps include centrifugal pumps, which are typically ineffective at low Reynolds numbers and have only been miniaturized to a limited extent, as well as pumps in which an electromagnetic field interacts directly with the working fluid to produce pressure and flow (electrohydrodynamic pumps, electroosmotic pumps and magnetohydrodynamic pumps) and acoustic-wave micropumps[1].

In figure 1, open boxes represent pump categories of which operational micropumps have been reported. In our use of the term micropump, we adhere to the convention for microelectromechanical systems, with the prefix *micro* considered to be appropriate for devices with prominent features having length scales of order 100 μm or smaller. Many pumps that meet this criterion are micromachined, meaning that they are fabricated using tools and techniques originally developed for the integrated circuit industry or resembling such tools and techniques (e.g., tools involving photolithography and etching). Techniques such as plastic injection molding and precision machining have also been used to produce micropumps. In keeping with the nomenclature associated with nanotechnology, we consider the term nanopump to be appropriate only for devices with prominent features having length scales of order 100 nm or smaller (so pumps that pump nanoliter volumes of liquid are not necessarily nanopumps). We suggest, that, in general, that the term nanopump should be used judiciously, with terms that more accurately describe the operation of a nanoscale device used when appropriate. Of course, subcontinuum effects may be important in nanopumps and some micropumps, particularly in the case of devices that pump gases [47]. As an aside, we note that electric-motor-driven miniature reciprocating displacement pumps that are compact relative to most macroscopic pumps (but larger than the micropumps discussed here) are commercially available. The performance of several such pumps is reviewed by Wong *et al* [31].

In this review, we consider the various categories of micropumps individually. We review important features, analyze operation, describe prominent examples and discuss applications. We then compare micropumps of all categories, recognizing that the enormous variation among micropumps makes such comparisons difficult. Throughout this review, we pay particular attention to the maximum measured volumetric flow rate reported for micropumps, $Q_{\rm max}$, and the maximum measured micropump differential pressure, $\Delta p_{\rm max}$. Since many of the micropumps discussed here are explicitly targeted for applications where compactness is important, we also consider micropump overall package size, $S_{\rm p}$. When $S_{\rm p}$ is not explicitly reported, we attempt to estimate size from images, by making inferences from known dimensions, etc. An interesting metric is the ratio of maximum flow rate $Q_{\rm max}$ to package size $S_{\rm p}$, which we refer to as the self-pumping frequency, $f_{\rm sp}$. We also discuss certain micropump operating parameters, particularly operating voltage, V, and operating frequency, f. These parameters partially determine the electronics and other components needed to operate the micropump—important considerations for size- and/or cost-sensitive applications. Power consumption P and thermodynamic efficiency η are also important operational parameters, but unfortunately these measures are rarely reported. We urge the community to collect and report power consumption and thermodynamic efficiency data on all micropumps of interest. The most useful definition of thermodynamic efficiency for a pump producing a flow rate Q against a back pressure Δp is $\eta = Q^* \Delta p/P$ [48]. We further suggest that the community report values of P reflecting the total power consumed by the pump (including power consumed by motors and other actuators, voltage conversion, power transmission, etc). In any case, the adopted definitions of η and P should be described in detail for each reported micropump. In this paper, we recount efficiency for micropumps for which measured values are specifically reported. For micropump papers which do not report η but do report $Q_{\rm max}$, $\Delta p_{\rm max}$ and P, we use these values to calculate estimated thermodynamic efficiency, $\eta_{\rm est}$, by assuming that pump flow rate is an approximately linear function of load pressure. Estimated thermodynamic efficiency $\eta_{\rm est}$ is then $0.25 Q_{\rm max} \Delta p_{\rm max}/P$.

As a supplement to this review, the reader may wish to refer to other reviews of micropump technologies [49–51], surveys of micro total analysis systems [27, 28, 52, 53], more general surveys of microfluidics [54–58] and surveys of microelectromechanical systems [59–63].

[1] Krutzch and Cooper refer to noncentrifugal dynamic pumps as 'special effect' pumps, a classification that is abandoned here in favor of identifying the specific physical mechanism that imparts momentum to the working fluid.

2. Displacement micropumps

2.1. Reciprocating displacement micropumps

The vast majority of reported micropumps are reciprocating displacement micropumps—micropumps in which moving boundaries or surfaces do pressure work on the working fluid in a periodic manner. Pistons are the moving boundaries in many macroscale reciprocating displacement pumps, but traditional, sealed piston structures have not been used in micropumps. In most reciprocating displacement micropumps, the force-applying moving surface is instead a deformable plate—the pump diaphragm—with fixed edges. Common pump diaphragm materials include silicon, glass, and plastic. Figure 2 depicts the structure and operation of a generic diaphragm-based reciprocating displacement micropump. The basic components are a pump chamber (bounded on one side by the pump diaphragm), an actuator mechanism or driver and two passive check valves—one at the inlet (or suction side) and one at the outlet (or discharge side). The generic reciprocating displacement micropump shown in figure 2 is constructed from four layers of material. Micropumps made from as few as two and as many as seven layers of material have been reported.

During operation, the driver acts on the pump diaphragm to alternately increase and decrease the pump chamber volume. Fluid is drawn into the pump chamber during the chamber expansion/suction stroke and forced out of the pump chamber during the contraction/discharge stroke. The check valves at the inlet and outlet are oriented to favor flow into and out of the pump chamber, respectively, rectifying the flow over a two-stroke pump cycle. The basic design illustrated in figure 2 is perhaps most directly attributable to Harald van Lintel and coworkers, who reported a two-valve, single-chamber reciprocating displacement micropump in the journal *Sensors and Actuators* in 1988 [64]. Van Lintel *et al*'s micropump comprises an entire 2 inch silicon wafer bonded between two like-sized glass plates and is therefore relatively large ($S_{\rm p} \cong 4$ cm^3). The pump chamber is a 12.5 mm

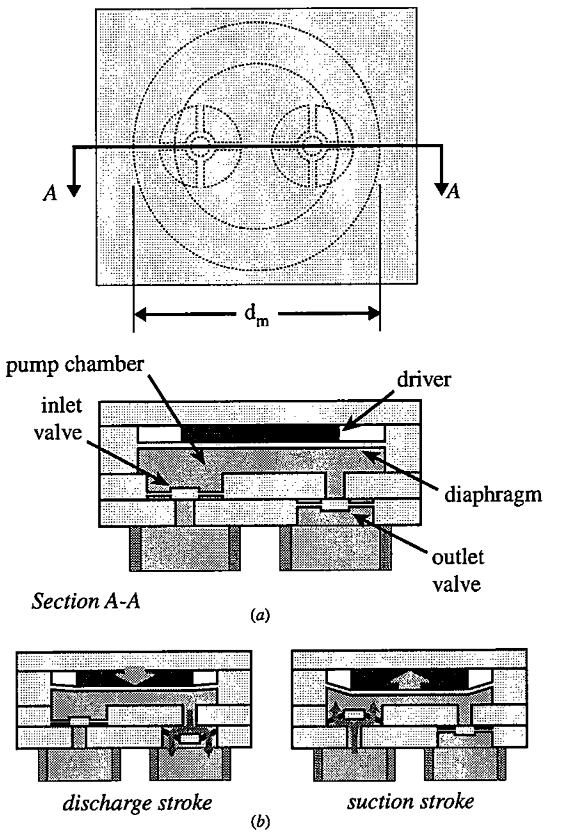

Figure 2. Structure and operation of a typical reciprocating displacement micropump. (*a*) Top view and section. (*b*) Discharge and suction strokes. During the discharge stroke, the driver acts to reduce the pump chamber volume, expelling working fluid through the outlet valve. During the suction stroke, the pump chamber is expanded, drawing working fluid in through the inlet valve.

diameter, 130 μm deep cavity etched in the silicon wafer using an ethylene diamine/pyrocatechol/pyrazine solution (EDP) with a silicon oxide mask. Diaphragm-like check valves and connecting channels are also etched in the silicon substrate. A 0.19 mm thick glass plate seals the pump chamber side of the device; a thicker piece of glass seals the other side. The portion of the thin glass plate above the pump chamber is the pump diaphragm; a piezoelectric disk actuator is affixed to this glass diaphragm. Van Lintel *et al*'s micropump is driven by lateral strain in the piezoelectric disk. This design was patented in 1992 [65, 66]. Reported performance is $Q_{max} = 8\ \mu$l min^{-1} and $\Delta p_{max} = 10$ kPa at $f = 1$ Hz and $V = 125$ V.

Reciprocating displacement micropumps with a wide range of designs have been reported. Key features and measured performances characteristics of reported reciprocating displacement micropumps are summarized (and referenced) in table 1. While most micropump designs have a single pump chamber, a few micropumps have multiple pump chambers arranged either in series or in parallel as listed in the table. Driver types and configurations vary widely; reciprocating displacement micropumps with piezoelectric, electrostatic, thermopneumatic and pneumatic drivers among others, have been reported. Various valve designs based on flaps or other moving structures have been developed, as have fixed-geometry structures that rectify flow using fluid inertial effects. Variations among reciprocating displacement micropumps are discussed further below.

2.1.1. Modeling reciprocating displacement micropump operation. The operation of reciprocating displacement micropumps often involves the interaction of several types of mechanics including electromechanical forces, solid mechanics and fluid mechanics. Because of this complexity, accurate, tractable, broadly applicable analytical models of reciprocating displacement micropump operation are not readily available. Low-order lumped-parameter models provide significant insight on key aspects of micropump operation [67–69]. Finite element analysis is also a useful tool in studying reciprocating displacement micropumps. Commercial packages such as ANSYS and ALGOR have been used to analyze the response of micropump diaphragms subjected actuator forces [69–71]. A variety of numerical and semianalytical approaches have been taken in the study of fluid flows in reciprocating displacement micropumps [72–74]; commercial packages suitable for such analysis include CFDRC, Coventor, FEMLAB and ANSYS FLOTRAN [75, 115].

In an effort to elucidate certain aspects of reciprocating displacement micropump operation, we present a simple analysis assuming quasi-static flow and ideal valve operation. The Reynolds number, $Re = \rho U D_h/\mu$, and the Strouhal number, $Sr = f D_h/U$, of the fluid flow within the micropump impact the validity of this model. The analysis below is especially useful for reciprocating displacement micropumps operating in flow regimes characterized by both very low Reynolds number and low Reynolds number and Strouhal number product [47, 76, 77].

The pressure and flow rate generated by reciprocating displacement pumps depend on the (1) stroke volume ΔV, or the difference between the maximum and minimum volumes of the pumping chamber over the course of the pump cycle; (2) pump dead volume V_0, or the minimum fluid volume contained between the inlet and outlet check valves at any point during the pump cycle; (3) pump operating frequency, f; (4) properties of the valves; and (5) properties of the working fluid. For ideal valves ($\Delta p_{forward} = 0$ and $\Delta p_{reverse} \to \infty$) and an incompressible working fluid, conservation of mass dictates that the flow rate is simply the product of the stroke volume ΔV and the operating frequency f. ΔV depends strongly on the characteristics of the micropump driver. For example, some piezoelectrical drivers essentially function as displacement sources, while other drivers are well modeled as pressure sources. For displacement source-like drivers, diaphragm displacement (and therefore ΔV) is limited by the mechanical failure criteria of the diaphragm. For pressure source-like drivers, the diaphragm stiffness and dynamic response limit ΔV and f. In either case, analysis of the mechanical properties of a generic pump diaphragm is informative. For a micropump diaphragm with diameter d_d and uniform thickness t_d clamped at its perimeter and subjected to a uniform applied driver force per unit cross-sectional area p_a, the diaphragm centerline displacement y_0 is [78]

$$\frac{p_a d_d^4}{16 E_y t_d^4} = \frac{5.33}{(1-\nu^2)}\frac{y_0}{t_d} + \frac{2.6}{(1-\nu^2)}\left(\frac{y_0}{t_d}\right)^3, \qquad (1)$$

Table 1. Reciprocating displacement micropumps.

Author and year	Driver	Valves	Construction	Pump chambers	Diaphragm material	S_p (approx.) (mm^3)	Diaphragm thickness (mm)	Working fluid	V (V)	f (Hz)	Δp_{max} (kPa)	Q_{max} (ml min^{-1})
van Lintel 1988 [64]	Piezoelectric (lateral)	Flap (diaphragm-ring mesa)	glass–Si–glass	1	Glass	4100	0.3 0.19	Water Water	125 100	0.1 1	24 9.8	0.0006 0.008
Smits 1990 [16]	Piezoelectric (lateral)	None	glass–Si–glass	3 (S)	Glass	1500	n/r	Water	100	15	5.9	0.1
Stemme 1993 [91]	Piezoelectric (lateral)	Fixed-geometry (nozzle-diffuser)	Brass	1	Brass	2500	0.2	Water Water Air	20 20 20	110 310 6000	21 4.9 0.78	4.4 16 35
Gass 1994 [111]	Piezoelectric (lateral)	Flap (diaphragm-ring mesa)	glass–Si–glass	1	Glass	11 800	0.3	Water	250	40	9.0	0.55
Forster 1995 [180]	Piezoelectric (lateral)	Fixed-geometry	Si–glass	1	Glass	n/r	0.15	Water	150	114	n/r	0.038
Carrozza 1995 [95]	Piezoelectric (lateral)	Ball	Polymer–brass	1	Brass	1270	0.1	Water	300	70	25	2.7
Gerlach 1995 [179]	Piezoelectric (lateral)	Fixed-geometry (nozzle-diffuser)	Si–Si–glass	1	Glass	200	0.12	Water Methanol	50 50	3000 5000	3.2 7	0.39 0.32
Olsson 1995 [88]	Piezoelectric (lateral)	Fixed-geometry (nozzle-diffuser)	Brass	2 (P)	Brass	1600	0.35	Water	130	540	16	16
Olsson 1996 [89]	Piezoelectric (lateral)	Fixed-geometry (nozzle-diffuser)	Si–glass	2 (P)	Glass, silicon	270	0.3 (Si), 0.5 (glass)	Methanol	n/r	1318	17	0.23
Bardell 1997 [286]	Piezoelectric (lateral)	Fixed-geometry (tesla)	Si–glass	1	Glass	n/r 220	0.15 0.5	Water Water	300 290	100 3000	2.3 47	0.085 0.75
Olsson 1997 [110]	Piezoelectric (lateral)	Fixed-geometry (nozzle-diffuser)	Si–glass	2 (P)	Glass	260	0.5	Water	200	3500	74	1.1
Kamper 1998 [92]	Piezoelectric (lateral)	Flap (diaphragm-ring mesa)	Molded polycarbonate (two layers)	1	Brass/ polycarbonate	500	0.15	Water Air	n/r n/r	70 n/r	200 50	0.4 3.5
Koch 1998 [114]	Piezoelectric (lateral)	Flap (cantilever)	Si–Si–Si	1	Silicon	n/r	0.07	Ethanol	600	200	1.8	0.12
Linnemann 1998 [81]	Piezoelectric (lateral)	Flap (cantilever)	Si–Si–Si	1	Silicon	111	0.04	Water	160	220	n/r	1.2
Richter 1998 [80]	Piezoelectric (lateral)	Flap (cantilever)	Si–Si	1	Silicon	n/r	0.04	Water Air	160 n/r	220 300	n/r n/r	0.7 1.4
Bohm 1999 [94]	Piezoelectric (lateral)	Flap (diaphragm-ring mesa)	Molded plastic	1	Brass	290	0.075	Water	350	50	12	1.9
Andersson 2001 [182]	Piezoelectric (lateral)	Fixed-geometry (nozzle-diffuser)	Si–glass	1	Silicon	n/r	n/r	Water	97	700	n/r	0.0023
Schabmueller 2002 [116]	Piezoelectric (lateral)	Fixed-geometry (nozzle-diffuser)	Si–Si	1	Silicon	120	0.07	Ethanol Air	190 190	2400 3400	1.0 n/r	1.5 0.69
ThinXXS2000 2003 [93]	Piezoelectric (lateral)	Flap (diaphragm-ring mesa)	Micro-injection molded/laser welded plastic	1	Plastic	4600	n/r	Water	450	20	35	2.5
MIP Implantable 2003 [98]	Piezoelectric (lateral)	Flap (diaphragm-ring mesa)	Glass–Si–glass–Si	1	Silicon	357	n/r	Water	150	0.2	55	0.0017

n/a: not applicable; n/r: not reported; S: series configuration; P: parallel configuration.

Author and year	Driver	Valves	Construction	Pump chambers	Diaphragm material	S_p (approx.) (mm^3)	Diaphragm thickness (mm)	Working fluid	V (V)	f (Hz)	Δp_{max} (kPa)	Q_{max} (ml min^{-1})
Stehr 1996 [101]	Piezoelectric (lateral/ cantilever)	None	Perspex-Si	1	Silicon	n/r	0.018 (bossed)	Water	200	190	17	1.5
Esashi 1989 [100]	Piezoelectric (axial)	Flap (tethered plate)	Si–Si w/spun-on glass layer	1	Silicon	800	0.05	Water	90	30	6.4	0.015
Shoji 1990 [85]	Piezoelectric (axial)	Flap (tethered plate)	Glass–Si–glass	1	Silicon	4000	0.05	Water	100	50	n/r	0.022
				2 (P)	Silicon	4000	0.05	Water	100	50	n/r	0.042
				2 (S)	Silicon	4000	0.05	Water	100	25	10.7	0.018
Li 2000 [102]	Piezoelectric (axial)	Flap (diaphragm-ring mesa)	Si, glass (7 layers)	1	Silicon	3300	0.025 (bossed)	Silicone oil	1200	3500	304	3
Zengerle 1995 [90]	Electrostatic	Flap (cantilever)	Si	1	Silicon	98	n/r	Water	200	300	29	0.16
Richter 1998 [80]	Electrostatic	Flap (cantilever)	Si–Si	1	Silicon	n/r	n/r	Water	n/r	400	n/r	0.26
van de Pol 1990 [123]	Thermo-pneumatic (air)	Flap (diaphragm-ring mesa)	Glass–Si–Si–Si–glass	1	Silicon	3000	0.018	Water	6	1	5.1	0.034
Folta 1992 [131]	Thermo-pneumatic (air)	None	Si–Si–Si	3 (S)	Silicon	n/r	0.002	Water	n/r	1	n/r	n/r
Elwenspoek 1994 [124]	Thermo-pneumatic (air)	Flap (diaphragm-ring mesa)	Glass–Si–glass	1	Silicon	n/r	n/r	Water	n/r	5	n/r	0.055
Schomburg 1994 [125]	Thermo-pneumatic (air)	Flap (diaphragm-ring mesa)	Polymer (polysulphone)	1	Polyimide	n/r	0.0025	Air	15	5	3.8	0.044
Grosjean 1999 [126]	Thermo-pneumatic (air)	None	Acrylic, silicon, glass	3 (S)	Parylene/ silicone rubber	970	0.12	Water	n/r	2	3.4	0.0063
Jeong 2000 [127]	Thermo-pneumatic (air)	Fixed-geometry (nozzle-diffuser)	Glass–Si–glass	1	Silicon	n/r	0.002	Water	8	4	0	0.014
Wego 2001 [96]	Thermo-pneumatic (air)	Flap (diaphragm-ring mesa)	Printed circuit board (4 layers)	1	Polyimide	780	0.0078	Water		2	12	0.53
Yoon 2001 [97]	Thermo-pneumatic (water/phase-change)	Flap (cantilever)	Si–glass	1	Silicone rubber	72	0.03	Water	10	0.5	0.10	0.006
Tsai 2002 [132]	Thermo-pneumatic (bubble)	Fixed-geometry (nozzle-diffuser)	Glass–Si	1	n/a	n/r	n/a	Isopropyl alcohol	20	400	0.38	0.0045
Zimmermann 2004 [133]	Thermo-pneumatic (bubble)	Flap (in-plane)	Glass–Si	1	n/a	n/r	n/a	Isopropyl alcohol	n/r	10	16	0.009
Rapp 1994 [142]	Pneumatic	None	Gold, polyimide, glass	3 (S)	Titanium	n/a	0.003	Water	n/a	5	2.3	n/r
Grosjean 1999 [126]	Pneumatic	None	Acrylic, silicon, glass	3 (S)	Parylene/ silicone rubber	n/a	0.122	Water	n/a	16	34.5	0.1
Meng 2000 [146]	Pneumatic	Flap (tethered plate)	Si, thermoplastic, silicone rubber	1	Silicone rubber	n/a	0.14	Water	n/a	5	5.9	3.5

n/a: not applicable; n/r: not reported; S: series configuration; P: parallel configuration.

Table 1. (Continued.)

Author and year	Driver	Valves	Construction	Pump chambers	Diaphragm material	S_p (approx.) (mm^3)	Diaphragm thickness (mm)	Working fluid	V (V)	f (Hz)	Δp_{max} (kPa)	Q_{max} (ml min^{-1})
Unger 2000 [143]	Pneumatic	None	Multi-layer elastomer	3 (S)	Elastomer	n/a		Water	n/a	75	n/r	0.000 14
Grover 2003 [144]	Pneumatic	Flap (diaphragm)	Glass–PDMS–glass	1	PDMS	n/a	0.254	Water	n/a	<1	30	0.0028
Berg 2003 [87]	Pneumatic	None	PDMS, glass	2 (S)	PDMS	n/a	2.3	Water	n/a	1	0.17	0.006
Benard 1998 [150]	Shape-memory alloy	Flap (tethered plate)	Silicon	1	TiNi	560	0.003	Water	n/r	0.9	0.53	0.05
Dario 1996 [145]	electromagnetic	Flap (double opposing cantilevers)	Molded plastic	1	Rubber	2500	n/r	Water	14	264	4.6	0.78
Bohm 1999 [94]	Electromagnetic	Flap (diaphragm-ring mesa)	Molded plastic	1	Silicone rubber	1000	0.2	Water Air	5 5	50 400	10 n/r	2.1 40
Yun 2002 [86]	Electrowetting	Flap (cantilever)	Glass–SU8–Si–Si	2	Silicone rubber	n/r	0.08	Water	2.3	25	0.70	0.07

n/a: not applicable; n/r: not reported; S: series configuration; P: parallel configuration.

where E_y and ν are the Young's modulus and Poisson ratio, respectively, of the diaphragm material. The maximum stress σ in the diaphragm is given by

$$\frac{\sigma d_d^2}{4E_y t_d^2} = \frac{4}{(1-\nu^2)}\frac{y_0}{t_d} + 1.73\left(\frac{y_0}{t_d}\right)^2. \quad (2)$$

The first mechanical resonance f_r of a 'dry' diaphragm (i.e. one not subject to significant pressure forces from a liquid) is [79]

$$f_r = 2\pi(1.015/d_d)^2\sqrt{\frac{E_y t_d^2}{12\rho(1-\nu^2)}} \quad (3)$$

where ρ is the density of the diaphragm material. Equations (1) and (2), taken together, can be used to estimate the absolute upper limit on ΔV for a given diaphragm geometry, regardless of choice of driver. Equation (1) can be used to determine ΔV directly (absent an external fluid pressure differential and for quasi-static operation) for the subset of reciprocating displacement micropumps with drivers that resemble pressure sources, while equation (3) can be used to determine the range of operating frequencies for which the assumption of quasi-static response is valid. Dynamic effects are relevant in micropumps operating at or near the diaphragm resonant frequency, potentially increasing performance but also making pump performance more dependent on valve characteristics and external conditions. Dynamic effects are discussed further in section 2.1.7 below.

Δp_{max} for reciprocating displacement micropumps with physical drivers and valves is ultimately limited by the driver force and by the valve characteristics. In the operating regime where the driver pressure is much greater than the back pressure and the valve behavior is nearly ideal, the compressibility κ of the working fluid limits pressure generation. For a reciprocating displacement pump with ideal valves, theoretical Δp_{max} is [80]

$$\Delta p_{max} = \frac{1}{\kappa}\varepsilon_C = \frac{1}{\kappa}\left(\frac{\Delta V}{V_0}\right), \quad (4)$$

where the ratio between the stroke volume ΔV and the dead volume V_0 is the pump compression ratio ε_C. Because of this dependence of Δp_{max} on κ, reciprocating displacement micropumps are generally capable of achieving higher pressures with liquid-phase working fluids than with gas-phase. For a liquid-phase working fluid with low, uniform compressibility, Δp_{max} is determined by the compression ratio ε_C, which is (to a degree) at the discretion of the pump designer. However, complications arise due to the very real possibility that bubbles might be present in the working fluid, increasing its compressibility and decreasing Δp_{max} for a given ε_C. Although steps can be taken to minimize the likelihood of bubbles reaching the pump chamber, susceptibility to bubbles is a significant problem for reciprocating displacement micropumps. If bubbles are unavoidable, the compression ratio must be sufficiently large that the pump can accommodate a highly compressible working fluid.

Richter *et al* [80] and Linnemann *et al* [81] studied the relationship between ε_C and bubble tolerance by testing three micropumps very similar to one another but with different compression ratios. A micropump with $\varepsilon_C = 0.002$ was found to pump water effectively, but stalled when an 8 μl bubble entered the pump chamber. A micropump with $\varepsilon_C = 0.017$ exhibited limited bubble tolerance, stalling after two bubbles entered the chamber in succession. A micropump with $\varepsilon_C = 0.085$ consistently passed bubbles that entered the chamber. Other recent papers have discussed pressure generation by reciprocating displacement micropumps [82, 83].

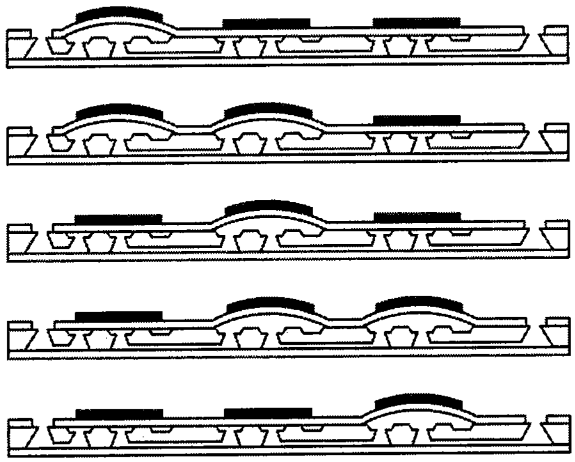

Figure 3. Reciprocating displacement micropump with three pump chambers in series developed by Smits [16]. The micropump is made from an etched silicon substrate bonded between two glass plates. Piezoelectric disks are bonded to the glass above each of the three pump chambers etched in the silicon. Applying a voltage to a piezoelectric actuator causes the glass to bow away from the pump chamber beneath, drawing in fluid. Staggered actuation as shown results in net fluid flow from the inlet at left to the outlet at right.

2.1.2. Chamber configuration. Most reported reciprocating displacement micropumps have a single pump chamber, like the design shown in figure 2. The micropump reported by Smits [16], however, introduced a different chamber configuration, shown in figure 3, in which the working fluid passes through three pump chambers linked in series by etched channels. Channels leading to the first and from the third chambers function as the pump's inlet and outlet. Piezoelectric actuators drive each of the three pump chamber diaphragms individually. Actuating the three piezoelectric disks 120° out of phase with one another produces net flow through the pump. Operating in this manner, the micropump requires no valves to rectify the flow. Micropumps with multiple chambers in series and no valves operate in a manner somewhat similar to macroscale peristaltic pumps, and accordingly are sometimes referred to as peristaltic micropumps. Smits' micropump, which consists of a single etched silicon substrate sandwiched between two glass plates, was patented in the United States in 1990 [84]. It is relatively large ($S_p \cong 1.5$ cm^3) and pumps water with $Q_{max} = 100$ μl min^{-1} and $\Delta p_{max} = 600$ Pa operating at $f = 15$ Hz and $V = 100$ V$_{p\text{-}p}$.

In 1990, Shoji *et al* reported a micropump with two pump chambers in series [85]. Unlike Smits' design, this micropump requires check valves. However, the two-chamber design was reported to operate effectively at higher frequencies than an otherwise-similar single-chamber micropump. Shoji *et al*'s micropump is piezoelectrically driven and fabricated from glass and silicon; its size is $S_p \cong 4.0$ cm^3. $Q_{max} = 18$ μl min^{-1}

and $\Delta p_{max} = 10.7$ kPa operating at $f = 25$ Hz and $V = 100$ V. Yun *et al* reported a reciprocating displacement micropump with two chambers in series driven by electrowetting-induced oscillation of a mercury plug [86]. This micropump pumps water with $Q_{max} = 70\ \mu l\ min^{-1}$ and $\Delta p_{max} = 700$ Pa operating at $f = 25$ Hz and $V = 2.3$ V. P is 0.17 mW and η_{est} is 0.12%. Berg *et al* [87] demonstrated that pressure and flow can be generated by phased actuation of two chambers in series without use of check valves.

Shoji *et al* also reported reciprocating displacement micropumps with two pump chambers arranged in parallel [85]. This configuration was intended to reduce oscillation in the pump output due to periodic driver operation. A micropump with this parallel-chamber configuration pumps water at $Q_{max} = 42\ \mu l\ min^{-1}$ operating at $f = 50$ Hz and $V = 100$ V; Δp_{max} was not reported. Olsson *et al* reported reciprocating displacement micropumps with two pump chambers in parallel in which drivers are attached to both the top and bottom surfaces of each pump chamber [88, 89]. A precision-machined brass micropump ($S_p \cong 1.6\ cm^3$) with this two-chamber, four-diaphragm design pumps water at $Q_{max} = 16\ ml\ min^{-1}$ and $\Delta p_{max} = 16.2$ kPa operating at $f = 540$ Hz and $V = 130$ V. Performance improvements realized with a multi-chamber design must be balanced against increases in fabrication complexity and overall size inherent in this approach. A recent study suggests two-chamber micropump designs are particularly effective when combined with fixed-geometry valves (discussed further below) [69].

2.1.3. Materials and fabrication techniques. The most common method for fabricating micropumps is micromachining of silicon combined with glass bonding layers, as seen in van Lintel *et al*'s and Smits' micropumps. These early micropumps are large by micromachining standards, each occupying an entire 2 inch silicon wafer. In 1995, Zengerle *et al* reported a reciprocating displacement micropump with $S_p \cong 0.1\ cm^3$ [90]. With the pump components efficiently arranged in four layers and a compact electrostatic driver, this micropump pumps water with $Q_{max} = 850\ \mu l\ min^{-1}$—corresponding to a self-pumping frequency $f_{sp} \cong 1.6$. In comparison, $f_{sp} \cong 0.002$ for van Lintel *et al*'s micropump and $f_{sp} \cong 0.07$ for Smits' micropump.

A number of reciprocating displacement micropumps have been fabricated through means other than traditional silicon/glass micromachining. Piezo-driven micropumps made by precision machining of brass were reported by Stemme and Stemme in 1993 [91]. These micropumps are $S_p \cong 2.5\ cm^3$ in size. Two micropumps (with different valves) were reported; one pumps water with $Q_{max} = 4.4\ ml\ min^{-1}$ and $\Delta p_{max} = 20.6$ kPa operating at $f = 110$ Hz and $V = 20$ V, while the other pumps water with $Q_{max} = 15.5\ ml\ min^{-1}$ and $\Delta p_{max} = 4.9$ kPa operating at $f = 310$ Hz. The two-chamber reciprocating displacement micropump reported by Olsson *et al* was made by precision machining of brass, but with planar geometries rather than the three-dimensional geometries of the Stemme and Stemme micropumps [88].

Improvements in techniques for fabricating precision components from plastic have led to increasing use of plastics in reciprocating displacement micropumps. Indeed, the only micropump currently in widespread commercial distribution, produced by thinXXS GmbH of Germany (a spin-off company of the Institut für Mikrotechnik Mainz GmbH (IMM)) is made from microinjection molding of plastic [92, 93]. The size of this micropump is $S_p \cong 4.6\ cm^3$; it produces $Q_{max} = 2\ ml\ min^{-1}$ and $\Delta p_{max} = 35$ kPa at $V = 450$ V and $f = 20$ Hz. A number of other plastic reciprocating displacement pumps have been reported, including one reported by Bohm *et al* [94] with $S_p \cong 0.28\ cm^3$. Carrozza *et al* [95] reported a micropump fabricated by stereolithography of an ultraviolet-photocurable polymer. The size of this micropump is $S_p \cong 1.3\ cm^3$; a portion of the micropump is made of brass. It pumps water with $\Delta p_{max} = 25$ kPa and $Q_{max} = 2.7\ ml\ min^{-1}$ operating at $V = 300$ V and $f = 70$ Hz. A reciprocating displacement micropump made from printed circuit boards has also been reported [96].

The choice of pump diaphragm material can be particularly important. For micropumps driven by low-frequency and/or low-force actuators, a low-modulus diaphragm material generally allows ΔV to be maximized, favorably impacting performance. Mylar [94] and silicone rubber [97] pump diaphragms have been used in thermopneumatically driven reciprocating displacement micropumps for this reason. Since the pump diaphragm comes into contact with the working fluid, however, the stability of soft polymer diaphragms is a concern. A micropump commercially produced by Debiotech S.A. of Switzerland and targeted for implanted drug delivery has a glass diaphragm, even though it operates at $f < 1$ Hz [98, 99]. This micropump produces flow rates of up to a few $\mu l\ min^{-1}$, suitable for therapeutic agent dispensation. For drivers capable of operating at high frequency and which produce ample force, the fast mechanical response of a stiff diaphragm generally yields the best performance. For this reason, silicon and glass are the most common diaphragm materials in piezoelectric-driven reciprocating displacement micropumps.

2.1.4. Diaphragm geometry. Most reported reciprocating displacement micropumps are roughly planar structures between 1 mm and 4 mm thick. The overall size of the micropump depends heavily on the in-plane dimensions, which must be large enough to accommodate the pump diaphragm. To estimate the effects of reducing diaphragm diameter, we consider a generic reciprocating displacement micropump with ideal check valves and a circular, planar diaphragm. Figure 4(*a*) shows the dependence of diaphragm centerline displacement y_0 on diaphragm diameter d_d for a 100 μm thick silicon diaphragm subjected to a spatially uniform driver force per unit diaphragm area p_a. Centerline displacement y_0, obtained using equation (1), is plotted for $p_a = 10^5$ Pa, 10^6 Pa and 10^7 Pa. Also plotted is y_0 for σ equal to the yield stress of single-crystal silicon ($\sigma_y = 7.0$ GPa [59]), obtained using equations (1) and (2) above; and the first resonant frequency of a 'dry' diaphragm, from equation (3). Centerline displacement and first resonance for a 10 μm thick silicon diaphragm are plotted in figure 4(*b*). For $y_0 \ll t_d$, centerline displacement scales with the fourth power of diameter, so reducing diaphragm diameter without undue decrease in ΔV generally necessitates the use of a high-force driver. Even with a driver capable of supplying effectively unlimited force, y_0 is limited by the diaphragm's

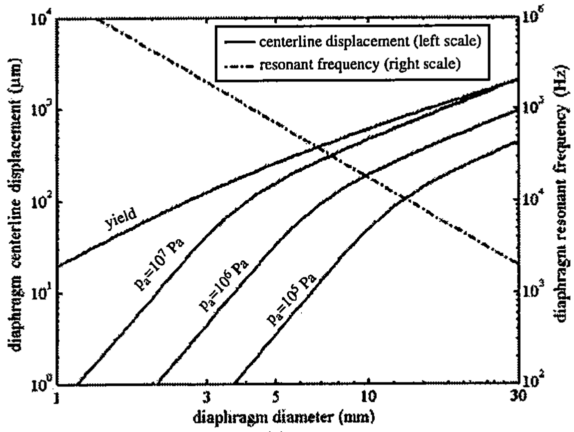

(*a*)

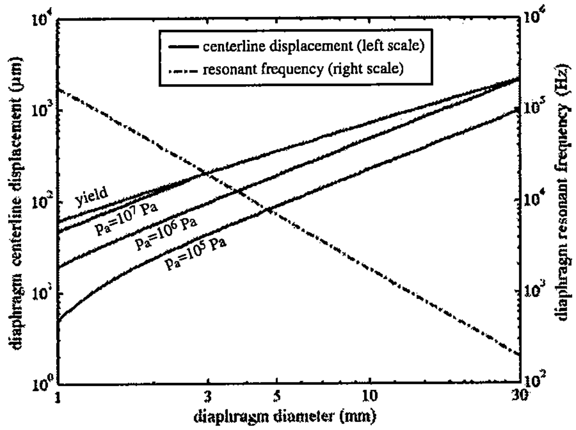

(*b*)

Figure 4. Scaling of pump diaphragm mechanical properties with diaphragm diameter d_d. A spatially uniform, circular diaphragm clamped at its perimeter is assumed. Centerline displacement y_0 is calculated for the driver pressures shown using equation (1). Centerline displacement at the yield point of the diaphragm is calculated using equations (1) and (2). Diaphragm resonant frequency is calculated using equation (3). (*a*) 100 μm thick silicon diaphragm; (*b*) 10 μm thick silicon diaphragm.

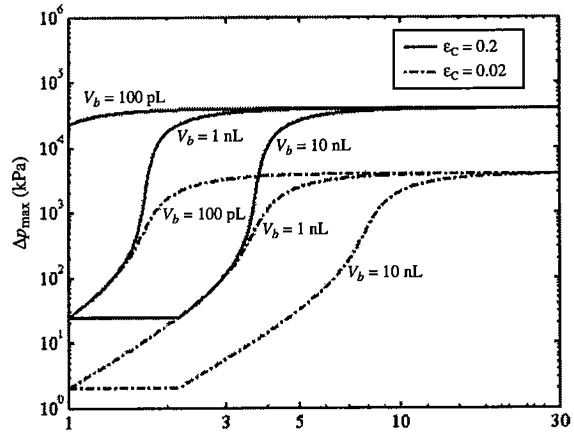

Figure 5. Theoretical scaling with diaphragm diameter d_d of maximum generated pressure Δp_{max} for reciprocating displacement micropumps. As shown in equation (4), Δp_{max} is a function of the micropump's compression ratio, ε_C, and of the compressibility, κ, of the fluid in the pump chamber. For ε_C = constant and κ = constant, pressure generation is independent of diaphragm diameter. As the diaphragm diameter is scaled down, the impact of a bubble of a given volume V_b in the pump chamber on κ—and therefore on Δp_{max}—increases. When the bubble fills the entire pump chamber, Δp_{max} reaches its minimum. A dead volume of $V_0 = 0.001 d_d^3$ is assumed in calculations.

failure criteria—which also scale unfavorably with decreasing diaphragm diameter. Note that, for sinusoidal forcing functions, resonance frequencies that are large compared to the frequency of operation imply that the inertia of the diaphragm can be neglected and its mechanical response becomes quasi-static (although the inertia of the fluid may still be important).

The scaling of bubble-dependent Δp_{max} with d_d is shown in figure 5. This analysis is independent of pump geometry except for V_0, which is assumed to equal 0.001 d_d^3. The working fluid is assumed to be nearly incompressible (κ = 0.5 m^2 N^{-1}). When no bubbles are present in the working fluid, Δp_{max} is given by equation (4) and is independent of d_d for a given compression ratio ε_C. However, Δp_{max} falls off precipitously with diaphragm diameter when a bubble of volume comparable to V_0 is present. Scaling down pump diaphragm diameter presents a significant challenge for designers of reciprocating displacement micropumps.

Nonplanar diaphragm geometries have been applied to a limited extent in reciprocating displacement micropumps. Piezoelectrically driven reciprocating displacement micropumps reported by Esashi *et al* [100], Shoji *et al* [85] and Stehr *et al* [101] have diaphragms with bosses at their centers. The diaphragm in a high-performance reciprocating displacement micropump reported by Li *et al* [102] and discussed further below is made from two layers of silicon with interior center bosses to yield piston-like behavior.

2.1.5. Drivers. Figure 6 shows common reciprocating displacement micropump driver designs. Figures 6(*a*) and (*b*) illustrate piezoelectric drivers in lateral and axial configurations. The free strain that can be produced in the driver places an upper limit on the stroke volume of a piezoelectric-driven micropump. The available driving voltage and the polarization limit of the piezoelectric material, in turn, determine the maximum piezoelectric free strain. PZT-5H, a high-performance piezoceramic, has a d_{31} strain coefficient of -274×10^{-12} C N^{-1} (for strain normal to the polarization direction) and a d_{33} strain coefficient of 593×10^{-12} C N^{-1} (for strain parallel to the polarization direction). Piezoelectrics can be driven at frequencies over 1 kHz by electric fields on the order of 10 kV cm^{-1} or higher. The efficiency of electromechanical conversion in piezoelectrics is typically between 10 and 30% (excluding the finite efficiency of the voltage conversion and AC voltage control) [103].

The use of piezoelectrics to drive micropumps can be traced to a class of ink jet printheads developed in the 1970s, illustrated schematically in figure 7. A piezoelectric actuator contracts a chamber in the printhead, causing a droplet of ink to be ejected from the nozzle. During expansion, a vacuum in

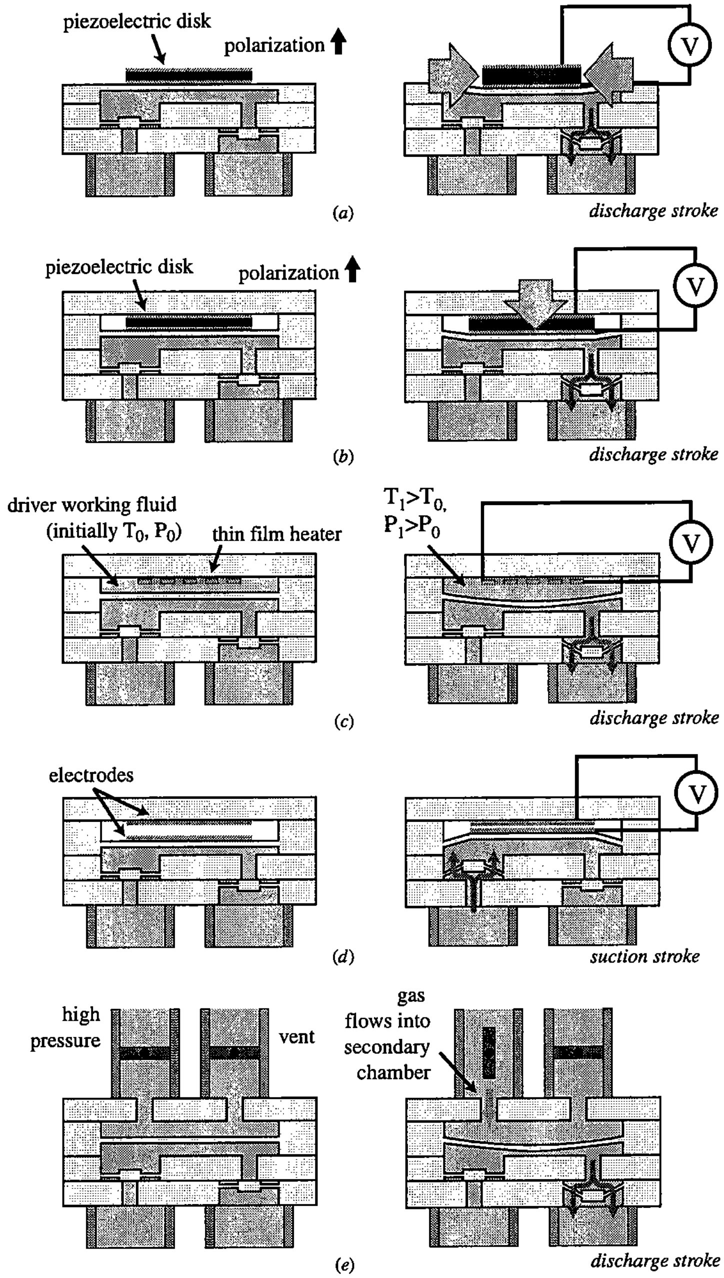

Figure 6. Reciprocating displacement micropumps with various drivers. (*a*) Piezoelectric driver in the lateral-strain configuration. The bottom surface of the piezoelectric disk is bonded to the pump diaphragm the top surface is unconstrained. During operation, the pump diaphragm deflects under a bending moment produced by radial strain in the piezoelectric disk. An axial electric field is applied to the disk. (*b*) Piezoelectric driver in the axial-strain configuration, where a piezoelectric disk is mounted between the pump diaphragm and a rigid frame. During operation, the pump diaphragm deflects primarily as a result of axial strain in the piezoelectric disk. As in (*a*), an axial electric field is applied to the disk. (*c*) Thermopneumatic driver, in which a thin-film resistive element heats the driver working fluid in a secondary chamber above the pump chamber. The heated fluid expands, exerting pressure on the pump diaphragm. (*d*) Electrostatic driver, in which the pump diaphragm deflects upward when an electric potential difference is applied between parallel electrodes. Electrostatically driven reciprocating displacement micropumps typically have a powered suction stroke and an unpowered discharge stroke. Dielectric coatings are used to prevent shorting. (*e*) External pneumatic driver, in which active valves alternately pressurize and vent a secondary chamber above the pump diaphragm.

the main liquid chamber fills it with ink from the ink supply, while the pressure difference associated with surface tension at the ejector orifice prevents air from entering the chamber. In this way, surface tension and capillary pressure are used as an inherent check valve with no solid moving parts. IBM was issued a US patent for this design in 1974 [104]. Researchers

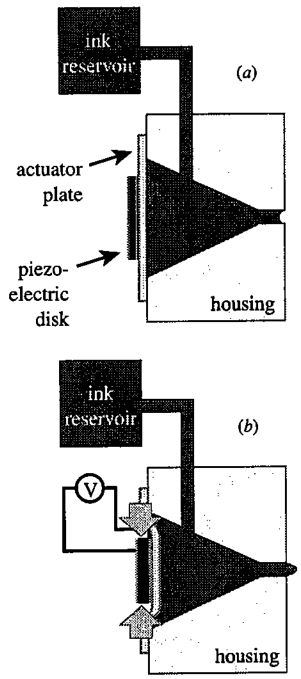

Figure 7. IBM ink jet printhead schematic. The volume of the chamber is varied by using a piezoelectric disk actuator to deform the plate that seals the back side of the chamber. Surface tension at the ejector orifice (on the right side) acts as a check valve to rectify the flow. From US patent no. 4,266,232 [106].

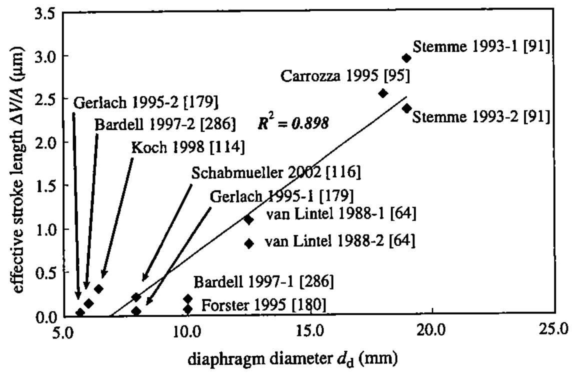

Figure 8. Scaling of effective stroke length ($= \Delta V/A$) with diaphragm diameter for reported reciprocating displacement micropumps with lateral-strain configuration piezoelectric actuators acting directly on the diaphragm. Effective stroke volume ΔV is determined by dividing the reported flow rate at minimal back pressure $Q_{\max}$ by the operating frequency f.

later conceived of fabricating the ink chamber using then-nascent silicon micromachining technology [105].

In piezoelectric inkjet printheads, chamber actuation results from lateral strain induced in the piezoelectric disk. In many piezo-driven micropumps, including van Lintel *et al*'s [64] and Smits' [16], piezoelectric actuators are employed in a similar manner. As shown in figure 6(*a*), one face of a piezoelectric disk is bonded to the chamber diaphragm (typically using epoxy); the other face of the disk is unconstrained. The piezoelectric disk is polarized in the axial direction, and each face is covered with an electrode. Applying an axial electric field across the piezoelectric disk produces both a lateral and an axial response in the disk, described by the d_{31} and d_{33} piezoelectric strain coefficients, respectively. For this configuration, the chamber diaphragm bows to balance the lateral stress in the piezoelectric disk. If the induced lateral stress in the disk is compressive, the diaphragm bows into the chamber; if tensile, it bows away from the chamber. In some micropumps, the piezoelectric actuators are driven bidirectionally to maximize stroke volume [16]. Progress has been made recently on the development of analytical solutions for the mechanical response of piezo-bonding layer-diaphragm structures [107]. Morris and Forster used numerical simulations to identify optimal diaphragm and piezoelectric disk geometries for lateral-strain piezo-driven reciprocating displacement micropumps [71]. Other researchers have also used numerical methods to study lateral-strain piezo-driven reciprocating displacement micropumps [67, 108]. In some micropumps stroke volume is increased by using multiple electrodes to apply a spatially varying field across the piezoelectric disk [84].

A sufficiently large number of lateral-configuration piezo-driven reciprocating displacement micropumps has been reported to permit empirical analysis of how micropump performance scales with diaphragm diameter. Figure 8 shows the correlation between effective stroke length ($\Delta V/A_d$) of reported micropumps and the diaphragm diameter, d_d. Micropumps with planar diaphragms to which the piezoelectric disk is directly attached and for which diaphragm diameter has been reported are considered. Effective stroke length decreases with decreasing d_m, in part because of generally increasing diaphragm stiffness as reflected in equation (1) above.

Micropumps that rely on piezoelectric coupling parallel to the applied field (described by the d_{33} piezoelectric strain coefficient), as shown in figure 6(*b*), have also been reported. In this configuration, both faces of the piezoelectric disk are constrained—one by a rigid support and the other by the pump diaphragm. The axial strain induced in the disk by applying an external axial electric field causes the pump diaphragm to deflect, expanding and contracting the pump chamber. Esashi *et al* [100] reported the first reciprocating displacement micropump driven by a piezoelectric actuator in this configuration. This micropump was fabricated from two layers of silicon with an intermediate layer of sputtered glass. A glass housing fixes a piezoelectric actuator above a 2 mm square bossed silicon diaphragm. The size of this micropump is $S_p \cong 0.8$ cm^3; it pumps water with $Q_{\max} = 15$ μl min^{-1} and $\Delta p_{\max} = 6.4$ kPa at $f = 30$ Hz and $V = 90$ V$_{\text{p-p}}$.

Many reported piezo-driven reciprocating displacement micropumps operate at very high frequencies, taking advantage of the fast temporal response of piezoelectric actuators. A two-chamber piezo-driven reciprocating displacement micropump reported by Olsson *et al* [109, 110] operates at $f = 3$ kHz and pumps water with $Q_{\max} = 2.3$ ml min^{-1}. Fluid dynamic effects, rather than traditional mechanical check valves, are used to produce net flow through this micropump, an approach discussed in more detail below. Li *et al* [102] reported an axial-configuration piezo-driven reciprocating displacement micropump driven by multiple stacks of high-performance piezoelectric materials. This micropump, intended for microrobotics and shoe strike power conversion, has an $S_p \cong 3.2$ cm^3 and pumps silicone oil (in a closed, pressurized system) with $Q_{max} = 3$ ml min^{-1} and $\Delta p_{max} = 300$ kPa operating at $f = 3.5$ kHz and $V = 1.2$ kV. A number of other piezoelectric-driven reciprocating displacement micropumps have been reported [111, 112].

Inserting and attaching piezoelectric actuators may increase manufacturing costs relatively to a fully batch process. Koch *et al* sought to address this limitation by screen-printing a PZT thick film to function as a lateral-strain-configuration reciprocating displacement micropump driver [113–115]. This micropump produced $Q_{max} = 120$ μl min^{-1} and $\Delta p_{max} = 1.8$ kPa operating at 200 Hz and 600 V$_{p-p}$; an otherwise-identical micropump with a bulk piezoelectric driver produced $Q_{max} = 150$ μl min^{-1} and $\Delta p_{max} = 3.5$ kPa operating at $f = 200$ Hz and $V = 200$ V$_{p-p}$. A modified version of this micropump with a bulk piezoelectric driver produced $Q_{max} = 1.5$ ml min^{-1} and $\Delta p_{max} = 1$ kPa [116]. Stehr *et al* [101] reported a reciprocating displacement micropump driven by a piezoelectric actuator with the tip of a bimorphic piezoelectric cantilever attached to the center of the pump diaphragm. This micropump pumps water with $Q_{max} = 1.5$ ml min^{-1} and $\Delta p_{max} = 17$ kPa operating at $f = 190$ Hz and $V = 200$ V. Further discussion of the design and performance of piezoelectric drivers and their applications in reciprocating displacement micropumps can be found in several recent papers [117–121].

Figure 6(*c*) illustrates the design of a typical thermopneumatically driven reciprocating displacement micropump. A chamber opposite the primary pump chamber holds a secondary working fluid. Heating the secondary working fluid (usually with an integrated thin-film resistive heater) causes it to expand, deflecting the pump diaphragm and discharging primary working fluid through the pump outlet. The intake stroke occurs when the heater is deactivated, allowing the diaphragm to relax. The secondary chamber is usually vented to speed the relaxation. The first thermopneumatically driven reciprocating displacement micropump was reported by van de Pol *et al* in 1989 [122, 123]. This relatively large micropump ($S_p \cong 4$ cm^3) consists of three layers of silicon and two layers of glass with an evaporated aluminum thin film heater element. With air as the secondary working fluid, it pumps water with $Q_{max} = 34$ μl min^{-1} and $\Delta p_{max} = 5$ kPa operating at $f = 1$ Hz and $V = 6$ V; $\eta_{est} = 3.6 \times 10^{-5}$% (i.e. less than one part in 1000 000 of the input power is converted to work on the fluid).

The temporal response of thermopneumatic actuators is limited by the rate of heat transfer into and out of the secondary working fluid, and so thermopneumatically driven reciprocating displacement micropumps typically operate at relatively low frequencies. Elwenspoek *et al* sought to maximize f with a design that minimizes heat transfer into the substrate (instead of the secondary working fluid) during the heating step [124]. This micropump pumps water with $Q_{max} = 55$ μl min^{-1} operating at $f = 5$ Hz; Δp_{max} was not reported.

Low-modulus pump diaphragm materials are often used in thermopneumatically driven reciprocating displacement micropumps in order to maximize ΔV. Schomburg *et al* [125] reported a thermopneumatically driven reciprocating displacement micropump in which the pump diaphragm is a 2.5 μm thick polyimide layer. This micropump is fabricated by polymer injection molding; the heater is titanium. With air as the secondary working fluid, this micropump pumps air with $Q_{max} = 44$ μl min^{-1} and $\Delta p_{max} = 3.8$ kPa operating at $f = 5$ Hz and $V = 15$ V; $\eta_{est} = 1.6 \times 10^{-4}$%. S_p was not reported, but the lateral dimensions of the pump are 7 mm × 10 mm. Grosjean and Tai reported a thermopneumatically driven reciprocating displacement micropump with a 120 μm thick silicone rubber diaphragm [126]. The silicone rubber is coated with a thin layer of parylene, which functions as a vapor barrier. With air as the secondary working fluid, this device pumps water with $Q_{max} = 4.2$ μl min^{-1} and $\Delta p_{max} = 3$ kPa at $f = 2$ Hz. Power consumption is 0.3 W ($\eta_{est} = 3 \times 10^{-4}$%). Jeong and Yang [127] reported a thermopneumatically driven reciprocating displacement micropump with a corrugated silicon pump diaphragm. The corrugations are intended to increase diaphragm deflection (and therefore stroke volume) for a given secondary chamber pressure. This micropump produces $Q_{max} = 14$ μl min^{-1} operating at $f = 4$ Hz and $V = 8$ V; Δp_{max} was not reported. Sim *et al* [128] attempted to increase the thermopneumatic actuator force using a phase change of the secondary working fluid. This micropump is highly compact ($S_p = 0.070$ cm^3), has a 30 μm thick silicone rubber diaphragm and aluminum flap valves and uses water as the secondary working fluid. Operating at $f = 0.5$ Hz and $P = 0.6$ W, this micropump pumps water with $Q_{max} = 6$ μl min^{-1} and $\Delta p_{max} = 100$ Pa. Maximum thermodynamic efficiency was reported to be $\eta = 3.6 \times 10^{-7}$%. Advantages of thermopneumatic actuation include ready fabrication using standard micromachining processes and low operating voltages. Whereas the stroke length piezoelectrically driven and electrostatically driven micropumps is typically limited to a few microns, the stroke length of thermopneumatically driven micropumps can be much larger, limited only by the available driver force and the mechanical properties of the diaphragm. The diaphragm in the pump reported by Schomburg *et al* deflects 100 μm during operation, yielding a compression ratio large enough to pump gases [125]. Schomburg *et al*'s plastic micropump is bonded to a silicon heat sink to increase the rate of cooling of the secondary working fluid during the intake stroke and thereby allow higher frequency micropump operation. A number of papers discuss thermopneumatically driven reciprocating displacement micropumps (including heat transfer aspects) in detail [129–131].

A subset of thermopneumatically driven reciprocating displacement micropumps are so-called 'bubble' pumps, in which pumping is driven by phase change of the primary working fluid, rather than of a secondary working fluid in a separate chamber. Tsai and Lin reported a thermal bubble-driven reciprocating displacement micropump fabricated from only two layers of material [132]. This micropump pumps isopropyl alcohol with $Q_{max} = 45$ μl min^{-1} and $\Delta p_{max} = 400$ Pa operating at $f = 400$ Hz and $V = 20$ V; power consumption is $P = 0.5$ W ($\eta_{est} = 1.4 \times 10^{-6}$%). Zimmermann *et al* [133] reported a thermal bubble micropump in which the heated chamber is offset from the main flow path, reducing heating of the working fluid. This micropump pumps isopropyl alcohol with $Q_{max} = 9\ \mu l\ min^{-1}$ and $\Delta p_{max} = 16$ kPa operating at $f = 10$ Hz; power consumption is $P = 0.18$ W.

Electrostatic forces are widely used for actuation in MEMS devices. The comb-drive configurations that are widely used in large-displacement electrostatically actuated MEMS devices [134] are difficult to implement in reciprocating displacement micropumps, however. Instead, electrostatically driven reciprocating displacement micropumps typically have the parallel-plate actuator design shown in figure 6(*d*). Although the pump diaphragm (and therefore the bottom electrode) typically bows during pump operation, the driver force at the very beginning of the pump stroke (when both electrodes are flat plates) can be easily calculated. The capacitance between a pump diaphragm of diameter d_d and a counterelectrode of equal size separated by a distance s is

$$C = \frac{\varepsilon \pi d_d^2}{4s}. \tag{5}$$

The electrostatic force between the two plates is therefore

$$F = \frac{1}{2}\frac{\partial C}{\partial s}V^2 = -\frac{\varepsilon \pi d_d^2}{8s^2}V^2 \tag{6}$$

where ε is the permittivity of the medium separating the plates and V is the potential difference between them [135]. To generate an initial driver force per unit diaphragm area p_a of 100 kPa with an electrostatic driver operating in a vacuum or in air ($\varepsilon = 8.85 \times 10^{-12}\ C^2\ J^{-1}\ m^{-1}$) requires a voltage-separation distance ratio V/s of 150 V μm^{-1}. With adequate control over out-of-plane feature size during fabrication, therefore, electrostatic drivers can produce appreciable forces at moderate voltages. Electrostatic actuation offers the further advantage of increasing driver force as the diaphragm deflects (and stiffens). The highly compact ($S_p \cong 0.1\ cm^3$) reciprocating displacement micropump reported by Zengerle *et al* and discussed above is electrostatically driven [90, 136]. This micropump exemplifies several favorable features of electrostatic drivers: it is fully micromachined, highly compact and capable of operating at high frequency. With $s = 5\ \mu m$, it pumps water with $Q_{max} = 850\ \mu l\ min^{-1}$ and $\Delta p_{max} = 29$ kPa operating at $V = 200$ V and $f = 800$ Hz. Power consumption is $P = 5$ mW ($\eta_{est} = 0.39\%$). Richter *et al* [80] compared the performance of two similar reciprocating displacement micropumps, one with an electrostatic driver and one with a lateral-configuration piezoelectric driver. The electrostatically driven micropump pumps water with $Q_{max} = 260\ \mu l\ min^{-1}$ operating at $f = 400$ Hz, compared to $Q_{max} = 700\ \mu l\ min^{-1}$ for the piezoelectric-driven micropump operating at $f = 220$ Hz. Cabuz *et al* reported an electrostatically driven micropump with three pump chambers in series [137]. Further analysis and review of the performance of electrostatically driven reciprocating displacement micropumps can be found in several recent papers [68, 138–141].

Reciprocating displacement micropumps driven pneumatically, as shown in figure 6(*e*), have been reported. These pumps require an external pneumatic supply and one or more high-speed valve connections and are therefore not strictly comparable to micropumps with fully integrated actuators. In settings where the necessary infrastructure is available, however, pneumatically driven reciprocating displacement micropumps can be effective. A pneumatically driven reciprocating displacement micropump fabricated using LIGA techniques was reported by Rapp *et al* in 1994 [142]. The three-chamber (series configuration) reciprocating displacement micropump reported by Grosjean *et al* and described above [126] exhibited much better performance when driven pneumatically than thermopneumatically ($Q_{max} = 100\ \mu l\ min^{-1}$ with pneumatic actuation versus $Q_{max} = 4.2\ \mu l\ min^{-1}$ with thermopneumatic actuation).

As with thermopneumatic drivers, low-modulus diaphragm materials are widely used in pneumatically driven reciprocating displacement micropumps. Unger *et al* [143] reported a class of pneumatically driven series multi-chamber reciprocating displacement micropumps made by lithographically patterning multiple layers of a soft elastomeric substrate. Individual layers of elastomer are first spun onto molds made from patterned photoresist, then stacked to form chambers and channels. The chambers and channels made using this 'soft' lithography technique have cross-sectional dimensions between 10–100 μm. The soft elastomer chambers are actuated by pneumatic pressure of order 100 kPa; separate, individually controlled valves of centimeter scale or larger are required to control chamber actuation. Pressure performance for these devices was not reported, but Q_{max} is of order 100 nl min^{-1}. Mathies and coworkers have performed extensive work on pneumatically driven reciprocating displacement micropumps for microchip-based laboratory systems for performing biological and chemical analysis [29, 144]. A representative micropump with a 3.0 mm diameter PDMS diaphragm was reported to pump water with $Q_{max} = 2.8\ \mu l\ min^{-1}$ and $\Delta p_{max} = 30$ kPa [144].

Other, less common micropump drivers have been reported. A version of the piezoelectrically driven reciprocating displacement micropump reported by Bohm *et al* was produced with an electromagnetic driver resembling a solenoid [94]. The choice of actuator had little impact on pump performance, but the micropump with the electromagnetic driver is substantially larger than the piezoelectrically driven version ($S_p = 8\ cm^3$ versus $S_p = 2.9\ cm^3$). Dario *et al* [145] reported a smaller ($S_p \cong 2.5\ cm^3$) electromagnetically driven reciprocating displacement micropump made by thermoplastic molding. Water is pumped with $Q_{max} = 780\ \mu l\ min^{-1}$ and $\Delta p_{max} = 4.6$ kPa operating at $V = 14$ V and $f = 264$ Hz. Meng *et al* [146] reported high-flow-rate micropumps with pneumatic and solenoid drivers. In handheld electronic medical diagnostic devices marketed by i-STAT Corporation, a solenoid actuates a rubber diaphragm to pump biological samples [147]. Gong *et al* [148] analyzed the theoretical performance of an optimized electromagnetically actuated reciprocating displacement micropump. Santra *et al* [149] reported a reciprocating displacement pump driven by the interaction of a stationary electromagnet with a permanent magnet diaphragm. Bernard *et al* [150] reported a reciprocating displacement micropump driven by shape-memory alloy actuators. This micropump was fabricated using five layers of micromachined silicon with a polyimide diaphragm and sputter-deposited titanium nickel and pumps water with $Q_{max} = 50\ \mu l\ min^{-1}$ and $\Delta p_{max} = 0.5$ kPa operating at $f = 0.9$ Hz. Power consumption is 0.63 W ($\eta_{est} = 1.7 \times 10^{-5}\%$). The use of shape-memory alloys in reciprocating displacement micropumps is discussed further by Makino *et al* [151]. As discussed above, Yun *et al* reported a reciprocating displacement micropump driven by electrowetting [86]. Micropump designs with bimetallic drivers [152–154] and magnetoelastic drivers [155] have also been reported.

2.1.6. Valves. The performance of check valves at the inlet and outlet of the pump chamber is critical to the operation of reciprocating displacement micropumps. Microvalves have been reviewed recently [56, 156]. Figures of merit for check valves include diodicity, or the ratio between the forward and reverse pressure drop across the valve, maximum operating pressure, ease of fabrication and reliability. Most micropumps incorporate some sort of normally closed, passive (non-actuated), mechanical flap structure. The valves in the reciprocating displacement micropump reported by van Lintel *et al* consist of a flexible, circular diaphragm with an opening at the center surrounded by a stiffening 'ring mesa' [64]. A number of other reported reciprocating displacement micropumps have similar valves [92, 94, 102, 123]. Flap valves based on cantilever structures are easily fabricated and widely used [80, 81, 90]. Several micropumps incorporating check valves with a tethered-plate structure (similar to that shown in figure 2) have been reported [85, 100, 150]. A micropump with in-plane flap valves has been reported [133]. The dynamic response of passive flap valves can be important for high-frequency pumps, and the flow can reverse direction above a mechanical resonance of the valves [90, 157]. Several recent papers discuss the mechanical response of passive flap valves [141, 148, 158–160]. The stereolithographically fabricated reciprocating displacement micropump reported by Carrozza *et al* [95] has ball-type check valves. The use of ball valves in micropumps is further discussed by Accoto *et al* [161].

Active valves—valves that are opened and closed by an actuating force—offer improved performance at the expense of fabrication and operational complexity. Active valves with bimetallic [162], electrostatic [163–166], thermopneumatic [167–170], piezoelectric [100, 171] and other drivers [156, 172–178] have been reported.

Fluid flow through reciprocating displacement micropumps can also be rectified by leveraging fluid dynamic effects in inlet and outlet channels with suitable geometries. Pumps with flow-rectifying channels instead of more traditional valves are referred to as having 'fixed-geometry' or 'no-moving-parts' valves, or, occasionally, as 'valveless' pumps. The brass micropumps reported in 1993 by Stemme and Stemme have nozzle-diffuser inlet and outlet channel geometries that function as fixed-geometry valves [91]. Flow separation in these structures causes pressure drop to be a function of flow direction. A micropump with 4 mm long nozzles with small and large diameters of 230 μm and 600 μm, respectively, pumps water with $Q_{max} = 4.4\ ml\ min^{-1}$ and $\Delta p_{max} = 20.6$ kPa at $f = 110$ Hz and $V = 20$ V. An otherwise-identical micropump with 3 mm long nozzles with small and large diameters of 530 μm and 1.1 mm, respectively, pumps water with $Q_{max} = 15.5\ ml\ min^{-1}$ and $\Delta p_{max} = 4.9$ kPa at $f = 310$ Hz.

Olsson *et al* reported a miniature brass pump with planar nozzle-diffuser elements [88]. A pump with this design and two pumping chambers produced $Q_{max} = 16\ ml\ min^{-1}$ and $\Delta p_{max} = 100$ kPa. In 1995, Gerlach reported a nozzle-diffuser micropump produced by micromachining silicon [179]. Much smaller than the brass pumps that preceded it ($S_p \cong 0.2\ cm^3$), this piezo-driven micropump pumps water with $Q_{max} = 400\ \mu l\ min^{-1}$ and $\Delta p_{max} = 3$ kPa at $f = 3$ kHz and $V = 50$ V. Forster *et al* [180] reported reciprocating displacement micropumps in which tesla valves, rather than the more widely used nozzle-diffuser structures, rectify the flow. A number of other micropumps with fixed-geometry valves have been reported, including those of Koch *et al* [113–115] and Jeong and Yang [127].

The absence of moving structures in fixed-geometry valves may be advantageous when the working fluid contains cells or other materials prone to damage or clogging. In 1999, Jang *et al* [181] reported pumping suspensions of polystyrene beads as large as 20 μm through piezo-driven reciprocating displacement micropumps with tesla-type fixed-geometry valves. Andersson *et al* [182] subsequently reported pumping liquid samples containing beads through a piezo-driven reciprocating displacement micropump with nozzle-diffuser valves. Recent studies discuss fixed-geometry valves in greater detail [74, 183–187].

Intriguing alternatives to the traditional valves used in micropumps have been proposed. Liu *et al* [188] reported using hydrogel swelling in response to changes in environmental chemistry to restrict flow through microchannels or close them off entirely. Matsumoto *et al* [189] reported a piezo-driven micropump in which temperature-induced viscosity changes at the inlet and outlet rectify the flow. Yun *et al* [190] proposed using electrohydrodynamic effects to improve the performance of fixed-geometry valves. Hasselbrink *et al* [191] reported the use of *in situ* polymerized plugs which act as piston in a passive check valve. This valve has an impressive open/closed flow ratio of 10^6 at pressures as high as 700 kPa.

2.1.7. Dynamic effects. Dynamic effects are relevant to the operation of many reciprocating displacement micropumps, particularly those with high-frequency drivers. Dynamic effects are routinely leveraged to maximize performance by operating at dynamically favorable conditions determined by the mechanical system/fluid system coupling. These dynamic conditions are a function of pump geometry, operating conditions and load conditions and can lead to substantial gains in performance. Recent papers have suggested that this approach is particularly effective for micropumps with fixed-geometry valves [67, 73]. As mentioned earlier, dynamic effects often cause flow reversal in micropumps with flap valves operated at high frequencies [85, 90]. For dynamic effects to be relevant to the operation of a reciprocating displacement micropump, the operation of the micropump must be such that (i) the operating frequency is on the order of (or greater than) the mechanical resonant frequency of the diaphragm and/or (ii) inertial effects in the fluid are important [47]. Figure 9 shows the importance

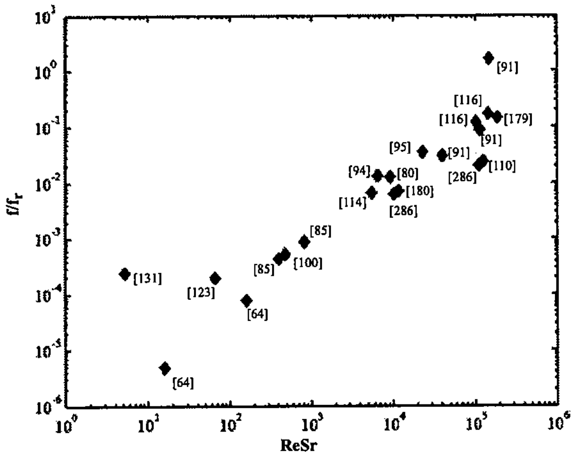

Figure 9. Dynamic effects in reported reciprocating displacement micropumps. The product of the Reynolds number *Re* and the Strouhal number *Sr* indicates the importance of fluid inertia in low *Re* flows. The ratio of the operating frequency f and the diaphragm resonant frequency f_r indicates the extent to which dynamic effects are relevant in the diaphragm mechanical response. Higher values of f/f_r and lower Re^*Sr is indicative of a micropump performance-limited by the mechanical time constant of the pump driver and/or diaphragm. Lower values of f/f_r and higher Re^*Sr are associated with pumps where fluid inertia is particularly important. Multiple data points shown for micropumps tested with more than one working fluid and/or at more than one operating frequency.

of dynamic effects in reported reciprocating displacement micropumps with simple diaphragm geometries. The ratio of the operating frequency f and the approximate diaphragm resonant frequency f_r (calculated from the reported diaphragm geometry and material properties using equation (3)) is plotted against the product of the Reynolds and Strouhal numbers. High values along either axis imply that the pump is operating in a regime where dynamic effects are important. A number of papers discuss dynamic effects in reciprocating displacement micropumps further [67, 90, 136, 161].

2.2. *Rotary displacement micropumps*

A small number of microscale rotary displacement pumps, mostly micro gear pumps, have been reported. Microfabricating released gear structures is achievable, but minimizing the gaps between the gears and the housing, through which backflow can occur, is a major challenge. Dopper *et al* [192] reported a gear micropump fabricated by LIGA and driven by a small electromagnetic motor. Two opposing in-line gears, 0.6 mm in diameter, pump a glycerin–water solution with $Q_{\max} = 180\ \mu\text{l min}^{-1}$ and $\Delta p_{\max} = 100$ kPa operating at 2250 rpm. The back pressure against which a gear pump can operate generally scales with the inverse of viscosity, making these pumps best suited for use with moderately high-viscosity liquids. Dopper *et al* tested a slightly larger gear pump (gear diameter 1.2 mm) with both the glycerine–water solution and with pure water. With this solution, $Q_{\max} = 190\ \mu\text{l min}^{-1}$ and $\Delta p_{\max} = 100$ kPa, while for pure water $Q_{\max} = 5.5\ \mu\text{l min}^{-1}$ and $\Delta p_{\max} = 2.4$ kPa. A gear micropump made of PMMA and also fabricated by LIGA was reported by Dewa *et al* [193]. The use of external motors with gear pumps limits the prospects for true miniaturization; the gear pump reported by Dopper *et al*, for example, is $S_p = 3\ \text{cm}^3$ in size. As an alternative to using an external motor, a planetary gear micropump driven by surface micromachined electrostatic comb drives has been reported [194, 195]. Terray *et al* [196] reported a gear micropump based on optically trapping 3 μm diameter colloidal silica. Several microspheres are arranged into a two-lobe gear within a fluid chamber. The microspheres are controlled individually by rapidly scanning a laser between the microspheres. This system produces a flow rate of around 1 nl h^{-1}. Flow generation through eccentric rotation of a cylinder in a microchannel has been proposed [197, 198].

Hatch *et al* [199] reported a micropump based on manipulating a ferrofluidic plug with an external magnet. The plug pushes the working fluid in front of it as it circulates through a closed path; inlet and outlet ports along the path produce net flow of the working fluid. This manner of operation resembles that of macroscale vane pumps. Key issues for such pumps include ensuring the immiscibility of the ferrofluidic plug and liquid being pumped; degradation of the ferrofluid over time; and the need to incorporate an external controller for the magnet.

2.3. *Aperiodic displacement micropumps*

A number of micropumps have been reported in which a moving surface or boundary exerts pressure on the working fluid, but in which the movement of the pressure surface is not generally reciprocating or otherwise periodic. These aperiodic displacement micropumps tend to be suitable only for pumping finite volumes of fluid. Aperiodic displacement pumping driven by a reservoir of compressed gas is used in the miniature implanted insulin delivery system marketed by Medtronic [23]. Electronically controlled solenoid-driven valves control the release of insulin from the secondary chamber, through a tube, and into diabetic's intraperitoneal cavity; the pressure reservoir is recharged when the device is refilled with insulin. The implanted device occupies a volume of over 50 cm^3. Sefton *et al* [200] discuss implanted pumps in detail. A valved pressure source is also the basis of a flow cytometry system under development by Cabuz *et al* [201] of the Honeywell Corporation. This device includes a 2 cm^3 pressurized chamber and produces regulated flow at around 50 μl min^{-1} against unspecified back pressure. The Honeywell device exemplifies both the advantages and the disadvantages of pneumatic aperiodic displacement pumps. The pump is inherently low power and robust, but requires closed-loop control because the driving pressure varies over time. A means of recharging the pressure source is required for long-term use. The inherently unidirectional flow produced by the pressure source is converted to bidirectional flow using active valves—increasing the versatility of the pump, but at a substantial cost in complexity.

Pneumatically driven aperiodic displacement pumping is readily implemented at the microscale. Interfacial tension effects often take the place of traditional moving surfaces for applying pressure on the working fluid [12]. Tas *et al* [202] reported an aperiodic displacement micropump based on injecting bubbles into a microchannel through a port midway along its length. Axial variations in surface tension due to discontinuities in the microchannel height produce net flow. Producing bidirectional flow at the microscale with valved pressure reservoirs is discussed by Jen and Lin [203].

Aperiodic displacement micropumps based on thermal or electrochemical phase change have also been reported. Evans *et al* [204] demonstrated an aperiodic displacement micropump based on locally boiling the liquid in a closed-end microchannel. A similar approach was taken by Handique *et al* [205], producing $Q_{max} = 20$ nl min^{-1}. Jun *et al* [206] and Song *et al* [207] reported using arrays of heating elements to generate flow in channels open on both ends. Several other aperiodic displacement micropumps based on phase change have been reported [208–210]. Lin *et al* [211] discusses thermal bubble formation in micromachined devices in detail.

Electrical control of interfacial tension was proposed as a microscale pumping mechanism by Matsumoto and Colgate [212, 213]. Electrowetting-driven aperiodic displacement micropumps and other electrowetting-based microfluidic devices have since been developed [214, 215]. A related class of micropumps based on thermocapillary effects has also been reported [216, 217]. Osmosis has been used as an aperiodic displacement pumping mechanism [218, 219]. Aperiodic pumping based on the interaction of local electric fields with DNA has been reported [220].

3. Dynamic micropumps

Centrifugal pumps are the most common type of traditional dynamic pump. Extensive miniaturization of centrifugal pumps has been precluded, however, by typically unfavorable scaling of efficiency with decreasing Reynolds number [221] and the limitations of microfabrication technologies. Microturbines with $S_p < 1$ cm^3 have been explored for applications such as microrocketry [222–225]. Axial flow pumps may generally be favored for other applications, particularly in space exploration, involving primarily gas phases. Miniature axial flow pumps are also being developed for certain biological applications [226].

There are a variety of alternatives to rotating machinery for continuously adding momentum (or directly imparting Lorentz forces into the fluid volume) at the microscale. Electrohydrodynamic, electroosmotic and magnetohydrodynamic micropumps are all based on interactions between the working fluid and an electromagnetic field. An additional category of dynamic micropumps are those which generate flow through acoustic effects. Key features and the performance of reported dynamic micropumps are summarized in table 2.

3.1. Electrohydrodynamic micropumps

Electrohydrodynamic micropumps are based on the interaction of electrostatic forces with ions in dielectric fluids. The electric body force density F_e that results from an applied electric field with magnitude E is given by

$$F_e = qE + P \cdot \nabla E - \frac{1}{2}E^2\nabla\varepsilon + \frac{1}{2}\nabla\left[E^2\left(\frac{\partial\varepsilon}{\partial\rho}\right)_T\rho\right] \quad (7)$$

where q is the charge density, ϵ is the fluid permittivity, ρ is the fluid density, T is the fluid temperature and P is the polarization vector [227]. Several EHD micropumps based on the Coulomb force acting on free charges in a field, represented by the qE term in equation (7), have been reported. Operation of these micropumps requires the existence of space charge in a dielectric fluid. Space charge can be produced because of inhomogeneities in the fluid, or through dissociation or direct charge injection. These three mechanisms for space charge generation are associated with *induction*, *conduction*, and *injection* EHD pumping, respectively.

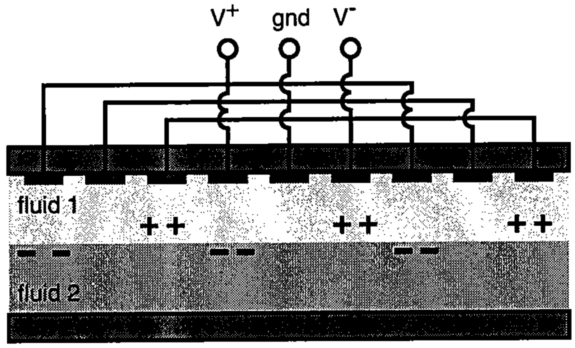

Figure 10. One type of traveling-wave (induction) electrohydrodynamic pump. Arrays of electrodes capacitively induce mirror charges at the interface between two fluids. Sequential switching of the electrode arrays results in net fluid flow.

In *induction* EHD pumps, charge is induced in an inhomogeneous working fluid through the application of a potential difference across the fluid. This can, for example, be achieved with an electric field with a component transverse to the flow direction, as shown in figure 10. The electrodes are then activated in a traveling wave configuration and axial components of the electric field result in net fluid flow. Bart *et al* [228] reported an induction EHD micropump that pumps silicone oil. Quantitative performance measures were not reported. Fuhr *et al* [229] reported an EHD micropump based on traveling waves applied to arrays of electrodes. Instead of inducing charge at an interface and relying on Coulomb forces, however, Fuhr's device uses the dielectric force that results from the application of an electric field to a fluid containing a permittivity gradient (see the third term in equation (7)). This pump generates $Q_{max} = 2$ µl min^{-1} operating at $V = 40$ V.

Applying a weak electric field (much less than 100 kV cm^{-1}) between electrodes immersed in a dielectric fluid causes dissociation of ionizable groups at the electrode/fluid interface. Coulomb forces acting on the ions produced through such dissociation give rise to conduction through the bulk liquid. *Conduction* EHD pumps rely on ion drag associated with this bipolar conduction [230, 231]. To our knowledge, no micropumps based on conduction EHD pumping have been reported, although a conduction EHD pump with high voltage-ground electrode modules 2.2 cm diameter by 4 cm long was reported by Jeong and Seyed-Yagoobi [230].

EHD micropumps based on the injection of ions into the working fluid at electrodes have also been reported. For specific electrode/liquid interfaces (typically a metal electrode with sharp features in contact with a dielectric liquid), application of a very high electric field (>100 kV cm^{-1})

Table 2. Dynamic micropumps.

Author and year	Description	Construction	Working fluid	Approximate size (mm^3)	Operating voltage (V)	Δp_{max} (kPa)	Q_{max} (ml min^{-1})
Richter 1991 [232]	Electrohydrodynamic (injection)	Si–Si	Ethanol	10	600	0.43	14
Fuhr 1994 [229]	Electrohydrodynamic (induction)	Si–glass	Water	n/r	40	n/r	0.002
Furuya 1996 [287]	Electrohydrodynamic (injection)	Polyimide	Ethanol	n/r	200	n/r	0.00012
Wong 1996 [233]	Electrohydrodynamic (injection)	Si–Si	Propanol	70	120	0.29	
Ahn 1998 [234]	Electrohydrodynamic (injection)	Si–glass	Ethyl alcohol	90	100	0.25	0.04
Darabi 2001 [236]	Electrohydrodynamic (polarization)	Quartz	R-134a (refrigerant)	250	120	0.25	n/r
Darabi 2002 [235]	Electrohydrodynamic (injection)	Ceramic	3M HFE-7100	640	250	0.78	n/r
Jacobson 1994 [247]	Electroosmotic (microchannel)	Glass	Water	n/a	2700	n/a	0.00002
Ramsey 1997 [249]	Electroosmotic (micromachined)	Glass	Water/methanol	1 250	2000	n/r	0.00009
Paul 1998 [251]	Electroosmotic (porous media)	Packed silica particles	80:20 acetonitrile:water with 4 mM aqueous sodium tetraborate buffer	120	1500	4000	0.00004
					6750	20 000	0.0002
Gan 2000 [260]	Electroosmotic (porous media)	Sintered glass beads	NH_4OH (0.35 mM)		500	150	3.0
McKnight 2001 [250]	Electroosmotic (microchannel)	PDMS-glass	TBE buffer (Tris, boric acid, EDTA)	n/a	40	0	5.4×10^{-6}
Yao 2001 [285]	Electroosmotic (porous media)	Sintered glass frit	Borate buffer	3800	200	250	7.0
Zeng 2001 [254]	Electroosmotic (porous media)	Packed silica particles	Water	85	2000	2000	0.0036
Takamura 2001 [266]	Electroosmotic (micromachined)	Quartz	Phosphate buffer	n/r	40	5.0	n/r
Chen 2002 [259]	Electroosmotic (micromachined)	Soda-lime glass	Water	9000	1000	33	0.015
Laser 2002 [255]	Electroosmotic (micromachined)	Si–glass	Borate buffer	120	400	10	0.014
Zeng 2002 [261]	Electroosmotic (porous media)	Packed silica particles	Water	1200	1250	250	0.9
Laser 2003 [26]	Electroosmotic (micromachined)	Si–glass	Borate buffer	120	400	10	0.17
Yao 2003 [256]	Electroosmotic (porous media)	Sintered glass frit	Borate buffer	9500	100	130	33
Jang 2000 [272]	Magnetohydrodynamic (DC)	Si–Si	Seawater	n/r	n/a	0.17	0.063
Lemoff 2000 [273]	Magnetohydrodynamic (AC)	Glass–Si–glass	1 M NaCl solution	n/r	n/a	0	0.018

n/a: not applicable; n/r: not reported.

causes ions to be injected into the bulk fluid. The Coulomb force acts on the injected charges; viscous interaction generates bulk flow. Richter *et al* reported a micromachined electrohydrodyamic micropump based on such charge injection [232]. The electrodes are mesh structures made by wet etching and metallizing a single-crystal silicon substrate. The electrode grids are separated by a distance of approximately 350 μm, across which an electrical potential difference of 600 V is applied. This micropump pumps ethyl alcohol with $Q_{max} = 14$ ml min^{-1} and $\Delta p_{max} = 2.5$ kPa. Charge injection with a similar electrode design is the basis for an EHD micropump reported by Wong that produces $\Delta p_{max} = 290$ Pa operating at $V = 120$ V with isopropyl alcohol as the working fluid [233]. Ahn and Kim reported an EHD micropump with multiple pairs of electrodes arrayed in the direction of flow [234]. This micropump produces $Q_{max} = 40$ μl min^{-1} and $\Delta p_{max} = 300$ Pa operating at $V = 100$ V with ethyl alcohol as the working fluid. Darabi *et al* reported an injection EHD micropump with transverse electrode pairs arrayed in the direction of flow [235]. The gap between the two electrodes in each pair is 50 μm; the pairs are spaced at 100 μm intervals. For this micropump, $S_p = 640$ mm^2. With 3M HFE-7100 ($\varepsilon_R = 7.4$) as the working fluid, this micropump produced $\Delta p_{max} = 2.5$ kPa; flow rate data was not reported. The use of electrodes with saw-tooth geometries was reported to reduce power consumption relative to linear electrodes.

Another category of EHD micropumps is those based on the polarization force term in equation (7) rather than on the Coulomb force. Darabi *et al* reported such a polarization EHD pump intended for microelectronics cooling applications that generates flow through electric field interactions with dipoles in a polarized medium [236]. The polarization-dependent functionality of this pump permits operation at relatively low voltages (150 V) and with a nondielectric working fluid (R-134a, chosen for its thermal properties). This EHD polarization micropump pumps the cooling liquid through a 250 Pa pressure difference; further details of pump performance were not reported. Other papers discuss EHD pumping [237, 238].

3.2. Electroosmotic micropumps

Electroosmotic (EO) pumping leverages the surface charge that spontaneously develops when a liquid comes in contact with a solid [239, 240]. Bulk liquid counter-ions shield this surface charge, completing the so-called electrical double layer (EDL). The characteristic thickness of the electric double layer is the Debye shielding length, λ_D, of the ionic solution, given by

$$\lambda_D = \left[\frac{\varepsilon k T}{e^2 \sum_i z_i n_{\infty,i}}\right]^{\frac{1}{2}}. \quad (8)$$

Here ε and T are the electrical permittivity and temperature of the solution, respectively; z_i and $n_{\infty,i}$ are the valence number and number density, respectively, of the ionic species i in solution; k is the Boltzmann constant; and e is the electron charge. Some portion of the counter-ions in the liquid phase of the EDL can be set into motion by applying an electric field parallel to the wall. The mobile ions drag bulk liquid in the direction of the electric force. In the case of silica-based ceramics (e.g., glass) at pH greater than about 4, surface silanol groups deprotonate and leave a negative surface charge [240]. Bulk flow is therefore induced in the direction of the electric field. This phenomenon is illustrated in figure 11 and discussed in detail by Probstein [76].

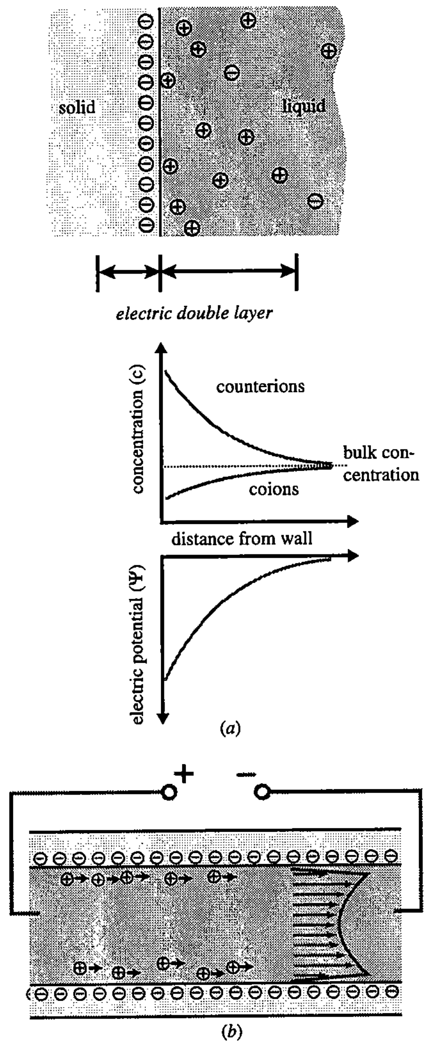

Figure 11. Electrochemistry of a solid–liquid interface and electroosmotic flow. (*a*) Chemical reactions at the interface leave the surface charged (shown as negative here). Counter ions in the liquid accumulate in the vicinity of the charged surface, forming the electric double layer. (*b*) An externally applied electric field causes motion of counter ions that shield a negative wall charge. Ion drag forces the flow against a pressure gradient.

The key parameters that dictate the performance of EO pumps are (i) the magnitude of the applied electric field and applied voltage, (ii) the cross-sectional dimensions of the structure in which flow is generated, (iii) the surface charge density of the solid surface that is in contact with the working liquid and (iv) ion density and pH of the working fluid. Rice and Whitehead's analysis of EO flow in a cylindrical capillary [241] shows how these parameters relate to EO pump performance. In a capillary of radius a and length l, the flow rate Q that results from applying a uniform axial electric field E_z is given by

$$Q = \frac{\pi a^4}{8\mu l}\Delta p - \frac{\pi a^2 \varepsilon \zeta E_z}{\mu} f(a/\lambda_D). \qquad (9)$$

Here μ is the viscosity of the liquid and Δp is the differential pressure from one end of the capillary to the other. The zeta potential, ζ, is the potential drop associated with the mobile region of counter-ions that shield the surface charge at the wall. The theoretical maximum flow rate and pressure that can be generated are

$$Q_{\mathrm{max,EO}} = -\frac{\pi a^2 \varepsilon \zeta E_z}{\mu} f(a/\lambda) \qquad (10)$$

and

$$\Delta p_{\mathrm{max,EO}} = \frac{8\varepsilon\zeta E_z l}{a^2} f(a/\lambda_D). \qquad (11)$$

For the simple case of a cylindrical capillary with a symmetric, univalent electrolyte and a zeta potential smaller than kT/e, $f(a/\lambda_D)$ can be expressed as

$$f(a/\lambda_D) = 1 - \frac{2}{a/\lambda_D}\frac{I_1(a/\lambda_D)}{I_0(a/\lambda_D)}, \qquad (12)$$

where I_0 and I_1 are, respectively, the zero-order and first-order modified Bessel functions of the first kind. This term arises from the finite effects of electrical double layers with Debye lengths comparable to the capillary radius. In the thin double layer limit where $(a/\lambda_D) \gg 1$, $f(a/\lambda_D)$ monotonically approaches unity. For capillary radii smaller than the thickness of the double layer, $f(a/\lambda_D)$ approaches $\frac{1}{8}(a/\lambda_D)^2$. For thin EDLs ($f \approx 1$) and a given working liquid and zeta potential, pressure per volt scales as a^{-2} and flow rate per unit electric field strength scales as the total cross-sectional area of the EO pumping channel. For a given working fluid, wall chemistry, and pump geometry, both maximum flow rate and maximum pressure are linear functions of applied voltage.

EO flow (as distinguished from EO pumping, in which the device generates both flow rate and a significant pressure) is used in a wide range of applications, including soil remediation, and has been used in chemical and biological analysis since at least 1974 [242]. A number of important techniques and processes used for μTAS incorporate EO flow, including electroosmosis-based microchannel flow injection analysis [243], on-chip electrophoretic separation [1, 244–246] and on-chip liquid chromatography [247].

The most basic EO pumps are simply capillaries or microchannel sections (either filled with porous media or filled only with liquid) with electrodes submerged within end-channel reservoirs and a flow resistance in series with the channel [248–250]. The flow rates produced by such pumps are typically very small ($Q_{\mathrm{max}} < 1\ \mu$l min^{-1}). For example, Ramsey and Ramsey applied a 350 V cm^{-1} electric field to a portion of a microchannel network to produce roughly 90 nl min^{-1} flow out of the chip through an exit port [249]. An EO micropump incorporating a 75 μm ID fused silica capillary packed with silica beads was reported by Paul *et al* [251, 252]. This pump produced only $Q_{\mathrm{max}} = 200$ nl min^{-1}, but exceptionally high pressures—reportedly up to 20 MPa—at an applied voltage of $V = 6.75$ kV. A detailed description of the history and development of EO pumps is presented by Yao and Santiago [253].

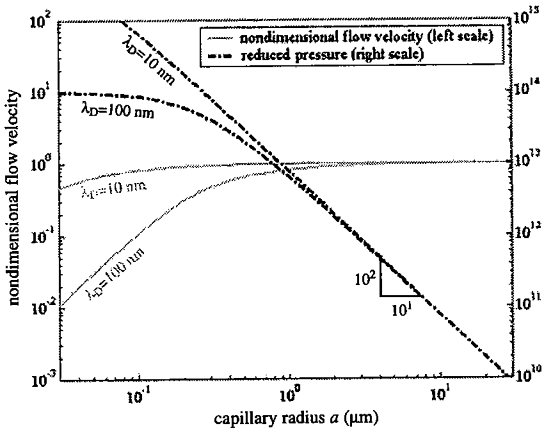

Figure 12. Theoretical performance of electrosmotic pumps with flow passages resembling cylindrical tubes. Scaling, as a function of cylindrical tube radius a, is shown for nondimensional flow velocity ($= -Q_{\mathrm{max}} \cdot \mu/(\pi a^2 n\varepsilon\zeta E_z)$) and reduced pressure ($= \Delta p_{\mathrm{max}} \cdot 1/(8\varepsilon\zeta E_z l)$). Scaling is for ionic solutions with Debye lengths $\lambda_D = 10$ nm (e.g., a 100 mM electrolyte) and $\lambda_D = 100$ nm (e.g., a 1 mM electrolyte). For $a/\lambda_D \ll 1$, this reduced pressure scale approaches an a^{-2} dependence associated with thin electrical double layers and nondimensional flow velocity approaches the theoretical maximum of unity. For $a/\lambda_D \cong 1$, finite EDL effects reduce both flow rate and pressure. Figure describes flow in a single tube. In practice, electroosmotic pumps use many small flow passages in parallel to achieve both high pressure and high flow rate.

Production of higher flow rates using EO pumping generally requires structures with larger dimensions in the directions normal to the flow than are found in single channels or capillaries. These pumps typically incorporate porous structures in which each pore acts as a tortuous capillary for generating EO flow. These pumps can be modeled as a bundle of n capillaries [253–255]. In figure 12, $Q_{\mathrm{max,EO}}$ (normalized by multiplying by $-\mu/(n\pi a^2\varepsilon\zeta E_z)$) (where n is the number of EO pumping channels in parallel) and $\Delta p_{\mathrm{max,EO}}$ (normalized by multiplying by $1/(8\varepsilon\zeta E_z l)$) are plotted as a function of capillary radius a for Debye lengths λ_D of 10 nm and 100 nm. Small λ_D operation allows high-pressure performance without a reduction in area-specific flow rate. However, decreasing λ_D via increases in ion density also increases the ionic current through the pump and thereby lowers thermodynamic efficiency. This tradeoff is a major consideration for practical implementations of EO pumping. The choice of working fluid also affects zeta potential, important to both pressure and flow rate performance. Zeta potential is a strong function of pH (although typically saturating in magnitude at high and low pH values), and a weaker function of ion density [239]. A simple relation for zeta potential as a function of pH and ion density for silica surfaces is presented by Yao *et al* [256]. This relation is a fit to a model by Yates *et al* [257], which was more recently experimentally validated by Scales *et al* [258]. Together, the effects of ion density on normalized flow rate, pressure and current performance result in an optimum value of thermodynamic efficiency for EO pumping. This optimization and other aspects of EO pump design and theory are discussed in detail by Chen and Santiago [259], Yao and Santiago [253] and Yao *et al* [256] for planar and porous-media pumps.

Operating voltages and geometries of high-flow rate EO pumps vary widely. Useful metrics for describing their performance are the maximum pressure normalized by applied voltage, $\Delta p_{\max,V}$ (kPa V^{-1}), and the maximum flow rate normalized by applied voltage and flow cross-sectional area, $Q_{\max,V,A}$ (μl min^{-1} V^{-1} cm^{-2}). Gan *et al* reported $\Delta p_{\max,V} = 0.3$ kPa V^{-1} and $Q_{\max,V,A} = 0.6$ μl min^{-1} V^{-1} cm^{-2} with a 3.5 cm inner diameter (ID) pump using a bed of sintered glass beads as a porous pumping medium [260]. Zeng *et al* [254] reported using large (500 μm to 700 μm diameter) capillaries packed with silica particles to produce $\Delta p_{\max,V} = 1$ kPa V^{-1} and $Q_{\max,V,A} = 1$ μl min^{-1} V^{-1} cm^{-2}. Maximum thermodynamic efficiency is $\eta = 1.3\%$. An EO micropump in which a 1 cm diameter porous polymer frit holds a bed of silica particles in place produced $\Delta p_{\max,V} = 0.2$ kPa V^{-1} and $Q_{\max,V,A} = 1$ μl min^{-1} V^{-1} cm^{-2} [261]. Yao *et al* [256] reported a pump in which EO flow is generated in a 4 cm diameter (1 mm thick) sintered glass frit. This pump produces $\Delta p_{\max,V} = 1.3$ kPa V^{-1} and $Q_{\max,V,A} = 26$ μl min^{-1} V^{-1} cm^{-2}. The absolute $\Delta p_{\max}$ and $Q_{\max}$ for the latter pump are 130 kPa and 33 ml min^{-1} operating at $V = 100$ V; maximum thermodynamic efficiency is $\eta = 0.3\%$.

A different approach to boosting flow rate was taken by Chen and Santiago, who used glass micromachining to fabricate a miniature EO pump consisting of a single channel 4 cm wide and 1 mm long in the flow direction, but only 1 μm deep [259, 262]. A detailed analysis of EO flow in this geometry is given by Burgreen and Nakache [263], and Chen and Santiago present an analysis of thermodynamic efficiency of this structure. Pressure generation is a function of the small (1 μm) gap height in this structure, which yielded $\Delta p_{\max,V} = 0.03$ kPa V^{-1}. Narrow structural ribs are the only obstruction in the flow direction, so this pump produces a high normalized flow rate of $Q_{\max,V,A} = 42$ μl min^{-1} V^{-1} cm^{-2}. The absolute $\Delta p_{\max}$ and $Q_{\max}$ for this micropump are 33 kPa and 15 μl min^{-1} operating at $V = 1$ kV; maximum thermodynamic efficiency is $\eta = 0.49\%$. Silicon micropumps based on the EO flow generated in narrow slots have also been reported [26, 255, 264]. Although the silicon substrate precludes use of voltages greater than a few hundred volts (to avoid breakdown of passivation layers), the capabilities of silicon micromachining make possible a high degree of geometrical optimization. A micropump with a 1 cm wide $\times$ 150 μm deep $\times$ 100 μm long pumping region containing 500 parallel etched slots produces $\Delta p_{\max,V} = 0.03$ kPa V^{-1} and $Q_{\max,V,A} = 53$ μl min^{-1} V^{-1} cm^{-2} operating at $V = 400$ V. The absolute $\Delta p_{\max}$ and $Q_{\max}$ for this micropump are 10 kPa and 170 μl min^{-1}; maximum thermodynamic efficiency is $\eta = 0.01\%$. Other implementations of EO pumping at the microscale have been reported [265–271].

3.3. Magnetohydrodynamic pumps

Several magnetohydrodynamic micropumps have been reported in which current-carrying ions in aqueous solutions are subjected to a magnetic field to impart a Lorentz force on the liquid and induce flow. A typical magnetohydrodynamic pump is shown in figure 13. In a rectangular channel with transverse current density J_y and perpendicular transverse magnetic flux density B_x, the maximum pressure is

$$P_{\max,\mathrm{MHD,th}} = J_y B_x l \tag{13}$$

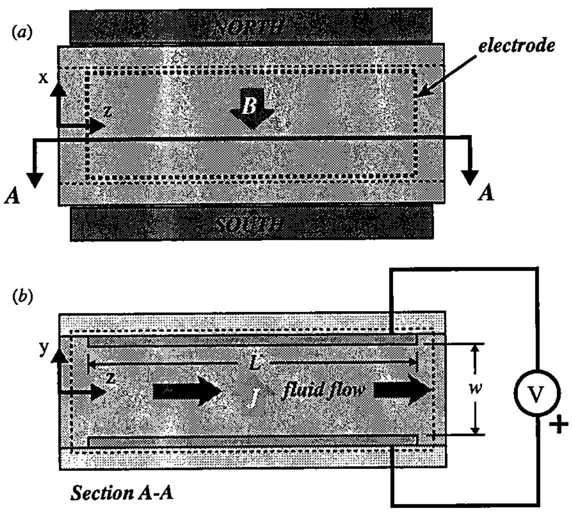

Figure 13. Top view (*a*) and section view (*b*) schematics of a simple magnetohydrodynamic micropump. A transverse magnetic field exerts a Lorentz force ($\vec{F} = \vec{J} \times \vec{B}w$) on current-carrying ions flowing across the channel, producing flow in the axial direction.

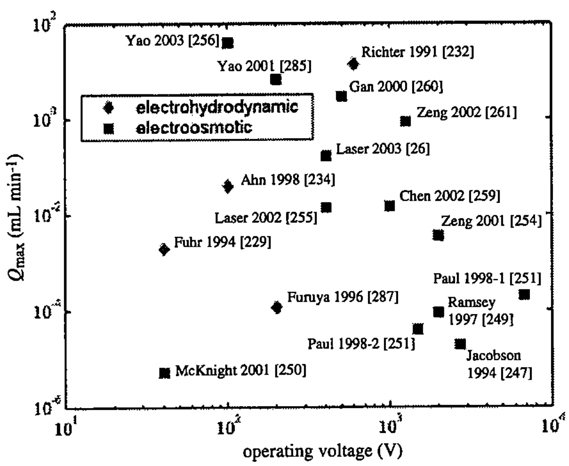

Figure 14. $Q_{\max}$ for reported electrohydrodynamic and electroosmotic micropumps, plotted as a function of operating voltage V.

and the maximum flow rate is on the order of

$$Q_{\max,\mathrm{MHD,th}} = J_y B_x \frac{\pi D_h^4}{128\mu} \tag{14}$$

where l is the length of the pumping channel and D_h is its hydraulic diameter (cross-sectional area multiplied by 4 and divided by its perimeter). The performance of magnetohydrodynamic pumps is typically limited by the magnetic flux density (up to approximately 1 T for miniature permanent magnets or 0.1 T for miniature electromagnetic coils); the scaling of flow rate with the fourth power of hydraulic diameter makes miniaturization challenging. Also, thermal effects often limit current density.

Jang and Lee [272] reported a magnetohydrodynamic micropump with a 40 nm long pumping channel with hydraulic

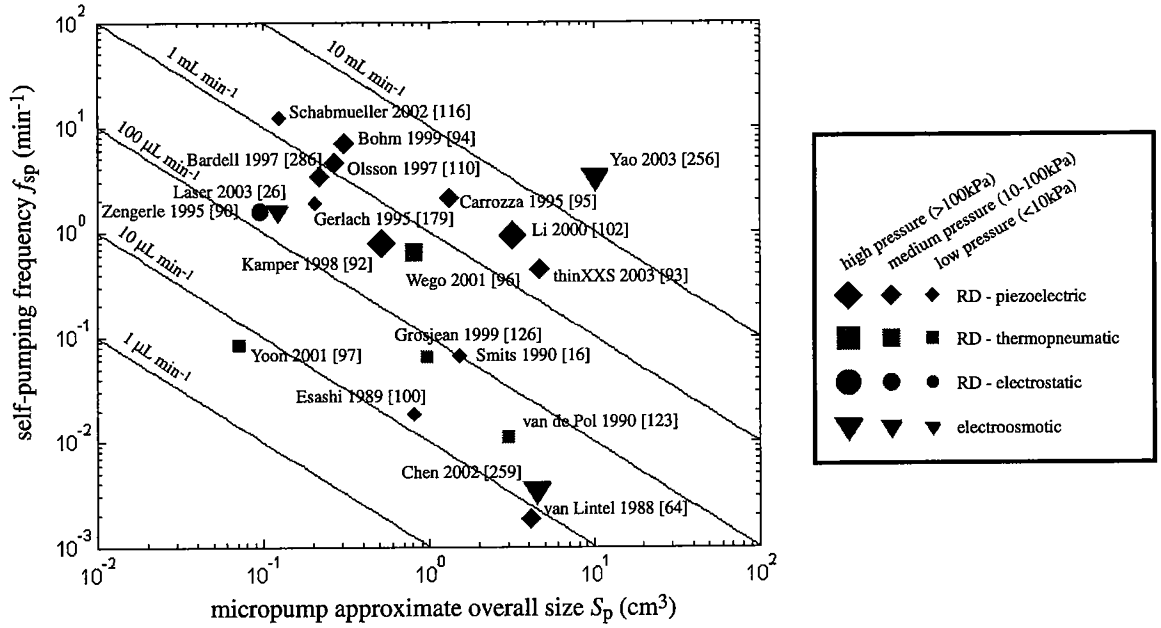

Figure 15. Comparison of several reported micropumps based on maximum flow rate, Q_{max}, maximum pressure Δp_{max}, and package size S_p. Self-pumping frequency is here defined as $f_{sp} = Q_{max}/S_p$.

diameter on the order of 1 mm. With permanent magnets producing a magnetic flux density of 0.44 T and total current between 1 and 100 μA, this pump produces $Q_{max} = 63\ \mu$l min^{-1} and $\Delta p_{max} = 170$ Pa. To avoid electrolysis associated with DC operation, Lemoff and Lee [273] used a miniature electromagnetic coil operating (along with the electric field) at 1 kHz. This micropump pumps a 1 M NaCl solution with $Q_{max} = 18\ \mu$l min^{-1}. Several papers have discussed microscale applications of magnetohydrodynamic effects [274–278].

3.4. Comparison of electrohydrodynamic, electroosmotic and magnetohydrodynamic micropumps

As with reciprocating displacement micropumps, various factors other than pressure and flow rate performance are relevant to the selection of a dynamic micropump. The magnitude of the electrical potential difference required to operate these field-driven micropumps is one important factor which can be compared directly and which varies widely. In figure 14, Q_{max} is plotted as a function of operating voltage for reported field-driven dynamic micropumps. Working fluid properties generally must also be taken into account in choosing a dynamic micropump. EO (and some magnetohydrodynamic) pumps can handle a wide range of working fluids, including many that are widely used in chemical and biological analysis such as deionized water and chemical buffers. In contrast, most EHD pumps require dielectric fluids. Electrolytic gas generation occurs at the electrodes of many field-driven dynamic micropumps. Lastly, current passing through the working fluid used in electrohydrodynamic, electroosmotic and magnetohydrodynamic pumps may, in some cases, cause significant Joule heating.

3.5. Other dynamic pumps

Net fluid flow can be induced by flexural waves propagating through a membrane in contact with the fluid. A micropump based on ultrasonic flexural plate waves was reported by Luginbuhl *et al* [279]. Piezoelectric actuators in this micropump operate at 2–3 MHz and actuate regions of a 2 × 8 mm membrane. A flow rate of $Q_{max} = 255$ nl min^{-1} was reported. Black and White [280] reported an ultrasonic flexural wave pump with a 2 × 8 mm membrane that produced $Q_{max} = 1.5\ \mu$l min^{-1}. The design and optimization of ultrasonic flexural wave pumps is further discussed in recent papers [281, 282]. Dynamic micropumps based on thermal transpiration have been reported [283, 284].

4. Comparison of reciprocating displacement micropumps and dynamic micropumps

As noted earlier, flow rate, pressure generation and overall size are important figures of merit for micropumps. Figure 15 compares reported micropumps of various types in terms of all three of these metrics (for papers where all three have been reported). S_p is plotted along the abscissa; estimates have been made in some cases based on available information. In the ordinance, Q_{max} is normalized by dividing by S_p, to give a self-pump frequency, f_{sp}. As shown in the legend, the size of the data point marker indicates the associated Δp_{max} range for each pump. A few observations may be made. The EO micropump reported by Yao *et al* [256] and the piezoelectric-driven reciprocating displacement micropump reported by Li *et al* [102] perform well in terms of absolute flow rate and pressure generation. The very different manufacturing process and operational nature of these pumps would likely dictate which is appropriate for a particular application. More compact piezo-driven reciprocating displacement micropumps deliver normalized flow rate performance superior to that of Li *et al*'s larger micropump, but generally at some cost in pressure generation. Given the comparatively high self-pumping frequency and small size of Zengerle *et al*'s electrostatically driven reciprocating displacement micropump [90], further research on electrostatic actuation for micropumps may be warranted. Thermopneumatically driven micropumps tend to produce low flow rates even relative to their size, as well as low $\Delta p_{\max}$, but this performance must be weighed against expected low manufacturing costs for these micropumps. Micromachined EO micropumps and reciprocating displacement micropumps of comparable size exhibit comparable performance.

5. Summary

Since the first micropumps were introduced in the early 1980s, progress in micropump development and analysis has been rapid. Reciprocating displacement micropumps, the most widely reported micropumps, have been produced with a wide variety of chamber configurations, valve types, drivers and constructions. Piezoelectrically driven reciprocating displacement micropumps have been the subject of particular attention and are now available commercially. Aperiodic displacement pumping based on localized phase change, electrowetting and other mechanisms are effective for transporting finite quantities of fluid in a generally unidirectional manner. Dynamic micropumps based on electromagnetic fields—electrohydrodynamic, electroosmotic and magnetohydrodynamic micropumps—are a subject of increasing interest. Electroosmotic micropumps are emerging as a viable option for a number of applications, including integrated circuit thermal management. As the reliability and ease of manufacture of micropumps improve, we can expect that micropumps will be increasingly used in a wide variety of systems in fields including life sciences, semiconductors and space exploration.

Acknowledgments

Many colleagues contributed knowledge, wisdom, and/or effort to the preparation of this review, for which the authors are grateful. We are particularly appreciative of Dr. Fred Forster's thought-provoking comments on an early draft and for Dr. Thomas Kenny's insights and encouragement throughout the paper's preparation. We also thank Dr. Alan Myers of Intel Corporation for useful discussion regarding silicon materials and microfabrication techniques.

Dan Laser's graduate study at Stanford was supported by a Semiconductor Research Corporation Graduate Fellowship and by funding from the Defense Advance Research Projects Agency. This work was also supported by funding from Intel Corporation with Drs Quat T Vu and Scott List as contract monitors.

References

[1] Manz A *et al* 1992 Planar chips technology for miniaturization and integration of separation techniques into monitoring systems: capillary electrophoresis on a chip *J. Chromatogr.* A **593** 253–8
[2] Woolley A T *et al* 1996 Functional integration of PCR amplification and capillary electrophoresis in a microfabricated DNA analysis device *Anal. Chem.* **68** 4081–6
[3] Khandurina J *et al* 2000 Integrated system for rapid PCR-based DNA analysis in microfluidic devices *Anal. Chem.* **72** 2995–3000
[4] Taylor M T, Nguyen P, Ching J and Petersen K E 2003 Simulation of microfluidic pumping in a genomic DNA blood-processing cassette *J. Micromech. Microeng.* **13** 201–8
[5] Zhang L *et al* 2002 Measurements and modeling of two-phase flow in microchannels with nearly constant heat flux boundary conditions *J. Microelectromech. Syst.* **11** 12–9
[6] Jiang L *et al* 2002 Closed-loop electroosmotic microchannel cooling system for VLSI circuits *IEEE Trans. Compon. Packag. Technol.* **25** 347–55
[7] Tuckerman D B and Pease R F W 1981 High-performance heat sinking for VLSI *IEEE Electron Device Lett.* **2** 126–9
[8] Liamos C T, Vivolo J A and Colman F C 1999 Small volume *in vitro* analyte sensor and methods *US Patent no.* 6,616,819
[9] Fan S-K, de Guzman P-P and Kim C J 2002 EWOD driving of droplet on $N \times M$ grid using single-layer electrode patterns *Proc. 2002 Solid-State Sensor, Actuator, and Microsystems Workshop (Hilton Head Island, SC)*
[10] Hobbs E D and Pisano A P 2003 Micro capillary-force driven fluidic accumulator/pressure source *Proc. Transducers '03 (Boston, MA)*
[11] Su Y-C and Lin L 2003 Geometry and surface assisted flow discretization *Proc. Transducers '03 (Boston, MA)*
[12] Burns M A *et al* 1998 An integrated nanoliter DNA analysis device *Science* **282** 484–7
[13] Blom M T *et al* 2002 A micro viscosity detector for use in miniaturized chemical separation systems *Proc. Micro Total Analysis Systems 2002 (Nara, Japan)*
[14] Kanai M *et al* 2003 Integrated micro chamber for living cell analysis with negligible dead volume sample injector *Proc. Transducers '03 (Boston, MA)*
[15] Selam J L, Micossi P, Dunn F L and Nathan D M 1992 Clinical trial of programmable implantable insulin pump for type I diabetes *Diabetes Care* **15** 877–85
[16] Smits J G 1990 Piezoelectric micropump with 3 valves working peristaltically *Sensors Actuators* A **21** 203–6
[17] Dash A K and Cudworth G C 1998 Therapeutic applications of implantable drug delivery systems *J. Pharmacol. Toxicol. Methods* **40** 1–12
[18] Coll J-L *et al* 1999 *In vivo* delivery to tumors of DNA complexed with linear polyethylenimine *Hum. Gene Ther.* **10** 1659–66
[19] Pickup J C, Keen H, Parsons J and Alberti K 1978 Continuous subcutaneous insulin infusion: an approach to achieving normoglycemia *Br. J. Med.* **1** 204–7
[20] Allen D G and Sefton M V 1986 A model of insulin delivery by a controlled release micropump *Ann. Biomed. Eng.* **14** 257–76
[21] Hanairebroutin H *et al* 1995 Feasibility of intraperitoneal insulin therapy with programmable implantable pumps in IDDM—a multicenter study *Diabetes Care* **18** 388–92
[22] Selam J L 2001 External and implantable insulin pumps: current place in the treatment of diabetes *Exp. Clin. Endocrinol. Diabetes* **109** S333–40
[23] Product information, Medtronic Minimed 2007 Implantable Insulin Pump System, www.minimed.com
[24] Semiconductor Industry Association 2001 International Technology Roadmap for Semiconductors
[25] Wang E N *et al* 2002 Micromachined jet arrays for liquid impingement cooling of VLSI chips *Proc. 2002 Solid State Sensor, Actuator, and Microsystems Workshop (Hilton Head, SC)*

[26] Laser D J *et al* 2003 Silicon electroosmotic micropumps for IC thermal management *Proc. Transducers '03 (Boston, MA)*
[27] Manz A and Becker H 1998 *Microsystems Technology in Chemistry and Life Science* (Berlin: Springer)
[28] Jakeway S C, de Mello A J and Russell E L 2000 Miniaturized total analysis systems for biological analysis *Fresnius J. Anal. Chem.* **366** 525–39
[29] Mathies R A *et al* 2002 Capillary array electrophoresis bioprocessors *Proc. 2002 Solid-State Sensor, Actuator, and Microsystems Workshop (Hilton Head Island, SC)*
[30] van der Schoot B H, Jeanneret S, van den Berg A and de Rooij N F 1992 A silicon integrated miniature chemical analysis system *Sensors Actuators* B **6** 57–60
[31] Wong C C, Flemming J H and Adkins D R 2002 Evaluation of mini/micro-pumps for micro-chem-lab *Proc. 2002 ASME Int. Mechanical Engineering Congress and Exposition (New Orleans, LA)*
[32] Clark R A, Hietpas P B and Ewing A G 1997 Electrochemical analysis in picoliter microvials *Anal. Chem.* **69** 259–63
[33] Grosvenor A L, Feltus A, Conover R C, Daunert S and Anderson K W 2000 Development of binding assays in microfabricated picoliter vials: an assay for biotin *Anal. Chem.* **72** 2590–4
[34] Li P C H and Harrison D J 1997 Transport, manipulation, and reaction of biological cells on-chip using electrokinetic effects *Anal. Chem.* **69** 1564–8
[35] Limbach P A and Meng Z 2002 Integrating micromachined devices with modern mass spectrometry *Analyst* **127** 693–700
[36] Terry S C, Jerman J H and Angell J B 1979 Gas-chromatographic air analyzer fabricated on a silicon wafer *IEEE Trans. Electron Devices* **26** 1880–6
[37] Mastrangelo C H, Burns M A and Burke D T 1998 Microfabricated devices for genetic diagnostics *Proc. IEEE* **86** 1769–87
[38] Feldman B *et al* 2000 FreeStyle: a small-volume electrochemical glucose sensor for home blood glucose testing *Diabetes Technol. Ther.* **2** 221–9
[39] Garcia M, Kirimoama S, Marlborough D, Leafasia J and Rieckmann K H 1996 Immunochromatographic test for malaria diagnosis *Lancet* **347** 1549
[40] Center for Disease Control and Prevention, Identification and diagnosis of parasites of public health concern: diagnostic procedures for blood specimens www.dpd.cdc.gov/DPDx/HTML/DiagnosticProcedures.htm
[41] Wiberg D, Eyre B, Shcheglov K, White V and Garkanian V 2001 Progress toward highly miniaturized vacuum pumps *2nd Workshop on Harsh-Environment Mass Spectrometry (St. Petersburg, FL)*
[42] Watson T J 1997 *Introduction to Mass Spectrometry* (Philadelphia, PA: Lippincott-Raven)
[43] DARPA Mesoscale Machines program documentation, www.darpa.mil/dso/trans/mesomach/pump/sarcos
[44] Micci M M and Ketsdever A D 2000 *Micropropulsion for Small Spacecraft* (Reston, VA: American Institute of Aeronautics and Astronautics)
[45] Bruschi P, Diligenti A and Piotto M 2002 Micromachined gas flow regulator for ion propulsion systems *IEEE Trans. Aerosp. Electron. Syst.* **38** 982–8
[46] Krutzch W C and Cooper P 2001 Introduction: classification and selection of pumps *Pump Handbook* ed I J Karassik *et al* (New York: McGraw-Hill)
[47] Deen W M 1998 *Analysis of Transport Phenomena* (New York: Oxford University Press)
[48] Beck W W 2001 Pump testing *Pump Handbook* ed I J Karassik *et al* (New York: McGraw-Hill)
[49] Shoji S and Esashi M 1994 Microflow devices and systems *J. Micromech. Microeng.* **4** 157–71
[50] Woias P 2001 Micropumps—summarizing the first two decades *Microfluidics and BioMEMS* ed Mastrangelo and Becker, *Proc. SPIE* **4560** pp 39–52
[51] Nguyen N T, Huang X Y and Chuan T K 2002 MEMS-micropumps: a review *Trans. ASME, J. Fluids Eng.* **124** 384–92
[52] Reyes D R, Iossifidis D, Auroux P A and Manz A 2002 Micro total analysis systems: 1. Introduction, theory, and technology *Anal. Chem.* **74** 2623–36
[53] Auroux P A, Iossifidis D, Reyes D R and Manz A 2002 Micro total analysis systems: 2. Analytical standard operations and applications *Anal. Chem.* **74** 2637–52
[54] Gravesen P, Branebjerg J and Jensen O S 1993 Microfluidics—a review *J. Micromech. Microeng.* **3** 168–82
[55] van den Berg A and Lammerink T S J 1998 Micro total analysis systems: microfluidic aspects; integration concept and applications *Top. Curr. Chem.* **194** 21–49
[56] Koch M, Evans A and Brunnschweiler A 2000 *Microfluidic Technology and Applications* (Hertfordshire: Baldock)
[57] Polson N A and Hayes M A 2001 Microfluidics: controlling fluids in small places *Anal. Chem.* **73** 312A–9A
[58] Nguyen N T and Wereley S 2002 *Fundamentals and Applications of Microfluidics* (Boston, MA: Artech House, International)
[59] Petersen K E 1982 Silicon as a mechanical material *Proc. IEEE* **70** 420–57
[60] Kovacs G T A 1998 *Micromachined Transducers Sourcebook* (Boston, MA: WCB)
[61] Judy J W 2001 Microelectromechanical systems (MEMS): fabrication, design and applications *Smart Mater. Struct.* **10** 2001
[62] Madou M J 2002 *Fundamentals of Microfabrication: The Science of Miniaturization* (Boca Raton, FL: CRC Press)
[63] Gad-el-Hak M (ed) 2002 *The MEMS Handbook* (Boca Raton, FL: CRC Press)
[64] van Lintel H T G, van de Pol F C M and Bouwstra S 1988 A piezoelectric micropump based on micromachining of silicon *Sensors Actuators* **15** 153–67
[65] van Lintel H T G 1992 Micropump having a constant output *US Patent no.* 5.085,562
[66] van Lintel H T G 1993 Micropump with improved priming *US Patent no.* 5,219,278
[67] Morris C J and Forster F K 2003 Low-order modeling of resonance for fixed-valve micropumps based on first principles *J. Microelectromech. Syst.* **12** 325–34
[68] Bourouina T and Grandchamp J P 1996 Modeling micropumps with electrical equivalent networks *J. Micromech. Microeng.* **6** 398–404
[69] Olsson A, Stemme G and Stemme E 1999 A numerical design study of the valveless diffuser pump using a lumped-mass model *J. Micromech. Microeng.* **9** 34–44
[70] Moussa W A and Gonzalez U F 2002 Simulation of MEMS piezoelectric micropump for biomedical applications *Proc. ASME Int. Mechanical Engineering Congress and Exposition (New Orleans, LA)*
[71] Morris C J and Forster F K 2000 Optimization of a circular piezoelectric bimorph for a micropump driver *J. Micromech. Microeng.* **10** 459–65
[72] Gerlach T 1998 Microdiffusers as dynamic passive valves for micropump applications *Sensors Actuators* A **69** 181–91
[73] Ullman A and Fono I 2002 The piezoelectric valve-less pump—improved dynamic model *J. Microelectromech. Syst.* **11** 655–64
[74] Pan L S, Ng T Y, Wu X H and Lee H P 2003 Analysis of valveless micropumps with inertial effects *J. Micromech. Microeng.* **13** 390–9
[75] Gamboa A R, Morris C J and Forster F 2003 Optimized fixed-geometry valves for laminar flow micropumps *Proc. ASME Int. Mechanical Engineering Congress and Exposition (Washington, DC)*
[76] Probstein R F 1994 *Physicochemical Hydrodynamics* (New York: Wiley)
[77] Kundu P K and Cohen I M 2002 *Fluid Mechanics* (New York: Academic)

[78] Young W C and Budynas R C 2002 *Roark's Formulas for Stress and Strain* 7th edn (New York: McGraw-Hill)

[79] Geradin M and Rixen D 1997 *Mechanical Vibrations: Theory and Applications to Structural Dynamics* 2nd edn (Chichester, NY: Wiley)

[80] Richter M, Linnemann R and Woias P 1998 Robust design of gas and liquid micropumps *Sensors Actuators* A **68** 480–6

[81] Linnemann R, Woias P, Senfft C-D and Ditterich J A 1998 A self-priming and bubble-tolerant piezoelectric silicon micropump for liquids and gases *11th Annual Int. Workshop on Micro Electro Mechanical Systems (Heidelberg, Germany)* (Piscataway, NJ: IEEE)

[82] Zengerle R and Richter M 1994 Simulation of microfluid systems *J. Micromech. Microeng.* **4** 192–204

[83] Veenstra T T *et al* 2001 Use of selective anodic bonding to create micropump chambers with virtually no dead volume *J. Electrochem. Soc.* **148** G68–72

[84] Smits J G 1990 Piezoelectric micropump with microvalves *US Patent no.* 4,938,742.

[85] Shoji S, Nakagawa S and Esashi M 1990 Micropump and sample-injector for integrated chemical analyzing systems *Sensors Actuators* A **21** 189–92

[86] Yun K-S, Cho I-J, Bu J-U, Kim C-J and Yoon E 2002 A surface-tension driven micropump for low-voltage and low-power operations *J. Microelectromech. Syst.* **11** 454–61

[87] Berg J M *et al* 2003 A two-stage discrete peristaltic micropump *Sensors Actuators* A **104** 6–10

[88] Olsson A, Stemme G and Stemme E 1995 A valve-less planar fluid pump with 2 pump chambers *Sensors Actuators* A **47** 549–56

[89] Olsson A, Enoksson P, Stemme G and Stemme E 1996 A valve-less planar pump isotropically etched in silicon *J. Micromech. Microeng.* **6** 87–91

[90] Zengerle R, Ulrich J, Kluge S, Richter M and Richter A 1995 A bidirectional silicon micropump *Sensors Actuators* A **50** 81–6

[91] Stemme E and Stemme G 1993 A valveless diffuser/nozzle-based fluid pump *Sensors Actuators* A **39** 159–67

[92] Kamper K-P, Dopper J, Ehrfeld W and Oberbeck S 1998 A self-filling low-cost membrane micropump *Proc. 11th Annual Int. Workshop on Micro Electro Mechanical Systems (Heidelberg, Germany)* (Piscataway, NJ: IEEE)

[93] IMM *thinXXS XXS2000 Data Sheet* www.thinxxs.com

[94] Bohm S, Olthuis W and Bergveld P 1999 A plastic micropump constructed with conventional techniques and materials *Sensors Actuators* A **77** 223–8

[95] Carrozza M C, Croce N, Magnani B and Dario P 1995 A piezoelectric-driven stereolithography-fabricated micropump *J. Micromech. Microeng.* **5** 177–9

[96] Wego A and Pagel L 2001 A self-filling micropump based on PCB technology *Sensors Actuators* A **88** 220–6

[97] Yoon H J, Sim W Y and Yang S S 2001 The fabrication and test of a phase-change micropump *Proc. ASME Int. Mechanical Engineering Congress and Exposition (New York)*

[98] MIP Implantable product information, www.debiotech.sa

[99] Maillefer D, van Lintel H T G, Rey-Mermet G and Hirschi R 1999 A high-performance silicon micropump for an implantable drug delivery system *12th IEEE Int. Conf. on Micro Electro Mechanical Systems (Orlando, FL)* (Piscataway, NJ: IEEE)

[100] Esashi M, Shoji S and Nakano A 1989 Normally closed microvalve and micropump fabricated on a silicon-wafer *Sensors Actuators* **20** 163–9

[101] Stehr M, Messner S, Sandmaier H and Zengerle R 1996 The VAMP: a new device for handling liquids or gases *Sensors Actutators* A **57** 153–7

[102] Li H Q *et al* 2000 A high frequency high flow rate piezoelectrically driven MEMS micropump *Proc. 2000 Solid-State Sensor and Actuator Workshop (Hilton Head, SC)*

[103] Fraden J 1996 *Handbook of Modern Sensors: Physics, Designs, and Applications* (New York: Springer)

[104] Demer F M 1974 Ink jet printer *US Patent no.* 3,787,884

[105] Bassous E, Kuhn L and Taub H H 1976 Jet nozzle structure for electrohydrodynamic droplet formation and ink jet printing system therewith *US Patent no.* 3,949,410

[106] Juliana A, Koepcke R W, Mills R N and Talke F E 1981 Voltage modulated drop-on-demand ink jet method and apparatus *US Patent no.* 4,266,232

[107] Li S and Chen S 2003 Analytical analysis of a circular PZT actuator for valveless micropumps *Sensors Actuators* A **104** 151–61

[108] Chang S H and Du B C 2001 Optimization of asymmetric bimorphic disk transducers *J. Acoust. Soc. Am.* **109** 194–202

[109] Olsson A, Stemme G and Stemme E 1996 Diffuser-element design investigation for valve-less pumps *Sensors Actuators* A **57** 137–43

[110] Olsson A, Enoksson P, Stemme G and Stemme E 1997 Micromachined flat-walled valveless diffuser pumps *J. Microelectromech. Syst.* **6** 161–6

[111] Gass V, Vanderschoot B H, Jeanneret S and Derooij N F 1994 Integrated flow-regulated silicon micropump *Sensors Actuators* A **43** 335–8

[112] Park J H, Yokota S and Yoshida K 2002 A piezoelectric micropump using resonance drive with high power density *JSME Int. J.* C **45** 502–59

[113] Koch M *et al* 1997 A novel micropump design with thick-film piezoelectric actuation *Meas. Sci. Technol.* **8** 49–57

[114] Koch M, Harris N, Evans A G R, White N M and Brunnschweiler A 1998 A novel micromachined pump based on thick-film piezoelectric actuation *Sensors Actuators* A **70** 98–103

[115] Koch M, Evans A G R and Brunnschweiler A 1998 The dynamic micropump driven with a screen printed PZT actuator *J. Micromech. Microeng.* **8** 119–22

[116] Schabmueller C G J *et al* 2002 Self-aligning gas/liquid micropump *J. Micromech. Microeng.* **12** 420–4

[117] Rogacheva N N 1994 *The Theory of Piezoelectric Shells and Plates* (Boca Raton, FL: CRC Press)

[118] Dobrucki A B and Pruchnicki P 1997 Theory of piezoelectric axisymmetric bimorph *Sensors Actuators* A **58** 203–12

[119] Mu Y H, Hung N P and Ngoi K A 1999 Optimisation design of a piezoelectric micropump *Int. J. Adv. Manuf. Technol.* **15** 573–6

[120] Williams B E and Forster F K 2001 Micropump design for optimum pressure/flow characteristics *Proc. 2001 ASME Int.Mechanical Engineering Congress and Exposition (New York)*

[121] Roberts D C *et al* 2001 A high-frequency, high-stiffness piezoelectric micro-actuator for hydraulic applications *Proc. Transducers '01 (Munich)*

[122] van de Pol F C M, van Lintel H T G, Elwenspoek M and Fluitman J H J 1989 A thermopneumatic micropump based on micro-engineering techniques *Proc. 5th Int. Conf. on Solid-State Sensors and Actuators/Eurosensors III*

[123] van de Pol F C M, van Lintel H T G, Elwenspoek M and Fluitman J H J 1990 A thermopneumatic micropump based on micro-engineering techniques *Sensors Actuators* A **21** 198–202

[124] Elwenspoek M, Lammerink T S J, Miyake R and Fluitman J H J 1994 Towards integrated microliquid handling systems *J. Micromech. Microeng.* **4** 227–45

[125] Schomburg W K *et al* 1994 Microfluidic components in LIGA technique *J. Micromech. Microeng.* **4** 186–91

[126] Grosjean C and Tai Y C 1999 A thermopneumatic peristaltic micropump *Proc. Transducers '99 (Sendai, Japan)*

[127] Jeong O C and Yang S S 2000 Fabrication and test of a thermopneumatic micropump with a corrugated p+ diaphragm *Sensors Actuators* A **83** 249–55

[128] Sim W Y, Yoon H J, Jeong O C and Yang S S 2003 A phase-change type micropump with aluminum flap valves *J. Micromech. Microeng.* **13** 286–94

[129] Acero M C *et al* 1997 Design of a modular micropump based on anodic bonding *J. Micromech. Microeng.* **7** 179–82

[130] Carmona M, Marco S, Samitier J and Morante J R 1996 Dynamic simulations of micropumps *J. Micromech. Microeng.* **6** 128–30

[131] Folta J A, Raley N F and Hee E W 1992 Design, fabrication, and testing of a miniature peristaltic membrane pump *Proc. 1992 Solid-State Sensor and Actuator Workshop (Hilton Head Island, SC)* (Piscataway, NJ: IEEE)

[132] Tsai J H and Lin L 2002 A thermal-bubble-actuated micronozzle-diffuser pump *J. Microelectromech. Syst.* **11** 665–71

[133] Zimmermann S, Frank J A, Liepmann D and Pisano A P 2004 A planar micropump utilizing thermopneumatic actuation and in-plane flap valves *Proc. 17th IEEE Int. Conf. on Micro Electro Mechanical Systems (Maastricht, The Netherlands)*

[134] Tang W C, Nguyen T C H and Howe R T 1989 Laterally driven polysilicon resonant microstructures *Sensors Actuators* **20** 25–32

[135] Griffiths D J 1999 *Introduction to Electrodynamics* (Upper Saddle River, NJ: Prentice-Hall)

[136] Zengerle R *et al* 1995 Transient measurements on miniaturized diaphragm pumps in microfluid systems *Sensors Actuators* A **47** 557–61

[137] Cabuz C, Cabuz E I, Herb W R, Rolfer T and Zook D 1999 Mesoscopic sampler based on 3D array of electrostatically activated diaphragms *Proc. Transducers '99 (Sendai, Japan)*

[138] Bourouina T, Bosseboeuf A and Grandchamp J P 1997 Design and simulation of an electrostatic micropump for drug-delivery applications *J. Micromech. Microeng.* **7** 186–8

[139] Francais O, Dufour I and Sarraute E 1997 Analytical static modelling and optimization of electrostatic micropumps *J. Micromech. Microeng.* **7** 183–5

[140] Francais O and Dufour I 1998 Dynamic simulation of an electrostatic micropump with pull-in and hysteresis phenomena *Sensors Actuators* A **70** 56–60

[141] Voigt P, Schrag G and Wachutka G 1998 Electrofluidic full-system modelling of a flap valve micropump based on Kirchhoffian network theory *Sensors Actuators* A **66** 9–14

[142] Rapp R, Schomburg W K, Maas D, Schulz J and Stark W 1994 LIGA micropump for gases and liquids *Sensors Actuators* A **40** 57–61

[143] Unger M A, Chou H P, Thorsen T, Scherer A and Quake S R 2000 Monolithic microfabricated valves and pumps by multilayer soft lithography *Science* **288** 113–6

[144] Grover W H, Skelley A M, Liu C N, Lagally E T and Mathies R A 2003 Monolithic membrane valves and diaphragm pumps for practical large-scale integration into glass microfluidic devices *Sensors Actuators* B **89** 315–23

[145] Dario P, Croce N, Carrozza M C and Varallo G 1996 A fluid handling system for a chemical microanalyzer *J. Micromech. Microeng.* **6** 95–8

[146] Meng E, Wang X-Q, Mak H and Tai Y-C 2000 A check-valved silicone diaphragm pump *Proc. MEMS 2000: 13th Annual Int. Conf. on Micro Electro Mechanical Systems (Miyazaki, Japan)* pp 62–7

[147] Bisson C *et al* 1998 A microanalytical device for the assessment of coagulation parameters in whole blood *1998 Solid-State Sensor and Actuator Workshop (Hilton Head Island, SC)*

[148] Gong Q L, Zhou Z Y, Yang Y H and Wang X H 2000 Design, optimization and simulation on microelectromagnetic pump *Sensors Actuators* A **83** 200–7

[149] Santra S, Holloway P and Batich C D 2002 Fabrication and testing of a magnetically actuated micropump *Sensors Actuators* B **87** 358–64

[150] Benard W L, Kahn H, Heuer A H and Huff M A 1998 Thin-film shape-memory alloy actuated micropumps *J. Microelectromech. Syst.* **7** 245–51

[151] Makino E, Mitsuya T and Shibata T 2001 Fabrication of TiNi shape memory micropump *Sensors Actuators* A **88** 256–62

[152] Zou Q B, Sridhar U and Lin R M 1999 A study on micromachined bimetallic actuation *Sensors Actuators* A **78** 212–9

[153] Pang J T *et al* 1998 The study of single-chip integrated microfluidic system *IEEE 5th Int. Conf. on Solid-State and Integrated Circuit Technologies (Beijing)* pp 895–8

[154] Hsu C P and Hsu W S 2000 A two-way membrane-type micro-actuator with continuous deflections *J. Micromech. Microeng.* **10** 387–94

[155] Beskok A and Srinivasa A R 2001 Simulation and analysis of a magnetoelastically driven micro-pump *Trans. ASME, J. Fluids Eng.* **123** 435–38

[156] Yuen P K, Kricka L J and Wilding P 2000 Semi-disposable microvalves for use with microfabricated devices or microchips *J. Micromech. Microeng.* **10** 401–9

[157] Koch M, Evans A G R and Brunnschweiler A 1997 Characterization of micromachined cantilever valves *J. Micromech. Microeng.* **7** 221–3

[158] Carmona M *et al* 2001 An analytical model for passive microvalves *Sensors Mater.* **13** 373–83

[159] Voldman J, Gray M L and Schmidt M A 2000 An integrated liquid mixer/valve *J. Microelectromech. Syst.* **9** 295–302

[160] Paul B K and Terhaar T 2000 Comparison of two passive microvalve designs for microlamination architectures *J. Micromech. Microeng.* **10** 15–20

[161] Accoto D, Carrozza M C and Dario P 2000 Modelling of micropumps using unimorph piezoelectric actuator and ball valves *J. Micromech. Microeng.* **10** 277–81

[162] Jerman H 1994 Electrically activated, normally-closed diaphragm valves *J. Micromech. Microeng.* **4** 210–5

[163] Sato K and Shikida M 1994 An electrostatically actuated gas valve with an S-shaped film element *J. Micromech. Microeng.* **4** 205–9

[164] Yang X, Holke A and Schmidt M A 2002 An electrostatic, on/off MEMS valve for gas fuel delivery of a microengine *Proc. 2002 Solid-State Sensor, Actuator and Microsystems Workshop (Hilton Head Island, SC)*

[165] Yobas L, Huff M A, Lisy F J and Durand D M 2001 A novel bulk-micromachined electrostatic microvalve with a curved-compliant structure applicable for a pneumatic tactile display *J. Microelectromech. Syst.* **10** 187–96

[166] Vandelli N, Wroblewski D, Velonis M and Bifano T 1998 Development of a MEMS microvalve array for fluid flow control *J. Microelectromech. Syst.* **7** 395–403

[167] Fahrenberg J *et al* 1995 A microvalve system fabricated by thermoplastic molding *J. Micromech. Microeng.* **5** 169–71

[168] Goll C *et al* 1996 Microvalves with bistable buckled polymer diaphragms *J. Micromech. Microeng.* **6** 77–9

[169] Schomburg W K and Goll C 1998 Design optimization of bistable microdiaphragm valves *Sensors Actuators* A **64** 259–64

[170] Baechi D, Buser R and Dual J 2002 A high density microchannel network with integrated valves and photodiodes *Sensors Actuators* A **95** 77–83

[171] Chakraborty I, Tang W C, Bame D P and Tang T K 2000 MEMS micro-valve for space applications *Sensors Actuators* A **83** 188–93

[172] Capanu M, Boyd J G and Hesketh P J 2000 Design; fabrication; and testing of a bistable electromagnetically actuated microvalve *J. Microelectromech. Syst.* **9** 181–9

[173] Bohm S, Burger G J, Korthorst M T and Roseboom F 2000 A micromachined silicon valve driven by a miniature bi-stable electro-magnetic actuator *Sensors Actuators* A **80** 77–83

[174] Yoshida K, Kikuchi M, Park J H and Yokota S 2002 Fabrication of micro electro-rheological valves (ER valves) by micromachining and experiments *Sensors Actuators* A **95** 227–33

[175] Bosch D *et al* 1993 A silicon microvalve with combined electromagnetic/electrostatic actuation *Sensors Actuators* A **37** 684–92

[176] Kohl M, Dittmann D, Quandt E and Winzek B 2000 Thin film shape memory microvalves with adjustable operation temperature *Sensors Actuators* A **83** 214–9

[177] Ohori T, Shoji S, Miura K and Yotsumoto A 1998 Partly disposable three-way microvalve for a medical micro total analysis system (μTAS) *Sensors Actuators* A **64** 57–62

[178] Barth P W 1995 Silicon microvalves for gas flow control *Proc. Transducers '95/Eurosensors IX (Stockholm)*

[179] Gerlach T and Wurmus H 1995 Working principle and performance of the dynamic micropump *Sensors Actuators* A **150** 135–40

[180] Forster F, Bardell R, Afromowitz M, Sharma N and Blanchard A 1995 Design, fabrication and testing of fixed-valve micropumps *Proc. ASME Int. Mechanical Engineering Congress and Exposition (San Francisco, CA)* (New York: ASME)

[181] Jang L-S, Morris C J, Sharma N R, Bardell R L and Forster F K 1999 Transport of particle-laden fluids through fixed-valve micropumps *Proc. ASME Int. Mechanical Engineering Congress and Exposition (Nashville, TN)*

[182] Andersson H, van der Wijngaart W, Nilsson P, Enoksson P and Stemme G 2001 A valve-less diffuser micropump for microfluidic analytical systems *Sensors Actuators* B **72** 259–65

[183] Heschel M, Mullenborn M and Bouwstra S 1997 Fabrication and characterization of truly 3D diffuser/nozzle microstructures in silicon *J. Microelectromech. Syst.* **6** 41–7

[184] Jiang X N *et al* 1998 Micronozzle/diffuser flow and its application in micro valveless pumps *Sensors Actuators* A **70** 81–7

[185] Olsson A, Stemme G and Stemme E 2000 Numerical and experimental studies of flat-walled diffuser elements for valve-less micropumps *Sensors Actuators* A **84** 165–75

[186] Pan L S, Ng T Y, Liu G R, Lam K Y and Jiang T Y 2001 Analytical solutions for the dynamic analysis of a valveless micropump: a fluid-membrane coupling study *Sensors Actuators* A **93** 173–81

[187] Veenstra T T *et al* 2002 The design of an in-plane compliance structure for microfluidical systems *Sensors Actuators* B **81** 377–83

[188] Liu R H, Yu Q and Beebe D J 2002 Fabrication and characterization of hydrogel-based microvalves *J. Microelectromech. Syst.* **11** 45–53

[189] Matsumoto S, Klein A and Maeda R 1999 Development of bi-directional valve-less micropump for liquid *Proc. IEEE MEMS '99 (Orlando, FL)*

[190] Yun Y, Lee K M, Lim G, Lee J H and Pak Y E 2000 Modeling of diffuser/nozzle micropump under electrohydrodynamic backflow control *ASME FEDSM'00 (Boston, MA)*

[191] Kirby B J, Shepodd T J and Hasselbrink E F Jr 2002 Voltage-addressable on/off microvalves for high-pressure microchip separations *J. Chromatogr.* A **979** 147–54

[192] Dopper J *et al* 1997 Micro gear pumps for dosing of viscous fluids *J. Micromech. Microeng.* **7** 230–2

[193] Dewa A S *et al* 1997 Development of LIGA-fabricated, self-priming, in-line gear pumps *Proc. Transducers '97 (Chicago, IL)*

[194] Kilani M I, Galambos P C, Haik Y S and Chen C-J 2001 Electrostatically actuated surface micromachined offset planetary gear pump design *Proc. 2001 ASME Int. Mechanical Engineering Congress and Exposition (New York)*

[195] Kilani M I, Galambos P C, Halk Y S and Chen C-J 2002 A surface micromachined spiral-channel viscous pump *Proc. 2001 ASME International Mechanical Engineering Congress and Exposition (New Orleans, LA)*

[196] Terray A, Oakey J and Marr D W M 2002 Microfluidic control using colloidal devices *Science* **296** 1841–4

[197] Sen M, Wajerski D and Gad el Hak M 1996 A novel pump for MEMS applications *Trans. ASME, J. Fluids Eng.* **118** 624–7

[198] DeCourtye D, Sen M and Gad el Hak M 1998 Analysis of viscous micropumps and microturbines *Int. J. Comput. Fluid Dyn.* **10** 13–25

[199] Hatch A, Kamholz A E, Holman G, Yager P and Bohringer K F 2001 A ferrofluidic magnetic micropump *J. Microelectromech. Syst.* **10** 215–21

[200] Sefton M V 1987 Implantable pumps *CRC Crit. Rev. Biomed. Eng.* **14** 201–240

[201] Cabuz E *et al* 2002 MEMS-based flow controller for flow cytometry *Proc. 2002 Solid-State Sensors, Actuators and Microsystems Workshop (Hilton Head, SC)*

[202] Tas N R, Berenschot J W, Lammerink T S J, Elwenspoek M and van den Berg A 2002 Nanofluidic bubble pump using surface tension directed gas injection *Anal. Chem.* **74** 2224–7

[203] Jen C P and Lin Y C 1997 Design and simulation of bi-directional microfluid driving systems *J. Micromech. Microeng.* **12** 115–21

[204] Evans J, Liepmann D and Pisano A P 1997 Planar Laminar Mixer *Proc. IEEE MEMS '97 (Nagoya, Japan)*

[205] Handique K, Burke D T, Mastrangelo C H and Burns M A 2001 On-chip thermopneumatic pressure for discrete drop pumping *Anal. Chem.* **73** 1831–8

[206] Jun T K and Kim C J 1998 Valveless pumping using traversing vapor bubbles in microchannels *J. Appl. Phys.* **83** 5658–64

[207] Song Y J and Zhao T S 2001 Modelling and test of a thermally driven phase-change nonmechanical micropump *J. Micromech. Microeng.* **11** 713–9

[208] Bohm S, Timmer B, Olthuis W and Bergveld P 2000 A closed-loop controlled electrochemically actuated micro-dosing system *J. Micromech. Microeng.* **10** 498–504

[209] Lee S W, Jeong O C and Yang S S 1998 The fabrication of a micro injector actuated by boiling and/or electrolysis *Proc. 11th Annual Int. Workshop on Micro Electro Mechanical Systems (Heidelberg)* (Piscataway, NJ: IEEE)

[210] Li Z X, Wang M R and Tan L Y 2002 Experimental investigation on phase transformation type micropump *Chin. Sci. Bull.* **47** 518–22

[211] Lin L W, Pisano A P and Carey V P 1998 Thermal bubble formation on polysilicon micro resistors *Trans. ASME, J. Heat Transfer* **120** 735–42

[212] Colgate J E and Matsumoto H 1990 An investigation of electrowetting-based microactuation *J. Vac. Sci. Technol.* A **8** 3625–33

[213] Matsumoto H and Colgate J E 1990 Preliminary investigation of micropumping based on electrical control of interfacial tension *IEEE MEMS'90 (Napa Valley, CA)*

[214] Lee J and Kim C J 2000 Surface-tension-driven microactuation based on continuous electrowetting *J. Microelectromech. Syst.* **9** 171–80

[215] Lee J, Moon H, Fowler J, Schoellhammer T and Kim C J 2002 Electrowetting and electrowetting-on-dielectric for microscale liquid handling *Sensors Actuators* A **95** 259–68

[216] Kataoka D E and Troian S M 1999 Patterning liquid flow on the microscopic scale *Nature* **402** 794–7

[217] Sammarco T S and Burns M A 1999 Thermocapillary pumping of discrete drops in microfabricated analysis devices *AIChE J.* **45** 350–66

[218] Stolzenberg S J and Linkenheimer W H 1971 Osmotic fluid reservoir for osmotically activated long-term continuous injector device *US Patent no.* 3,604,417

[219] Su Y-C, Lin L and Pisano A P 2002 A water-powered micro drug delivery system *Proc. 2002 Solid-State Sensor, Actuator and Microsystem Workshop (Hilton Head, SC)*

[220] Ying L, Bruckbauer A, Rothery A M, Korchev Y E and Klenerman D 2002 Programmable delivery of DNA through a nanopipet *Anal. Chem.* **74** 1380–5

[221] Cooper P 2000 Centrifugal pump theory *Pump Handbook* ed I J Karassik *et al* (New York: McGraw-Hill)

[222] Frechette L G *et al* 2000 Demonstration of a microfabricated high-speed turbine supported on gas bearings *Proc. 2000 Solid-State Sensor and Actuator Workshop (Hilton Head, SC)*

[223] London A P, Epstein A H and Kerrebrock J L 2001 High-pressure bipropellant microrocket engine *J. Propulsion Power* **17** 780–7

[224] Deux A 2001 Design of a silicon microfabricated rocket engine turbopump *MIT Master's Thesis*

[225] Pennathur S 2001 Micro-scale turbopump blade cavitation *MIT Master's Thesis*

[226] Marseille O, Habib N, Reul H and Rau G 1998 Implantable micropump system for augmented liver perfusion *Artif. Organs* **22** 458–60

[227] Melcher J R 1981 *Continuum Electromechanics* (Cambridge, MA: MIT Press)

[228] Bart S F, Tavrow L S, Mehregany M and Lang J H 1990 Microfabricated electrohydrodynamic pumps *Sensors Actuators* A **21** 193–7

[229] Fuhr G, Schnelle T and Wagner B 1994 Traveling wave-driven microfabricated electrohydrodynamic pumps for liquids *J. Micromech. Microeng.* **4** 217–26

[230] Jeong S and Seyed-Yagoobi J 2002 Experimental study of electrohydrodynamic pumping through conduction phenomenon *J. Electrost.* **56** 123–33

[231] Atten P and Seyed-Yagoobi J 2003 Electrohydrodynamically induced dielectric liquid flow through pure conduction in point/plane geometry *IEEE Trans. Dielectr. Electr. Insul.* **10** 27–36

[232] Richter A, Plettner A, Hofmann K A and Sandmaier H 1991 A micromachined electrohydrodynamic (EHD) pump *Sensors Actuators* A **29** 159–68

[233] Wong C C, Adkins D R and Chu D 1996 Development of a micropump for microelectronic cooling *Microelectromechanical Systems* vol 59 (New York: ASME)

[234] Ahn S H and Kim Y K 1998 Fabrication and experiment of a planar micro ion drag pump *Sensors Actuators* A **70** 1–5

[235] Darabi J, Rada M, Ohadi M and Lawler J 2002 Design, fabrication and testing of an electrohydrodynamic ion-drag micropump *J. Microelectromech. Syst.* **11** 684–690

[236] Darabi J, Ohadi M M and DeVoe D 2001 An electrohydrodynamic polarization micropump for electronic cooling *J. Microelectromech. Syst.* **10** 98–106

[237] Crowley J M, Wright G S and Chato J C 1990 Selecting a working fluid to increase the efficiency and flow rate of an EHD pump *IEEE Trans. Ind. Appl.* **26** 42–9

[238] Watanabe M, Zheng J, Hara A, Shirai H and Hirai T 2003 A pumping technique using electrohydrodynamic flow inside a gel *IEEE Trans. Dielectr. Electr. Insul.* **10** 181–5

[239] Hunter R J 1981 *Zeta Potential in Colloid Science* (San Diego, CA: Academic)

[240] Adamson A W and Gast A P 1997 *Physical Chemistry of Surfaces* (New York: Wiley)

[241] Rice C L and Whitehead R 1965 Electrokinetic flow in a narrow cylindrical capillary *J. Phys. Chem.* **69** 4017

[242] Pretorius V, Hopkins B J and Schieke J D 1974 Electro-osmosis: new concept for high-speed liquid-chromatography *J. Chromatogr.* **99** 23–30

[243] Liu S and Dasgupta P K 1992 Flow-injection analysis in the capillary format using electroosmotic pumping *Anal. Chim. Acta* **268** 1–6

[244] Manz A *et al* 1994 Electroosmotic pumping and electrophoretic separations for miniaturized chemical-analysis systems *J. Micromech. Microeng.* **4** 257–65

[245] Harrison D J *et al* 1993 Micromachining a miniaturized capillary electrophoresis-based chemical analysis system on a chip *Science* **261** 895–7

[246] Knapp M R *et al* 2001 Commercialized and emerging lab-on-a-chip applications *Proc. Micro Total Analysis Systems 2001 (Monterey, CA)*

[247] Jacobson S C, Hergenroder R, Koutny L B and Ramsey J M 1994 Open-channel electrochromatography on a microchip *Anal. Chem.* **66** 2369–73

[248] Dasgupta P K and Liu S 1994 Auxiliary electroosmotic pumping in capillary electrophoresis *Anal. Chem.* **66** 3060–5

[249] Ramsey R S and Ramsey J M 1997 Generating electrospray from microchip devices using electroosmotic pumping *Anal. Chem.* **69** 1174–8

[250] McKnight T E, Culbertson C T, Jacobson S C and Ramsey J M 2001 Electroosmotically induced hydraulic pumping with integrated electrodes in microfluidic devices *Anal. Chem.* **73** 4045–9

[251] Paul P H, Arnold D W and Rakestraw D J 1998 Electrokinetic generation of high pressures using porous microstructures *Proc. Micro Total Analysis Systems 1998 (Banff, Canada)*

[252] Paul P H and Rakestraw D J 2000 Electrokinetic high pressure hydraulic system *US Patent no.* 6,019,882

[253] Yao S H and Santiago J G 2003 Porous glass electroosmotic pumps: theory *J. Colloid Interface Sci.* **268** 133–42

[254] Zeng S L, Chen C H, Mikkelsen J C and Santiago J G 2001 Fabrication and characterization of electroosmotic micropumps *Sensors Actuators* B **79** 107–14

[255] Laser D J, Goodson K E, Santiago J G and Kenny T W 2002 High-Frequency Actuation with Silicon Electroosmotic Micropumps *Proc. 2002 Solid-State Sensor, Actuator, and Microsystems Workshop (Hilton Head Island, SC)*

[256] Yao S H, Hertzog D E, Zeng S L, Mikkelsen J C and Santiago J G 2003 Porous glass electroosmotic pumps: design and experiments *J. Colloid Interface Sci.* **268** 143–53

[257] Yates D E, Levine S and Healy T W 1974 Site-binding model of electrical double layer at the oxide/water interface *J. Electrochem. Soc.* **74** 1807–18

[258] Scales P J, Grieser F and Healy T W 1992 Electrokinetics of the silica-solution interface: a flat plate streaming potential study *Langmuir* **8** 965–74

[259] Chen C-H and Santiago J G 2002 A planar electroosmotic micropump *J. Microelectromech. Syst.* **11** 672–83

[260] Gan W E *et al* 2000 Mechanism of porous core electroosmotic pump flow injection system and its application to determination of chromium(VI) in waste-water *Talanta* **51** 667–75

[261] Zeng S L *et al* 2002 Electroosmotic flow pumps with polymer frits *Sensors Actuators* B **82** 209–12

[262] Chen C-H, Zeng S L, Mikkelsen J C and Santiago J G 2000 Development of a planar electrokinetic micropump *Proc. 2000 ASME International Mechanical Engineering Congress and Exposition (Orlando, FL)*

[263] Burgreen D and Nakache F R 1964 Electrokinetic flow in ultrafine capillary slits *J. Phys. Chem.* **68** 1084–191

[264] Laser D J, Yao S, Chen C H, Mikkelsen J, Goodson K E, Santiago J G and Kenny T W 2001 A low-voltage silicon micromachined parallel-plate electrokinetic pump *Proc. Transducers '01 (Munich, Germany)*

[265] Kemery P J, Steehler J K and Bohn P W 1998 Electric field mediated transport in nanometer diameter channels *Langmuir* **14** 2884–9

[266] Takamura Y 2001 Low-voltage electroosmotic pump and its applications to on-chip linear stepping pneumatic pressure source *Proc. Micro Total Analytical Systems 2001 (Monterey, CA)*

[267] Selvaganapathy P, Leung Ki Y-S, Renaud P and Mastrangelo C H 2002 Bubble-free electrokinetic pumping *J. Microelectromech. Syst.* **11** 448–53

[268] Ajdari A 2002 Electrokinetic 'ratchet' pumps for microfluidics *Appl. Phys.* A **75** 271–4

[269] Morf W E, Guenat O T and de Rooij N F 2001 Partial electroosmotic pumping in complex capillary systems: 1. Principles and general theoretical approach *Sensors Actuators* B **72** 266–72

[270] Guenat O T, Ghiglione D, Morf W E and de Rooij N F 2001 Partial electroosmotic pumping in complex capillary systems: 2. Fabrication and application of a micro total analysis system (μTAS) suited for continuous volumetric nanotitrations *Sensors Actuators* B **72** 273–82

[271] Mosier B P, Crocker R W, Rognlien J L and Patel K D 2003 High-pressure microhydraulic actuator *Proc. 2003 ASME Int. Mechanical Engineering Congress and Exposition (Washington, DC)*

[272] Jang J S and Lee S S 2000 Theoretical and experimental study of MHD (magnetohydrodynamic) micropump *Sensors Actuators* A **80** 84–9

[273] Lemoff A V and Lee A P 2000 An AC magnetohydrodynamic micropump *Sensors Actuators* B **63** 178–85

[274] Huang L, Wang W, Murphy M C, Lian K and Ling Z G 2000 LIGA fabrication and test of a DC type magnetohydrodynamic (MHD) micropump *Microsyst. Technol.* **6** 235–40

[275] Zhong J H, Yi M Q and Bau H H 2002 Magneto hydrodynamic (MHD) pump fabricated with ceramic tapes *Sensors Actuators* A **96** 59–66

[276] Leventis N and Gao X R 2001 Magnetohydrodynamic electrochemistry in the field of Nd-Fe-B magnets. Theory; experiment; and application in self-powered flow delivery systems *Anal. Chem.* **73** 3981–92

[277] Bau H H, Zhong J H and Yi M Q 2001 A minute magneto hydro dynamic (MHD) mixer *Sensors Actuators* B **79** 207–15

[278] Bau H H 2001 A case for magneto hydro dynamics (MHD) *Proc. 2001 ASME Int. Mechanical Engineering Congress and Exposition (New York)*

[279] Luginbuhl P *et al* 1997 Microfabricated lamb wave device based on PZT sol-gel thin film for mechanical transport of solid particles and liquids *J. Microelectromech. Syst.* **6** 337–46

[280] Black J and White R M 2000 Microfluidic applications of ultrasonic flexural plate waves *Proc. 2000 Solid-State Sensors and Actuators Workshop (Hilton Head, SC)*

[281] Nguyen N T and White R M 1999 Design and optimization of an ultrasonic flexural plate wave micropump using numerical simulation *Sensors Actuators* A **77** 229–36

[282] Moroney R M, White R M and Howe R T 1991 Ultrasonically induced microtransport *Proc. IEEE MEMS '91 (Nara, Japan)*

[283] Young R M 1999 Analysis of a micromachine based vacuum pump on a chip actuated by the thermal transpiration effect *J. Vac. Sci. Technol.* B **17** 280–7

[284] Namasivayam V, Larson R G, Burke D T and Burns M A 2003 Transpiration-based micropump for delivering continuous ultra-low flow rates *J. Micromech. Microeng.* **13** 261–71

[285] Yao S, Huber D E, Mikkelsen J C and Santiago J G 2001 A large flow rate electroosmotic pump with micron pores *Proc. 2001 ASME Int. Mechanical Engineering Congress and Exposition (New York, NY)*

[286] Bardell R, Sharma N, Forster F, Afromowitz M and Penney R J 1997 Designing high-performance micro-pumps based on no-moving-parts valves *Proc. 1997 ASME Int. Mechanical Engineering Congress and Exposition* (Dallas, TX)

[287] Furuya A, Shimokawa F, Matsuura T and Sawada R 1996 Fabrication of fluorinated polyimide microgrids using magnetically controlled reactive ion etching (MC-RIE) and their applications to an ion drag integrated micropump *J. Micromech. Microeng.* **6** 310–19

EXHIBIT C

English Dictionary

Definition of "micropump"

micropump ('maɪkrəʊˌpʌmp)

Definitions

noun

(*medicine*) a small pump inserted under the skin to automatically deliver medicine at set intervals

Comments

Login to comment on this word.

b-ball
big data
blamestorm
cash mob
chillax

Related Terms

0 results

Browse nearby words

micropublishing
micropulsation
micropump
micropuncture
micropylar

All English words that begin with 'M'

"micropump" photos from Flickr

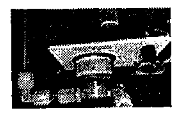

Word usage trends for "micropump"

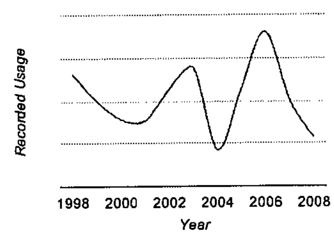

View usage over: Last 10 years

EXHIBIT D

THE SENSORS, ACTUATORS AND MICROSYSTEMS LABORATORY SAMLAB

Valveless Micro Pump

AC electrokinetic pumping of liquids

Most of the micropumps that are available today present major drawbacks that affect their reliability. These mainly depend on the intrinsic fragility of moving parts, such as diaphragms and membranes, and on the complexity of the fabrication process. The study presented here aims at addressing these issues through the implementation of an AC electroosmosis pumping solution with no moving parts.

The project deals with modelling, microfabrication and characterisation of prototype pumps, having high pressure capability and moving-part-free operation.

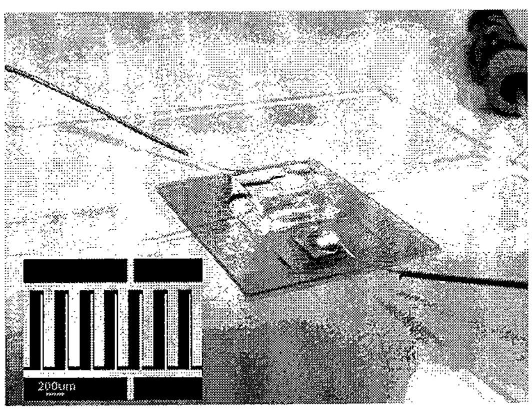

Prototype PDMS chip with 150-30µm electrode pattern.

Project partners:

Tronics Microsystems, Crolles, France

Scientific publications:

Improved Two-Side AC Electroosmotic Micropump, L. Ribetto, A. Homsy, and N.F. de Rooij, Oral presented at AMNAPLOC conference, Singapore, 2011

Flow recirculation when pumping liquids with AC electric fields, L. Ribetto, A. Homsy, N.F. de Rooij, Asia-Pacific Conference on Micro and Nano Transducers, Australia, 2010

Contact person:

Alexandra Homsy

SAMLAB'S MAIN TASKS

BioMEMS

EnviroMEMS

Micro and Nanofluidics

Nanotools

Optical MEMS

CONTACT

Sensors, Actuators and Microsystems Laboratory

Institute of Microengineering
EPFL STI
Rue Jaquet-Droz 1
Case postale 526
CH-2002 Neuchâtel, Switzerland

E-mail: lmt-ne-samlab@epfl.ch
Phone: ++ 41 32 720 51 21
Secretary: ++ 41 32 720 56 54
Fax: ++ 41 32 720 57 11

Location

EXHIBIT E

A HIGH-PERFORMANCE SILICON MICROPUMP FOR DISPOSABLE DRUG DELIVERY SYSTEMS

Didier Maillefer, Stephan Gamper, Béatrice Frehner, Patrick Balmer
Department of Microsystems, DEBIOTECH SA. (d.maillefer@debiotech.com), Lausanne, Switzerland
Harald van Lintel, Philippe Renaud
Institute of Microsystems, EPFL (Swiss Federal Institute of Technology), Lausanne, Switzerland

ABSTRACT

This paper describes the design, fabrication and experimental results of a new, low cost, high-performance silicon micropump developed for a disposable drug delivery system. The pump chip demonstrates linear and accurate (±5%) pumping characteristics for flow rates up to 2 ml/h with intrinsic insensitivity to external conditions. The stroke volume of 160 nl is maintained constant by the implementation of a double limiter acting on the pumping membrane. The actuator is dissociated from the pump chip.

The chip is a stack of three layers, two Pyrex wafers anodically bonded to the central silicon wafer. The technology is based on the use of SOI technology, silicon DRIE and the sacrificial etch of the buried oxide in order to release the structures. The result is a small size chip, suitable for cost-effective manufacturing in high volume.

The micropump chip is integrated into the industrial development of a miniature external insulin pump for diabetes care

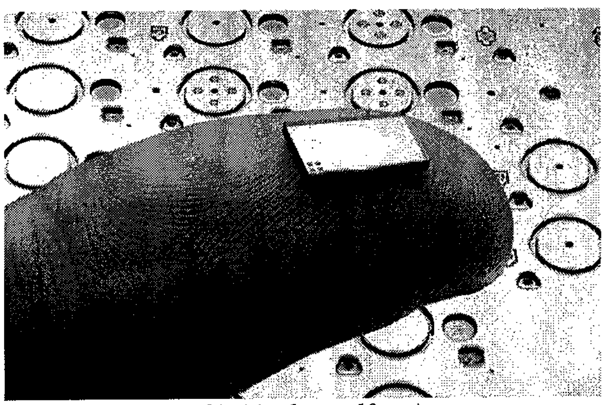

***Figure1:** micropump chip (size 6 mm x 10 mm)*

INTRODUCTION

Many micropumps recently described in the literature exhibit remarkable performances in terms of high flow rate (> 1 ml/min) and simple fabrication. In particular, the generation of single use, plastic based, valveless pumps demonstrates the validity of this approach. However, there are a number of applications requiring a low, precisely controlled flow rate (typically 10 µl/min). At MEMS'99, we reported on a high-performance micropump chip for an implantable drug delivery system **[1]**. The device presented here meets similar requirements of accuracy and reliability while achieving a drastic reduction of the manufacturing costs through a new design together with major size reduction and process simplification.

The micropump has been primarily developed for applications in drug delivery. Therefore it has to comply with specifications of accuracy better than ±5% over a wide range of external conditions such as pressure, temperature, viscosity. Being part of the drug's fluidic path, the micropump chip is defined as a single use device and included into the disposable set with a lifetime ranging from several days to several months depending on the application. Drug pumps are traditionally based on the peristaltic principle (rollers on a elastomeric tube) or a syringe drive. As compared with these pumping mechanism, the use of a silicon micropump offers major advantages in terms of system miniaturization and control over low flow rates. In our case, the dosage resolution (stroke volume 160 nl) is approximately one order of magnitude better than what is achievable with peristaltic or syringe pumps. These high performances make this pump chip particularly suited for critical application of delivery of very potent drugs such as subcutaneous injection of insulin for diabetes care.

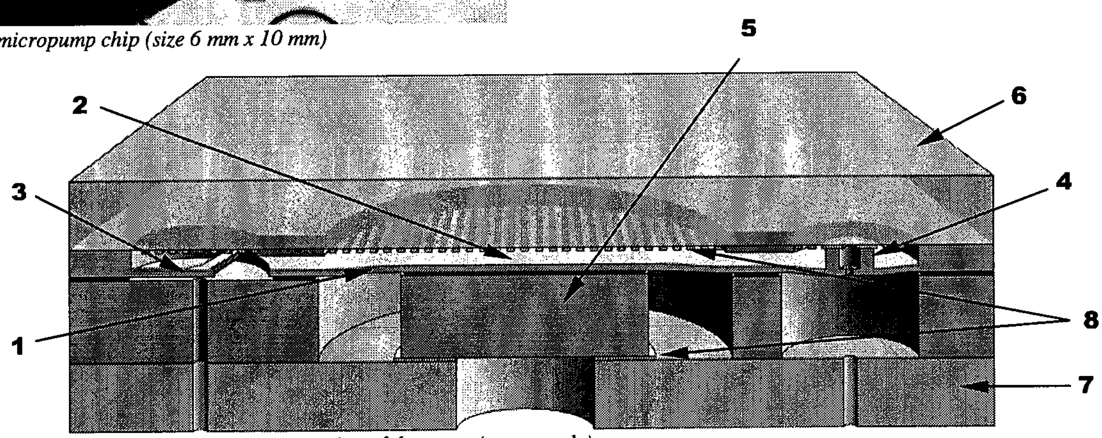

***Figure2**: Schematic cross section of the pump (not to scale)*

DESIGN

The micropump is based on the design published by Van Lintel and al. [5]. The working principle (shown in fig.2) is a volumetric pump with a pumping membrane (1) which compresses the pumping chamber (2). An inlet (3) and an outlet (4) check valves direct the liquid flow. The chip is a stack of three layers bonded together: one central silicon piece with micromachined pump structures sandwiched between two glass pieces, one having fluidic access holes. The actuator has not been integrated on the pump chip, essentially due to space constraints and the design of the pump being relatively independent of the nature and the characteristics of the actuator.

The performance of the pump is mainly determined by the implementation of a double limiter concept. The stroke amplitude of the pumping membrane (1) is mechanically defined by contact of its large mesa (5) to the upper (6) and lower (7) glass plates. By overdriving the actuator and controlling the range of the pumping membrane, the stroke volume is precisely determined and the pump becomes virtually insensitive to inlet pressure, outlet pressure, temperature and viscosity. Moreover this approach also allows for some latitude in the choice of actuator. Provided that the actuator is designed with enough displacement and force, the system can accommodate some tolerances of assembly and drift of characteristics. The actuator has been totally dissociated from the pumping mechanism. It is a single action (push) for the upward movement of the pumping membrane. The downward effect is ensured by the natural spring constant of the diaphragm. In our design, the membrane's displacement has been set to approximately 20 μm, yielding to a stroke volume of approximately 160 nl.

The pump chip has been optimized for compression ratio. The dead volume has been reduced to a minimum. The resulting compression ratio is: $\varepsilon = (\Delta V + V0) / V0 = 3.3$ where ΔV is the stroke volume and V0 is the dead volume. This ratio measures the ability of the pump to compress gas. The channels geometry have also been designed to offer minimum resistance to surface tension in the occurrence of an air-liquid interface. Consequently, the pump has the ability to pump gas, to self prime and to pump air bubbles through. In addition, the fluid dynamic of the pump has been improved by patterning the thin layer (8) deposited on the glass surface in contact with the silicon pumping membrane, thus avoiding important squeeze film effect.

In order to prevent free flow, the outlet valve is designed with a pretension of approximately 100 mbar obtained by pre-displacement of the valve seat. If required by the application, the micropump can be protected from particulate contamination through the integration of an on-chip barrier filter. The pump fluidic path is then virtually sealed in cleanroom condition as the stack of wafers is bonded. Such an on-chip particulate filter is described in [1].

This micropump chip has been developed for disposable applications. Therefore, acceptable manufacturing costs have been obtained by a drastic reduction of the chip size. The dimensions are now 6 mm x 10 mm, which is a factor 3.2 improvement as compared with the previous implantable pump chip [1].

TECHNOLOGY

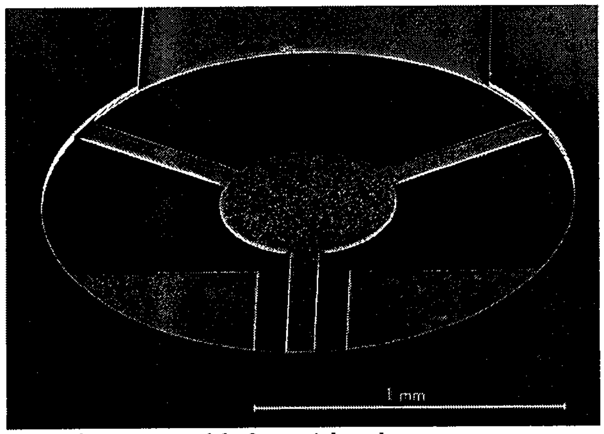

Figure 3: SEM view of the 3 arms inlet valve

The technology is based on the use of SOI (Silicon On Insulator) wafer, silicon DRIE (Deep Reactive Ion Etching) and the sacrificial etch of the buried oxide layer in order to release the structures. This approach brings several major advantages over the more traditional silicon bulk micromachining techniques:

- It permits the design of an original inlet valve (patent pending) optimal in terms of dead volume and process compatibility with the other elements of the pump.
- It represents a major simplification of the process and brings additional design freedom. As a comparison, this process only requires 3 etch steps in silicon and a total of 5 masks while the process of the previous chip required 5 different levels and a total of 12 masks.
- It achieves a very good control over the thickness of the membranes and fluidic channels thanks to the well defined SOI thickness and the etch stop oxide layer, leading to well defined mechanical characteristics. The membranes of the different elements are located on the same side of the wafer and the dead volume is minimized.
- The deep etch with vertical walls of the backside allow high aspect ratio structure and channels and the placement of the different elements in close proximity. It also allows small size circular membranes. As a result, the whole pump becomes very compact.

Extensive process development has been necessary for the dry etch of silicon with an etch stop on oxide. The critical parameters are the etch uniformity and lateral under-etch, given the important etch depth (> 300 μm) on the backside and the large distribution of area of the etched structures.

Besides this key technology, the process is also based on Pyrex-silicon anodic bonding for the assembly of the three wafers of the stack. Each of the glass plate has a thin layer of sputtered titanium (8) patterned to prevent bonding of the flexible membranes and to ensure pre-displacement of the pumping membrane and the outlet valve

With the current design, almost 100 chips are fabricated on a 100 mm wafer, raising to over 200 per 150 mm wafer. Consequently, despite the high initial cost of SOI wafers, the technology becomes very cost effective for high-volume production (> 1 M units/yr).

The back-end of this chip is very specific to the application. The packaging, fluidic and electrical connections as well as the design of the actuator are being developed with the specifications of the complete drug delivery system.

EXPERIMENTAL RESULTS

The present design is currently in the validation phase. The characterization is not complete yet and the following measurement results must be considered as preliminary.

The back-end operations necessary to permit adequate laboratory characterization of the chip simply consists of epoxy gluing the fluidic connectors for standard medical grade PVC tubes.

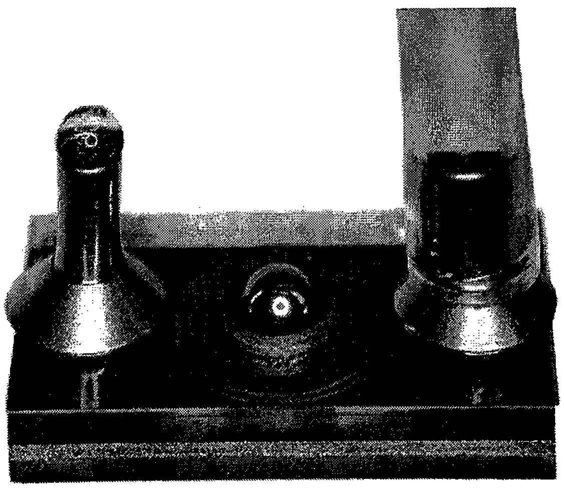

Figure 4: *Photo of the pump chip with laboratory back-end*

We have successfully implemented various types of actuators: piezoelectric bimorph discs, piezoelectric bimorph cantilevers and direct pneumatic (N_2 pressure) actuation on the back of the pumping membrane. We are also experimenting with electromagnetic and SMA (Shape Memory Alloy) actuation. We have obtained consistent results with various actuation methods, which validates the concept of the double limiter. Also visible on fig.4 is a steel ball glued on the pumping membrane's mesa. This part serves as a force transmitter between the actuator and the pump in order to ensure a single point contact and a minimum transmission of torque to the membrane.

All measurements of stroke volume and flow rate have been acquired using the gravimetric method with a micro-balance Sartorius MC5 (resolution 1 µg). Pure water has been used for the tests. Pressure variations on the inlet and outlet have been applied by a water column in the range -100 mbar to +100 mbar and by a pressurized water bottle for higher and lower pressure values.

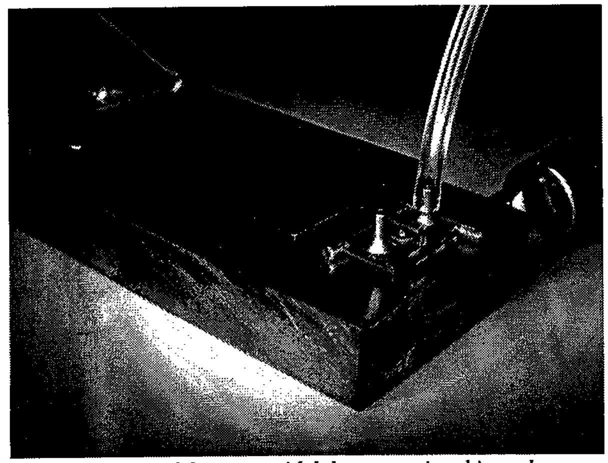

Figure 5: *Photo of the pump with laboratory piezo bimorph cantilever actuator*

- **Stroke volume:** 158 nl

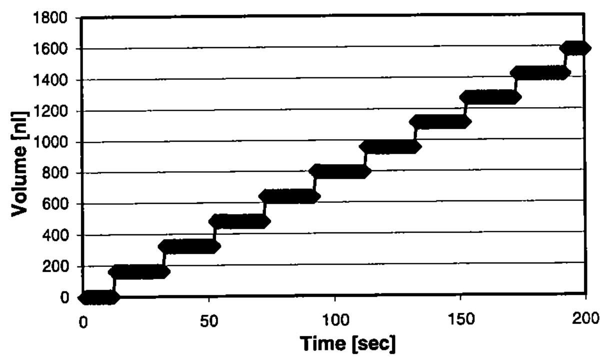

Figure 6: *Plot of the volume of liquid pumped vs. time at a frequency of 0.05 Hz. The acquisition frequency is 1 Hz. The pulsatile nature of the flow rate is clearly visible with a very reproducible stroke volume (standard deviation 1.1 nl)*

- **Flow rate**: 0 to 2 ml/hr

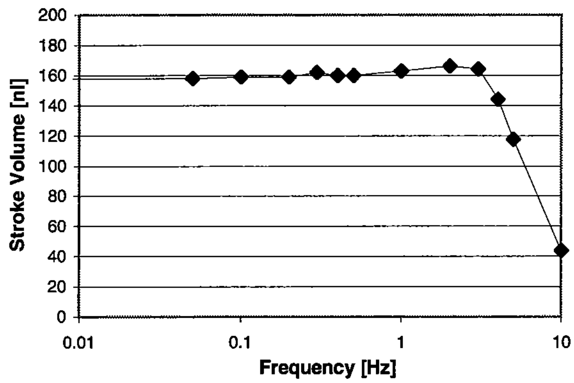

__Figure 7__: Plot of the stroke volume as function of the actuation frequency. This characteristic shows that the stroke volume is almost constant, i.e. the flow rate is proportional to the frequency up to approximately 3 Hz, corresponding to a flow rate of 1.7 ml/h or a maximum of 2 ml/h in the non proportional range.

- **Outlet pressure range**: -100 mbar to + 100 mbar
  (system specifications)

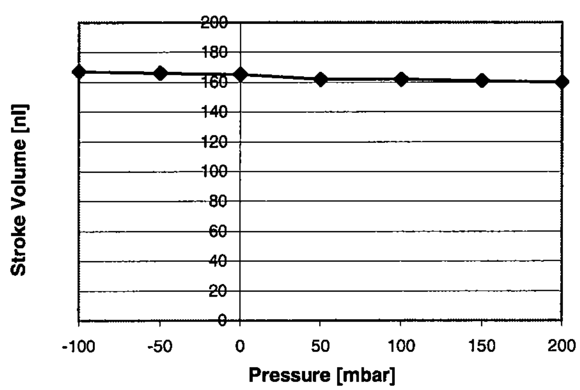

__Figure 8__: Plot of the stroke volume as a function of outlet pressure showing the relative insensitivity towards variations of pressure up to 200 mbar Note that the upper limit of outlet pressure essentially depends on the power of the actuator. This pump chip has demonstrated consistent stroke volume with pressure up to 1 bar.

- **Inlet pressure range**: -100 mbar to + 100 mbar
  (system specifications)

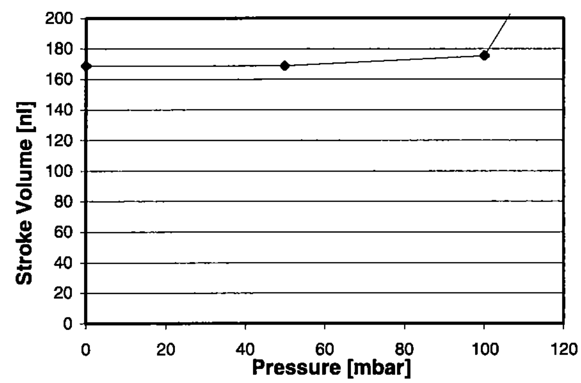

__Figure 9__: Plot of the stroke volume as a function of inlet pressure showing the relative insensitivity towards variations of pressure. Note that the upper limit of inlet pressure depends on the pretension of the outlet valve, after which the pump is in free flow mode.

- **Leakage**: The leak rate of the pump has not yet been properly characterized. However, tests on functional pumps with pressurized inlet (+50 mbar) and outlet (+100 mbar) have not revealed leak rates higher than 1 µl/h, which is sufficient for the required accuracy.

- **Viscosity**: The application require that the chip pumps liquids of various compositions at temperatures ranging from 5°C to 40°C within the nominal accuracy and without compensation table. This can be achieved because of the double limiter concept. This capability was already demonstrated by the previous generation of pump [1] up to 10 mPa s.

- **Accuracy**: We expect this pump to meet the required overall accuracy of ±5% within the specified conditions.

- **Longevity**: The expected lifetime of this pump chip used in a disposable drug delivery set is limited to a few weeks. However, for alternative applications, this requirement will likely be extended up to one year. Although this longevity has naturally not yet been demonstrated on this chip, we have acquired reliability data for almost two years with the previous generation of pump MIP.

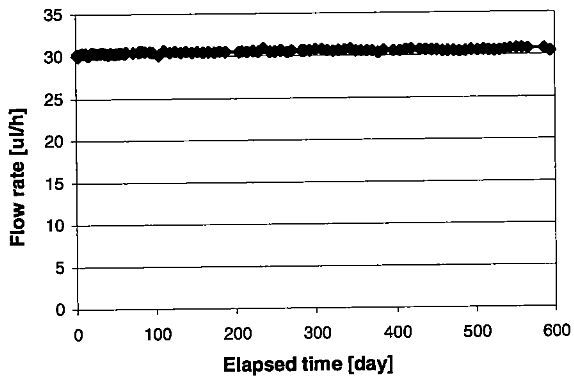

Figure 10: Plot of the flow rate stability of the MIP chip [1]. The actuation frequency is 0.05 Hz and the sampling period is one week.

- **Drug compatibility**: The materials in contact with the drug are exclusively silicon, silicon dioxide, pyrex glass and titanium, all known to be biocompatible. For a variety of drugs with a pH ranging from neutral to extreme acid, drug compatibility is ensured as follows:
  - No damage (corrosion) to the device
  - No damage to the PAI (Pharmaceutically Active Ingredient)
  - No release of toxic products in the drug

APPLICATIONS AND CONCLUSION

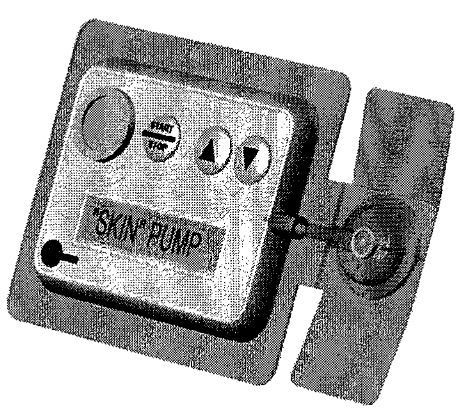

Figure11: Conceptual drawing of the tape-on-skin insulin pump

This micropump is the key component of the product in development aiming at the realization of a miniature pump for subcutaneous injection of insulin for diabetes care. The novelty of the system is essentially the level of miniaturization, allowing the patient to carry the pump directly taped onto the skin together with the injection soft needle. The system is conveniently operated from a remote control device through secured RF communication. Additional benefits of the use of MEMS pumping mechanism are the improved safety, resolution, programmability and autonomy. As part of the fluidic path, the micropump chip is fully disposable while the actuator remains together with the control electronics in the permanent pump housing.

Starting from this set of specifications, the pump is adaptable to a wide range of drugs with pH ranging from neutral to acidic. It is particularly suited for very potent drugs such as some peptides requiring accurate delivery at low flow rates. Besides this main application in drug delivery, it is believed that this micropump meets the requirements of a variety of micro-dosing applications such as μ-TAS or Bio-MEMS. We are currently evaluating the use of such micropumps for laboratory automation equipment. An array of pump chips would be assembled for micro-pipetting operations in 96, 384, and 1536 wells microplates.

In conclusion, this development demonstrates the feasibility of a silicon micropump with high requirements of accuracy and reliability, with manufacturing cost compatible with a single use application. This technology is now sufficiently mature to be integrated in a real industrial product development with target commercialization in three years.

ACKNOWLEDGEMENTS

The authors would like to thank Mr. Ph. Flückiger, Mr. C. Hibert and the whole team of CMI (EPFL) for the fruitful collaboration in the process development and the processing of prototype runs.

REFERENCES

1. D. Maillefer, H. van Lintel, G. Rey-Mermet, R. Hirschi., "A high-performance silicon micropump for an implantable drug delivery system", Proc. of the 12th *IEEE MEMS 1999 Technical Digest*, Orlando, FL, USA, 1/17-21/99, pp 541-546

2. M. Stehr, H. Gruhler, H. Straatmann, S. Messner, H. Sandmeier, R. Zengerle., "The selfpriming VAMP", Proc *Transducers 1997 Technical Digest*, Chicago, IL, USA, 6/16-19/97, pp 351-352.

3. K.-P. Kämper, J. Döpper, W. Ehrfeld, S. Oberbeck., A self-filling low-cost membrane micropump, Proc of the 11th *IEEE MEMS 1998 Technical Digest*, Heidelberg, Germany, 1/25-29/98, pp 432-437..

4. M. Richter, R. Linnemann, P. Woias, "Robust design of gas and liquid micropumps", *Sensors & Actuators* A68 (1998) pp.480-486

5. H. van Lintel ,.F. van de Pol, S. Bouwstra, "A Piezoelectric micropump based on micromachining of silicon", *Sensors & Actuators* A15 (1988) pp.153-168

EXHIBIT F

Micropump

From Wikipedia, the free encyclopedia

Although any kind of small pump is often referred to as **micropump**, a more accurate and up-to-date definition restricts this term to pumps with functional dimensions in the micrometre range. Such pumps are of special interest in microfluidic research, and have become available for industrial product integration in recent years. Their miniaturized overall size, potential cost and improved dosing accuracy compared to existing miniature pumps fuel the growing interest for this innovative kind of pump.

Contents

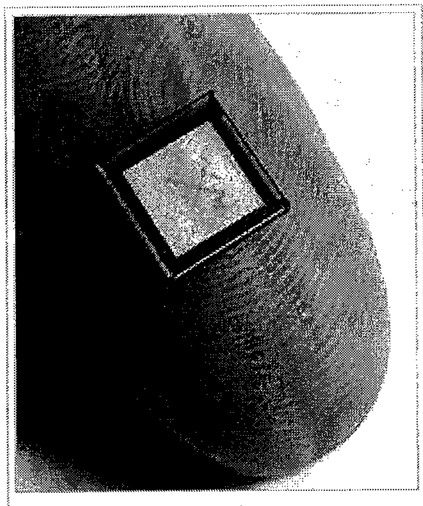

World's smallest micropump

Types and technology

In this sense, first true micropumps were reported on in 1975.[1] However, the micropumps developed by Jan Smits and Harald Van Lintel in the early 1980s are considered to be the first genuine MEMS micropumps,[2] and sparked the interest in shrinking the size of a fully functional pump to new dimensions.

Within the microfluidic world physical laws change their appearance: As an example, volumetric forces, such as weight or inertia, often become negligible, whereas surface forces can dominate fluidical behaviour, especially when gas inclusion in liquids is present. With only a few exceptions, micropumps rely on micro-actuation principles, which can reasonably be scaled up only to a certain size.

Micropumps can be grouped into mechanical and non-mechanical devices: Mechanical systems contain moving parts, which are usually actuation and valve membranes or flaps. The driving force can be generated by utilizing piezoelectric, electrostatic, thermo-pneumatic, pneumatic or magnetic effects. Non-mechanical pumps function with electro-hydrodynamic, electro-osmotic, electrochemical [3] or ultrasonic flow generation, just to name a few of the actuation mechanisms that are currently studied.

Industrial integration

Any kind of active microfluidic handling or analysis system (µTas, Lab-on-a-Chip System) requires some kind of micropump system. In addition, macro-fluidic systems which rely on miniature pumps might be reduced in size or enhanced in their functionality by integrating a micropump. Emerging technologies, such as portable fuel cell applications will benefit when smaller yet more energy efficient pumps become available on the market. In 2003, the first commercial availability of a micropump was announced. Other companies have followed with their own pumps. All commercially available micropumps depend on piezoelectric actuation and incorporate passive check valves.

Micropumps made of polymers appear to yield potentially low unit prices, while silicon micropumps prove to be the smallest pump devices in the world.

It has to be seen which of these pumps will be the first one to be successfully integrated into a commercially available product.

See also

- Electroosmotic pump
- Glossary of fuel cell terms

References

1. ^ L.J. Thomas, S.P. Bessman, Micropump powered by piezoelectric disk benders, United States Patent, Jan. 1975
2. ^ Woias, P, Micropumps - past progress and future prospects, Sensors and Actuators B. Vol. 105, no. 1, pp. 28-38. 14 Feb. 2005
3. ^ Neagu, C et al., An electrochemical microactuator: principle and first results. Journal of Microelectromechanical Systems, Vol. 5, no 1, pp 2–9, 1996

External links

- TCS Micropump Ltd (http://www.micropumps.co.uk)
- Osmotex AG (http://www.osmotex.ch)
- First commercialisation of a micropump (http://www.thinxxs.de/main/presse/pressemitteilungen/10-dezember-2004.html)
- Plastic micropump (http://www.bartels-mikrotechnik.de/index.php/Micropumps.html)
- Silicon micropump (http://www.debiotech.com/products/msys/mip.html)
- Low power consumption piezoelectric micropump (http://www.microjet.com.tw/english/micropump.htm)
- Low-cost electrochemical micropump (http://www.biflow-systems.com/technology_pumps.php)

EXHIBIT G

BIO-CHEM FLUIDICS

BIO-CHEM VALVE Solenoid Operated Micro-Pumps

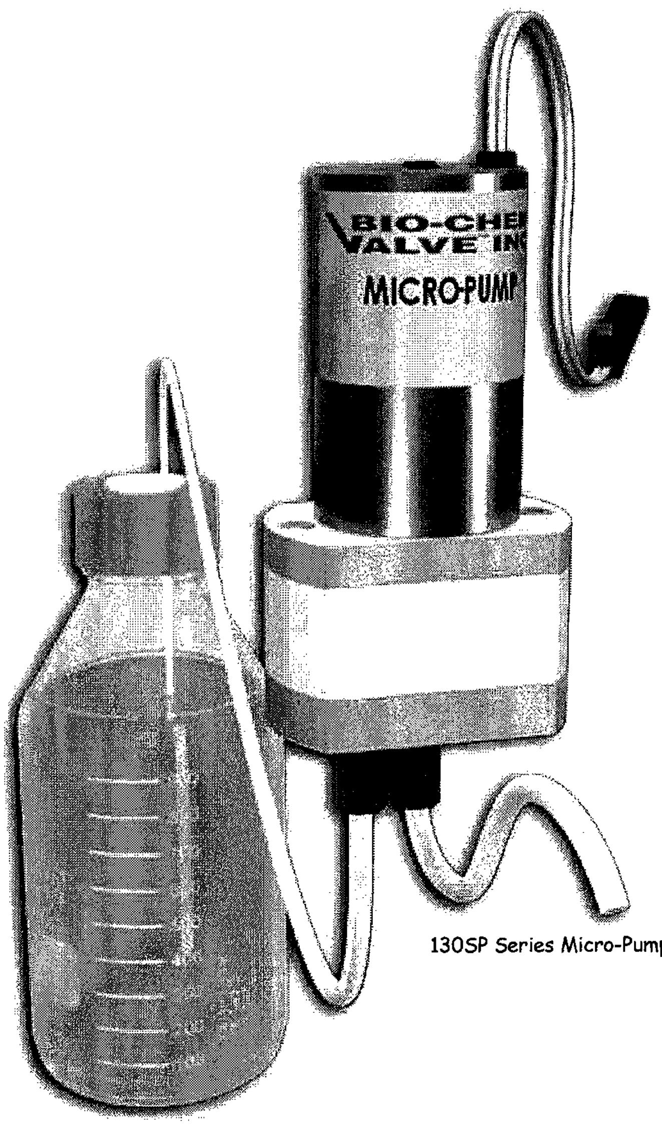

130SP Series Micro-Pump

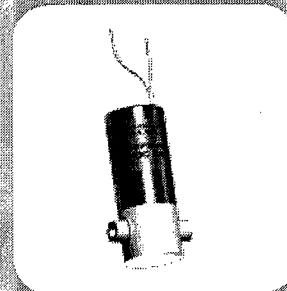

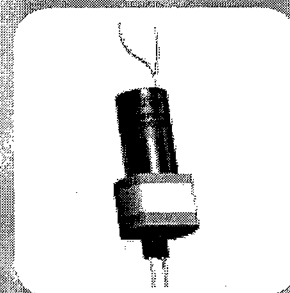

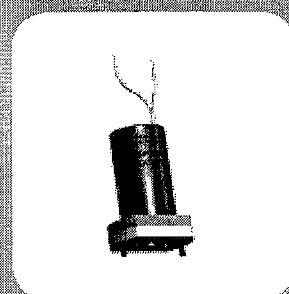

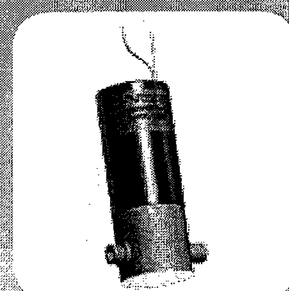

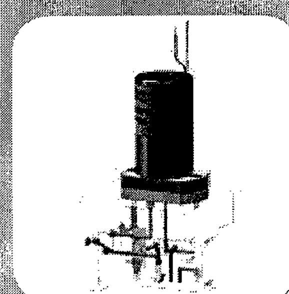

A HALMA COMPANY

INDEX

MICRO-PUMPS GENERAL INFORMATION

What is a Micro-Pump?

A Micro-Pump is a solenoid operated device designed to provide a precise, repeatable and discrete dispensed volume of fluid. The flow path is isolated from the operating mechanism by a flexible diaphragm. When the solenoid is energized, the diaphragm is retracted creating a partial vacuum within the pump body. This pulls liquid through the inlet check valve (A) and simultaneously closes the outlet check valve (B). When the solenoid is de-energized a spring pushes the diaphragm down, expelling a discrete volume of liquid through check valve B while simultaneously closing check valve A. Micro-Pumps require a complete on-off cycle for each discrete dispense. Repeatedly cycling the solenoid creates a pulsed flow *(refer to "Accurate discrete dispense volumes" in next column)*.

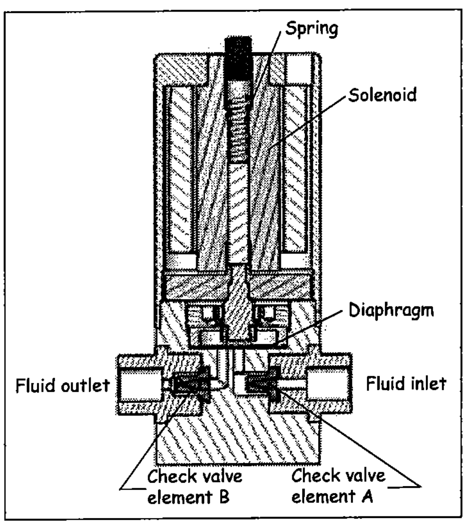

Features of the Bio-Chem Valve™ Micro-Pump

Inert materials

Our pumps provide a non-metallic inert fluid path for the dispensing of high purity or aggressive fluids. There is a range of different materials available for all the wetted parts of the pumps - body, diaphragm and check valve. Material combinations can be chosen to suit the application *(refer to individual product selection pages for standard combinations - custom combinations are available, refer to page 14)*.
Body materials: PPS, PTFE, PEEK™, POM
Diaphragm materials: EPDM, PTFE
Check valve materials: EPDM, FKM, FFKM

Self-priming

At start-up, pumps are able to draw air. The suction created by the pumps is sufficient to pull liquids from an unpressurized container located up to 4'3" (1.3m) beneath the pump. Once the pump is primed, it is able to generate around 5psi (0.3bar) pressure, equating to 11'6" (3.5m) of water.

Continuous duty

The pumps are capable of continuous duty. They are suitable for up to 20 million actuations, corresponding to nearly 3,000 hours of continuous use at a 2 Hz cycle rate.

Accurate discrete dispense volumes

Dispense volumes range from 20µl to 250µl per cycle. The pumps can be cycled at up to 2 Hz for the smallest version and 1.6 Hz for the largest. Pumps can be operated at less than the maximum cycle rate by increasing the length of the "off" time. The "on" time should remain unchanged to retain dispense accuracy.

Micro-Pump Selection Guide

1. Select pump style; either Ported or Manifold mount and work from the appropriate table:
    - Ported for direct connection with ¼"-28 fittings (*5⁄16"-24 for 150SP*)
    - Manifold mount for use with manifolds (see page 13)

Then:

2. Locate the volumetric characteristics that best suit your needs
3. Choose your preferred body material depending on the level of chemical inertness you require
4. Turn to the pages indicated to see full details and ordering information for each pump.

Ported

Volumetric output		Body Material			
Discrete Dispense Vol (µl)	Max flow rate (ml/min)	PTFE	PPS	PEEK™	POM
20	2.4				
30	3.6	130SP (pg. 7)	120SP (pg. 5)	120SP (pg. 5)	130SP (pg. 7)
40	4.8				
50	6.0				
60	7.2				
100	9.6				
125	12.0				
150	14.4				
175	16.8		150SP (pg. 9)	150SP (pg. 9)	
200	19.2				
225	21.6				
250	24.0				

Manifold mounted

Volumetric output		Body Material			
Discrete Dispense Vol (µl)	Max flow rate (ml/min)	PTFE	PPS	PEEK™	POM
20	2.4				
30	3.6	139SP (pg. 11)		139SP (pg. 11)	139SP (pg. 11)
40	4.8				
50	6.0				
60	7.2				

Polymers referenced in this brochure:

EPDM = ethylene-propylene-diene
ETFE = ethylene tetrafluoroethylene
FEP = fluorinated ethylene propylene
FKM = fluorinated elastomer
FFKM = perfluoro elastomer
PEEK™ = polyetheretherketone
POM = polyoxymethylene (Acetal resin)
PPS = polyphenelyne sulfide
PTFE = polytetrafluoroethylene.

Micro-Pump Applications

Waste effluent removal

Many types of analytical instruments incorporate a waste sump or container that collects any liquids that may have leaked inside the instrument. These waste streams can have many constituents and could be regarded as a biohazard if allowed to collect in the bottom of the instrument.

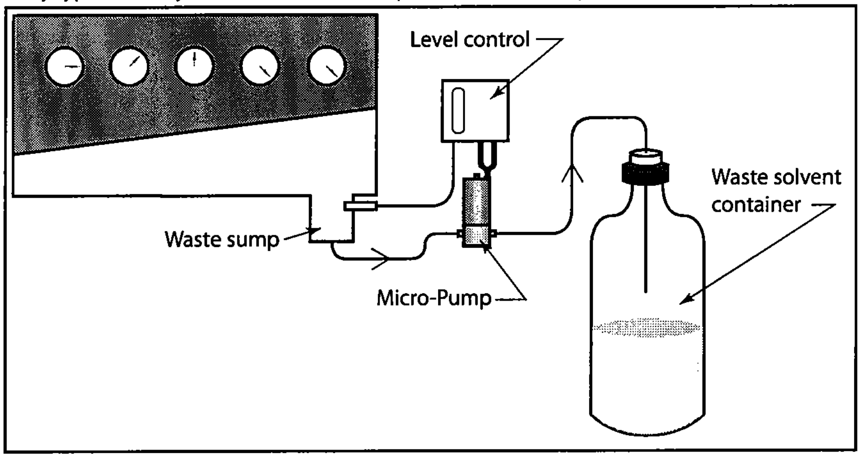

Bio-Chem Fluidics Micro-Pumps lend themselves to this application because they offer a completely inert flow path capable of handling the most aggressive of effluents, while maintaining repeatable and consistent pumping rates.

A Micro-Pump can be hooked up to the level control sensor and be cycled as necessary to empty the sump to an external waste solvent container.

Chemical dosing

In this application Bio-Chem Fluidics Micro-Pumps are used to pre-treat a liquid stream prior to analysis. The pumps are capable of pumping highly aggressive chemical reagents from a remote location (outside of the instrument) and accurately dispense predetermined volumes of the reagents directly into the main liquid stream.

This eliminates the need for an intermediate mixing step inside the instrument.

Micro-Pumps can be used in either continuous or intermittent mode depending on the demands of the instrument.

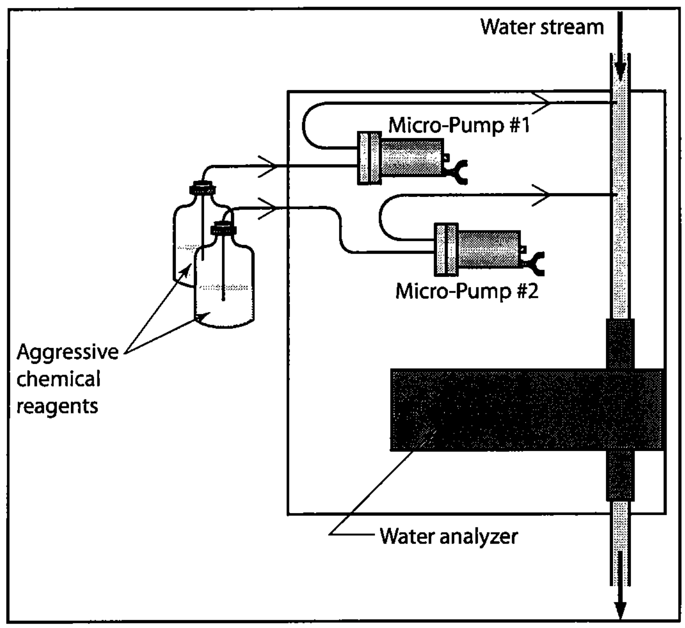

Sterilizing application

Sterilizing solution can be of a very high purity which almost always translates to additional expense. In this application a Bio-Chem Fluidics Micro-Pump takes small amounts of the sterilizing liquid from a reservoir and dispenses very accurate "drips" onto a heating panel inside a sterilizing chamber. When the liquid hits the panel, it instantly vaporizes forming a "sterilizing vapor" inside the chamber. The vapor is very efficient at sterilizing the internals of complicated components.

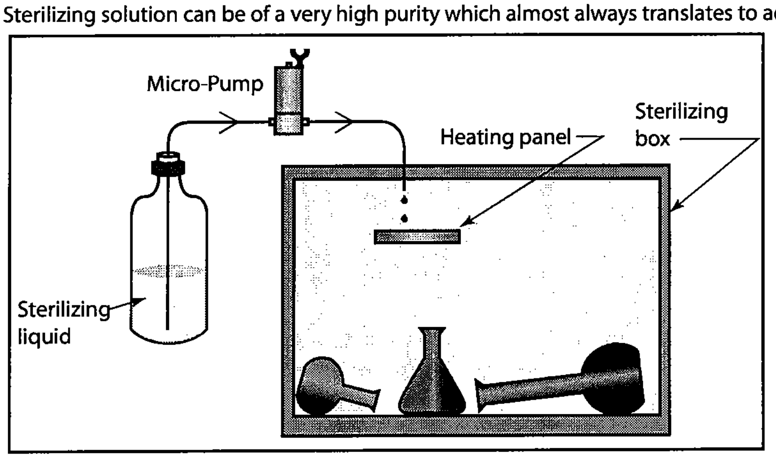

The Micro-Pumps provide highly repeatable and consistent delivery of the sterilizing fluid into the chamber. This safe and cost effective method of pumping high purity liquids has proved very successful.

120SP SERIES MICRO-PUMP

For precise dispensing between 20 and 60µl and flow rates up to 7.2 ml/min

- Self-priming
- 20-60µl discrete dispense volumes
- Up to 7.2 ml/min maximum flow rate
- ¼"-28 UNF threaded ports

The 120SP series Micro-Pumps are solenoid operated, with the operating mechanism isolated from the flow path by a diaphragm. Check valves situated at the inlet and outlet of the pump control the direction of flow. The combination of materials for each component can be selected to best suit your specific application.

Materials available for the wetted parts are:

- Body materials: PPS, PEEK™
- Diaphragm materials: PTFE, EPDM
- Check valve materials: EPDM, FKM, FFKM

ARRANGEMENT

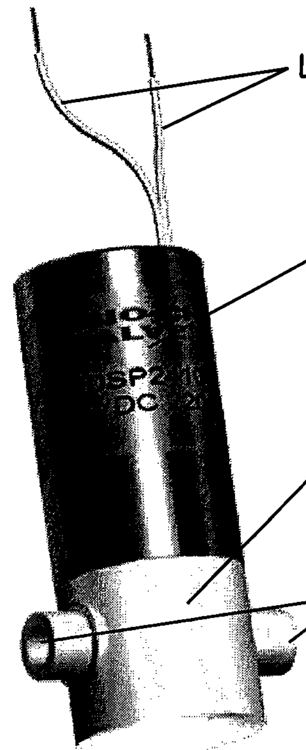

120SP series options

NOTE: For 24 VDC, replace 120SP12 with 120SP24 in any of the part numbers listed.

PART NO.	DISPENSE VOL (µL)	BODY MATERIAL	DIAPHRAGM MATERIAL	CHECK VALVE MATERIAL
12 VDC; 20µl dispense				
120SP1220-4EE	20	PPS	EPDM	EPDM
120SP1220-4TV	20	PPS	PTFE	FKM
120SP1220-4TP	20	PPS	PTFE	FFKM
120SP1220-5EE	20	PEEK™	EPDM	EPDM
120SP1220-5TV	20	PEEK™	PTFE	FKM
120SP1220-5TP	20	PEEK™	PTFE	FFKM
12 VDC; 30µl dispense				
120SP1230-4EE	30	PPS	EPDM	EPDM
120SP1230-4TV	30	PPS	PTFE	FKM
120SP1230-4TP	30	PPS	PTFE	FFKM
120SP1230-5EE	30	PEEK™	EPDM	EPDM
120SP1230-5TV	30	PEEK™	PTFE	FKM
120SP1230-5TP	30	PEEK™	PTFE	FFKM

PART NO.	DISPENSE VOL (µL)	BODY MATERIAL	DIAPHRAGM MATERIAL	CHECK VALVE MATERIAL
12 VDC; 40µl dispense				
120SP1240-4EE	40	PPS	EPDM	EPDM
120SP1240-4TV	40	PPS	PTFE	FKM
120SP1240-4TP	40	PPS	PTFE	FFKM
120SP1240-5EE	40	PEEK™	EPDM	EPDM
120SP1240-5TV	40	PEEK™	PTFE	FKM
120SP1240-5TP	40	PEEK™	PTFE	FFKM
12 VDC; 50µl dispense				
120SP1250-4EE	50	PPS	EPDM	EPDM
120SP1250-4TV	50	PPS	PTFE	FKM
120SP1250-4TP	50	PPS	PTFE	FFKM
120SP1250-5EE	50	PEEK™	EPDM	EPDM
120SP1250-5TV	50	PEEK™	PTFE	FKM
120SP1250-5TP	50	PEEK™	PTFE	FFKM
12 VDC; 60µl dispense (Note: EPDM diaphragm for all 60 µl options)				
120SP1260-4EE	60	PPS	EPDM	EPDM
120SP1260-5EE	60	PEEK™	EPDM	EPDM

INSTALLATION DRAWING

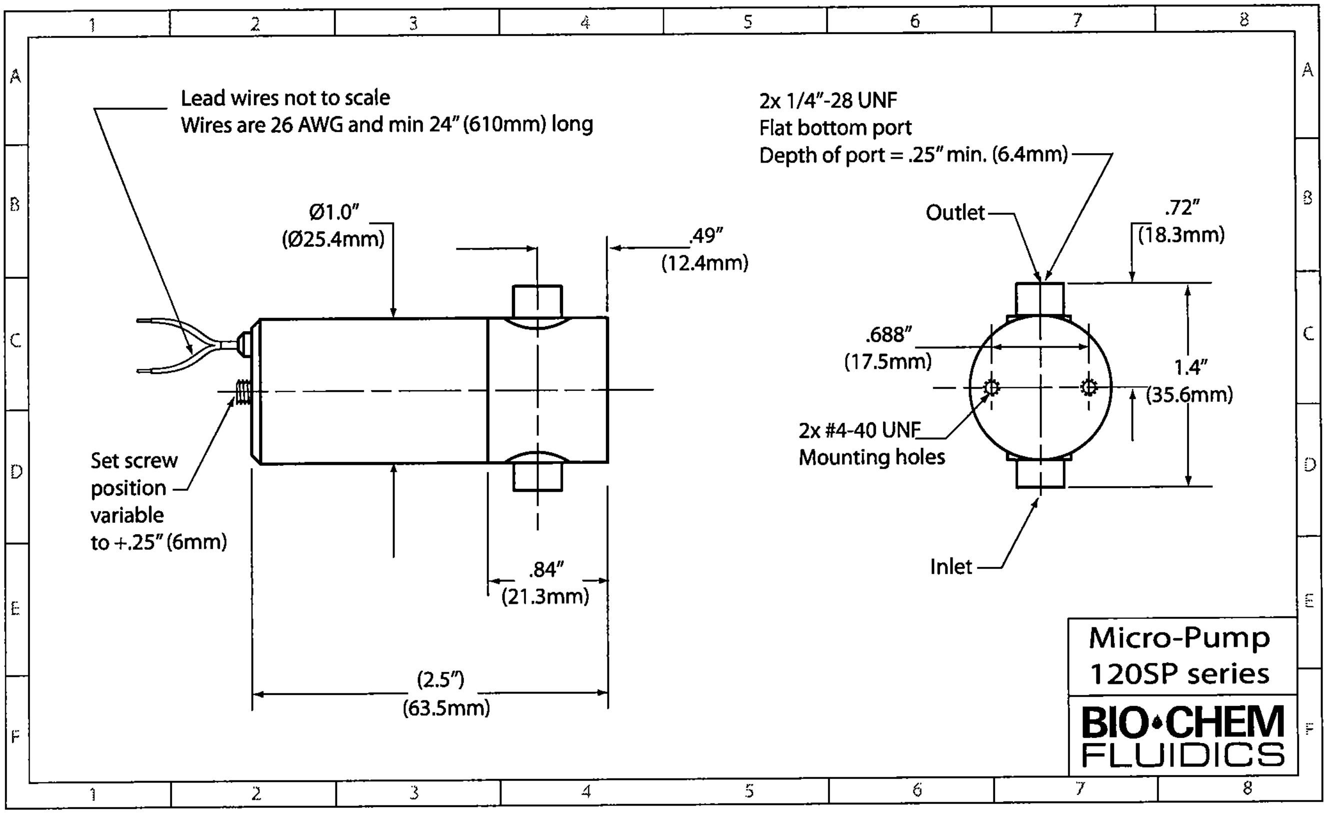

SPECIFICATIONS

120SP Fluid Data					
Dispense Volume (µl)	20	30	40	50	60
Set-point accuracy	+/- 10%	+/- 10%	+/- 10%	+/- 10%	+/- 10%
Repeatability	+/- 5%	+/- 5%	+/- 5%	+/- 5%	+/- 5%
Max flow rate (µl/min)	2400	3600	4800	6000	7200
Internal vol (µl)	105	105	105	105	105

120SP Electrical Data				120SP Cycle Rates		
Voltage	Power @70°F (21°C)	Current @70°F (21°C)	Effective continuous power @ max cycle rate	Fixed "on" time	Min "off" time	Max cycle rate
12 VDC	4.0 Watts	0.32 amps	1.2 Watts	150 msec	350 msec	2.0 Hz
24 VDC	4.0 Watts	0.16 amps	1.2 Watts			

Recommended tubing for 120SP
Inlet & outlet, 1/32" (0.80mm) ID, hardwall tubing, PART NO. 008T16-080

120SP Micro-Pumps can be cycled at up to 2 Hz. To maintain pumping precision the voltage "on" time should remain fixed - the pumping rate can be changed by increasing the "off" time.

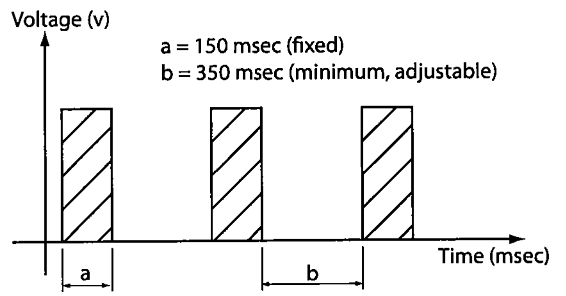

130SP SERIES MICRO-PUMP

For precise dispensing between 20 and 60µl and flow rates up to 7.2 ml/min

- Self-priming
- 20-60µl discrete dispense volumes
- Up to 7.2 ml/min maximum flow rate
- ¼"-28 UNF threaded ports
- Most inert body material for harshest applications

The 130SP series Micro-Pumps are solenoid operated, with the operating mechanism isolated from the flow path by a diaphragm. Check valves situated at the inlet and outlet of the pump control the direction of flow. The combination of materials for each component can be selected to best suit your specific application.

Materials available for the wetted parts are:

- Body materials: PTFE, POM
- Diaphragm materials: PTFE, EPDM
- Check valve materials: EPDM, FKM, FFKM

130SP series options

NOTE: For 24 VDC, replace 130SP12 with 130SP24 in any of the part numbers listed.

PART NO.	DISPENSE VOL (µL)	BODY MATERIAL	DIAPHRAGM MATERIAL	CHECK VALVE MATERIAL
12 VDC; 20µl dispense				
130SP1220-1TP	20	PTFE	PTFE	FFKM
130SP1220-6TV	20	POM	PTFE	FKM
130SP1220-6EE	20	POM	EPDM	EPDM
12 VDC; 30µl dispense				
130SP1230-1TP	30	PTFE	PTFE	FFKM
130SP1230-6TV	30	POM	PTFE	FKM
130SP1230-6EE	30	POM	EPDM	EPDM
12 VDC; 40µl dispense				
130SP1240-1TP	40	PTFE	PTFE	FFKM
130SP1240-6TV	40	POM	PTFE	FKM
130SP1240-6EE	40	POM	EPDM	EPDM
12 VDC; 50µl dispense				
130SP1250-1TP	50	PTFE	PTFE	FFKM
130SP1250-6TV	50	POM	PTFE	FKM
130SP1250-6EE	50	POM	EPDM	EPDM
12 VDC; 60µl dispense				
130SP1260-6EE	60	POM	EPDM	EPDM

ARRANGEMENT

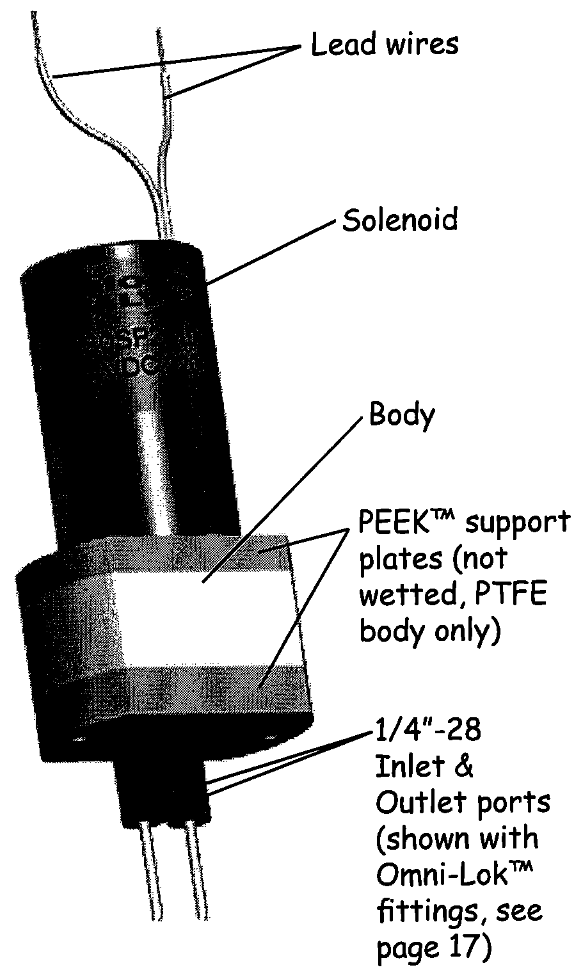

INSTALLATION DRAWING

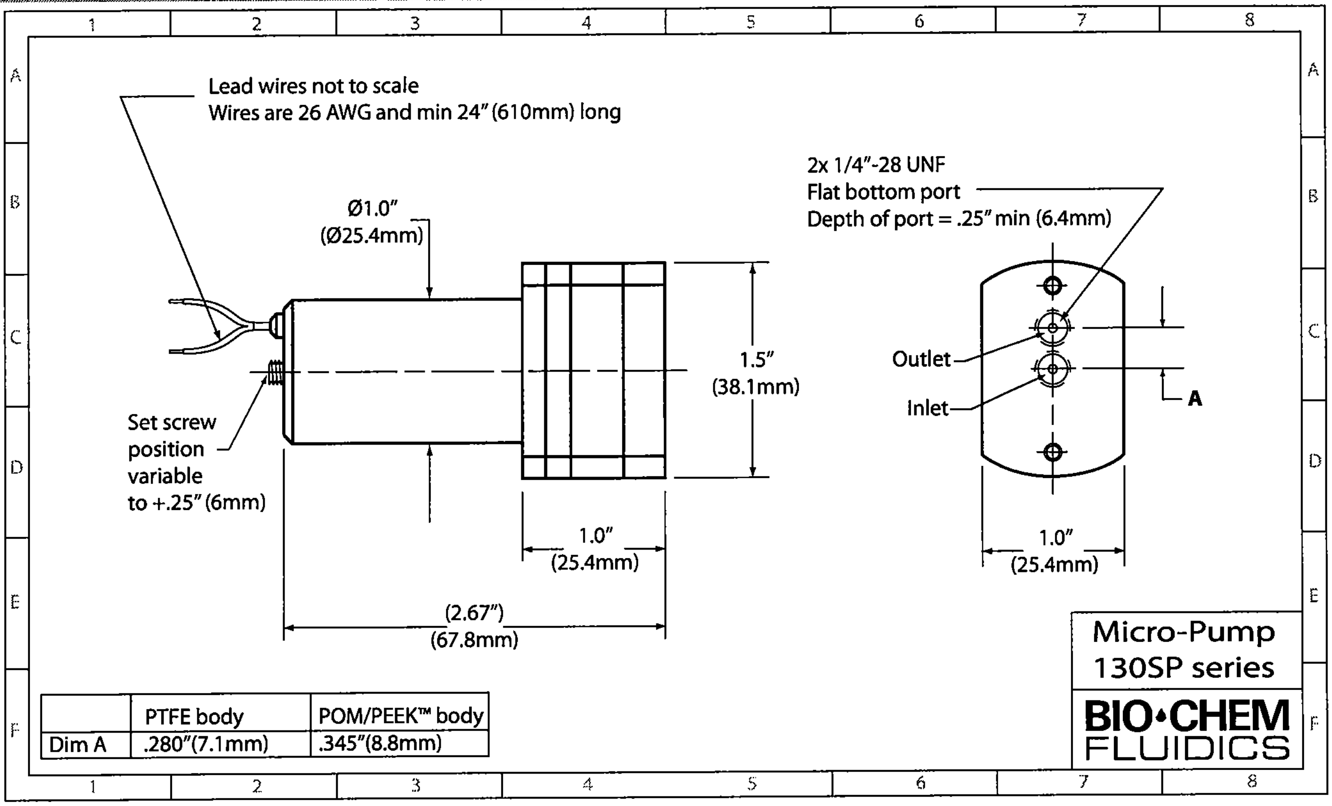

SPECIFICATIONS

130SP Volumetric Data					
Dispense Volume (µl)	20	30	40	50	60
Set-point accuracy	+/- 10%	+/- 10%	+/- 10%	+/- 10%	+/- 10%
Repeatability	+/- 5%	+/- 5%	+/- 5%	+/- 5%	+/- 5%
Max flow rate (µl/min)	2400	3600	4800	6000	7200
Internal vol (µl)	105	105	105	105	105

130SP Electrical Data				130SP Cycle Rates		
Voltage	Power @70°F (21°C)	Current @70°F (21°C)	Effective continuous power @ max cycle rate	Fixed "on" time	Min "off" time	Max cycle rate
12 VDC	4.0 Watts	0.32 amps	1.2 Watts	150 msec	350 msec	2.0 Hz
24 VDC	4.0 Watts	0.16 amps	1.2 Watts			

Recommended tubing for 130SP
Inlet & outlet, 1/32" (0.80mm) ID, hardwall tubing, PART NO. 008T16-080

130SP Micro-Pumps can be cycled at up to 2 Hz. To maintain pumping precision the voltage "on" time should remain fixed - the pumping rate can be changed by increasing the "off" time.

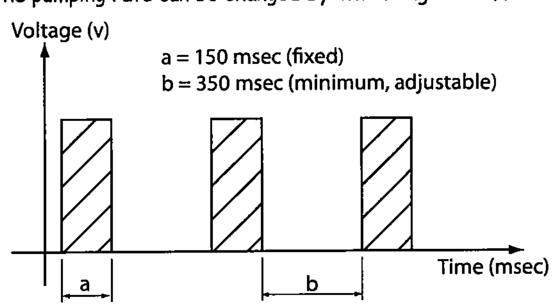

150SP SERIES MICRO-PUMP

For precise dispensing between 100 and 250µl and flow rates up to 24 ml/min

- Self-priming
- 100-250µl discrete dispense volumes
- Up to 24 ml/min maximum flow rate
- 5/16"-24 UNF threaded ports

The 150SP series Micro-Pumps are solenoid operated, with the operating mechanism isolated from the flow path by a diaphragm. Check valves situated at the inlet and outlet of the pump control the direction of flow. The combination of materials for each component can be selected to best suit your specific application.

Materials available for the wetted parts are:

- Body materials: PPS, PEEK™
- Diaphragm materials: EPDM
- Check valve materials: EPDM

150SP series options

NOTE: For 24 VDC, replace 150SP12 with 150SP24 in any of the part numbers listed.

PART NO.	DISPENSE VOL (µL)	BODY MATERIAL	DIAPHRAGM MATERIAL	CHECK VALVE MATERIAL
12 VDC; 100µl dispense				
150SP12100-4EE	100	PPS	EPDM	EPDM
150SP12100-5EE	100	PEEK™	EPDM	EPDM
12 VDC; 125µl dispense				
150SP12125-4EE	125	PPS	EPDM	EPDM
150SP12125-5EE	125	PEEK™	EPDM	EPDM
12 VDC; 150µl dispense				
150SP12150-4EE	150	PPS	EPDM	EPDM
150SP12150-5EE	150	PEEK™	EPDM	EPDM
12 VDC; 175µl dispense				
150SP12175-4EE	175	PPS	EPDM	EPDM
150SP12175-5EE	175	PEEK™	EPDM	EPDM
12 VDC; 200µl dispense				
150SP12200-4EE	200	PPS	EPDM	EPDM
150SP12200-5EE	200	PEEK™	EPDM	EPDM
12 VDC; 225µl dispense				
150SP12225-4EE	225	PPS	EPDM	EPDM
150SP12225-5EE	225	PEEK™	EPDM	EPDM
12 VDC; 250µl dispense				
150SP12250-4EE	250	PPS	EPDM	EPDM
150SP12250-5EE	250	PEEK™	EPDM	EPDM

ARRANGEMENT

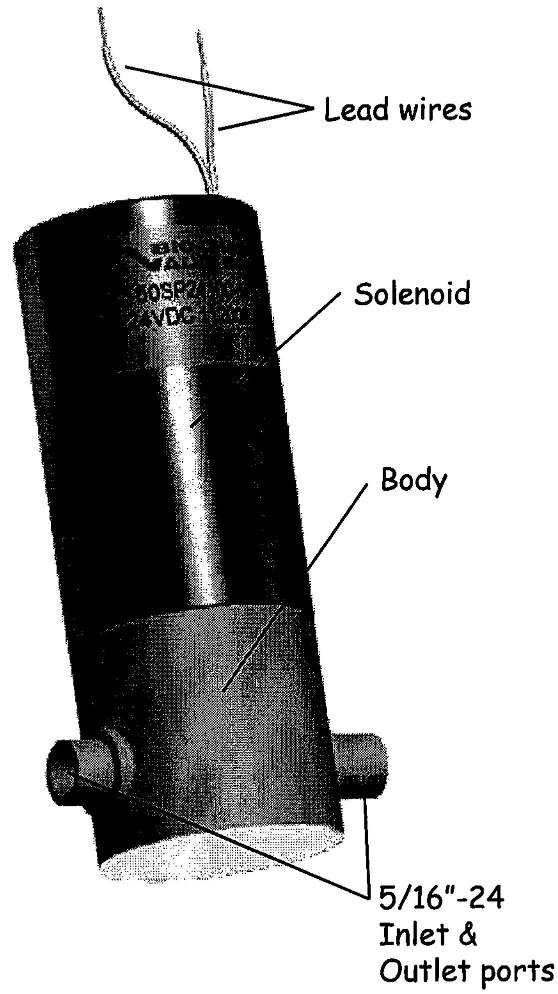

INSTALLATION DRAWING

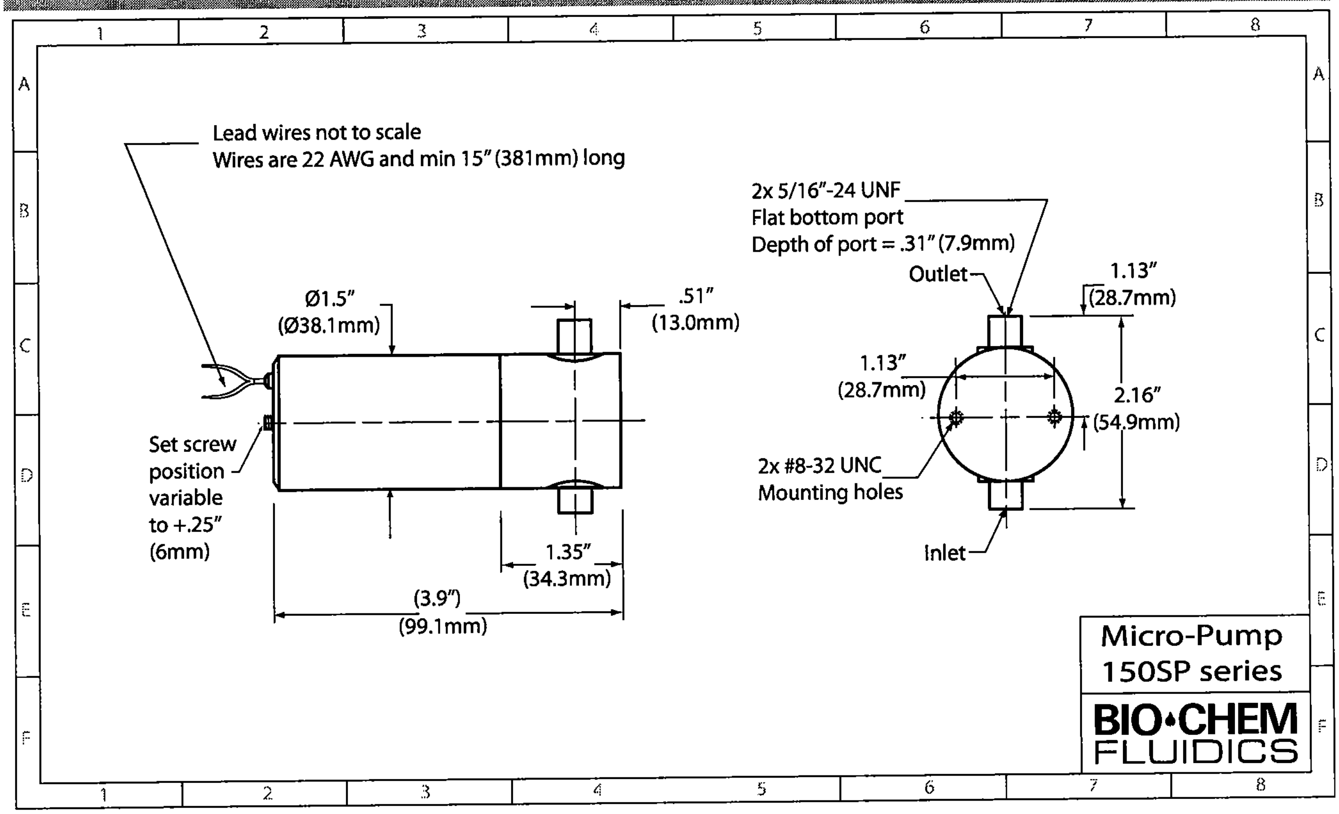

SPECIFICATIONS

150SP Fluid Data							
Dispense Volume (µl)	100	125	150	175	200	225	250
Set-point accuracy	+/- 10%	+/- 10%	+/- 10%	+/- 10%	+/- 10%	+/- 10%	+/- 10%
Repeatability	+/- 5%	+/- 5%	+/- 5%	+/- 5%	+/- 5%	+/- 5%	+/- 5%
Max flow rate (µl/min)	9600	12000	14400	16800	19200	21600	24000
Internal vol (µl)	710	710	710	710	710	710	710

150SP Electrical Data			
Voltage	Power @70°F (21°C)	Current @70°F (21°C)	Effective continuous power @ max cycle rate
12 VDC	8.0 Watts	0.66 amps	3.2 Watts
24 VDC	8.0 Watts	0.33 amps	3.2 Watts

150SP Cycle Rates		
Fixed "on" time	Min "off" time	Max cycle rate
200 msec	400 msec	1.6 Hz

Recommended tubing for 150SP
Inlet & outlet, 1/8" (3.2mm) ID, hardwall tubing, PART NUMBER 008T47-032

150SP Micro-Pumps can be cycled at up to 1.6 Hz. To maintain pumping precision the voltage "on" time should remain fixed - the pumping rate can be changed by increasing the "off" time.

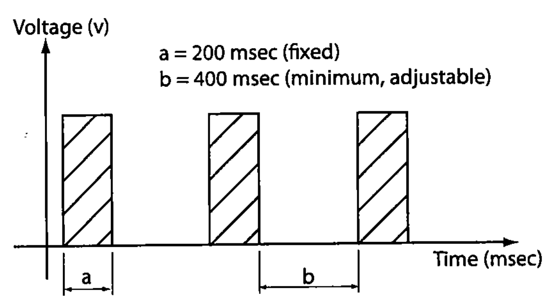

139SP SERIES MICRO-PUMP

For precise dispensing between 20 and 60µl and flow rates up to 7.2 ml/min in a manifold mountable design

- Self-priming
- 20-60µl discrete dispense volumes
- Up to 7.2 ml/min maximum flow rate
- Manifold mountable

This sibling to the 130SP Micro-Pump duplicates the performance characteristics but is supplied ready for mounting in your manifold. *Please contact us if you would like us to supply the manifold (see page 12).* Materials available for the wetted parts are:

- Body materials: PTFE, POM, PEEK™
- Diaphragm materials: PTFE, EPDM
- Check valve materials: EPDM, FKM, FFKM

ARRANGEMENT

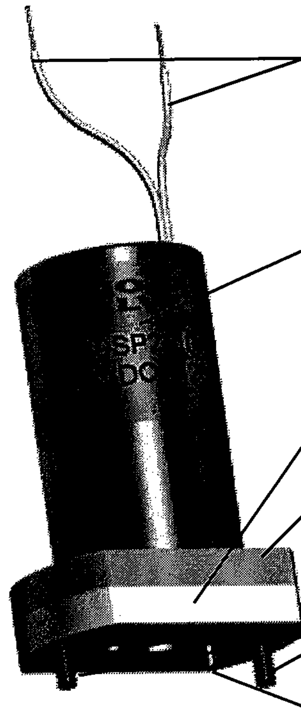

139SP series options

NOTE: For 24 VDC, replace 139SP12 with 139SP24 in any of the part numbers listed.

PART NO.	DISPENSE VOL (µL)	BODY MATERIAL	DIAPHRAGM MATERIAL	CHECK VALVE MATERIAL
12 VDC; 20µl dispense				
139SP1220-1TP	20	PTFE	PTFE	FFKM
139SP1220-5TP	20	PEEK™	PTFE	FFKM
139SP1220-5TV	20	PEEK™	PTFE	FKM
139SP1220-5TE	20	PEEK™	PTFE	EPDM
139SP1220-6TV	20	POM	PTFE	FKM
139SP1220-6EE	20	POM	EPDM	EPDM
12 VDC; 30µl dispense				
139SP1230-1TP	30	PTFE	PTFE	FFKM
139SP1230-5TP	30	PEEK™	PTFE	FFKM
139SP1230-5TV	30	PEEK™	PTFE	FKM
139SP1230-5TE	30	PEEK™	PTFE	EPDM
139SP1230-6TV	30	POM	PTFE	FKM
139SP1230-6EE	30	POM	EPDM	EPDM

PART NO.	DISPENSE VOL (µL)	BODY MATERIAL	DIAPHRAGM MATERIAL	CHECK VALVE MATERIAL
12 VDC; 40µl dispense				
139SP1240-1TP	40	PTFE	PTFE	FFKM
139SP1240-5TP	40	PEEK™	PTFE	FFKM
139SP1240-5TV	40	PEEK™	PTFE	FKM
139SP1240-5TE	40	PEEK™	PTFE	EPDM
139SP1240-6TV	40	POM	PTFE	FKM
139SP1240-6EE	40	POM	EPDM	EPDM
12 VDC; 50µl dispense				
139SP1250-1TP	50	PTFE	PTFE	FFKM
139SP1250-5TP	50	PEEK™	PTFE	FFKM
139SP1250-5TV	50	PEEK™	PTFE	FKM
139SP1250-5TE	50	PEEK™	PTFE	EPDM
139SP1250-6TV	50	POM	PTFE	FKM
139SP1250-6EE	50	POM	EPDM	EPDM
12 VDC; 60µl dispense				
139SP1260-6EE	60	POM	EPDM	EPDM

SPECIFICATIONS

The 139SP has the same specifications as the 130SP (see page 7)

INSTALLATION DRAWING

	PTFE body	POM/PEEK™ body
Dim ØA	.096"(2.4mm)	.125"(3.2mm)
Dim B	.50"(12.7mm)	.34"(8.6mm)
Dim C	.59"(15.0mm)	.62"(15.7mm)

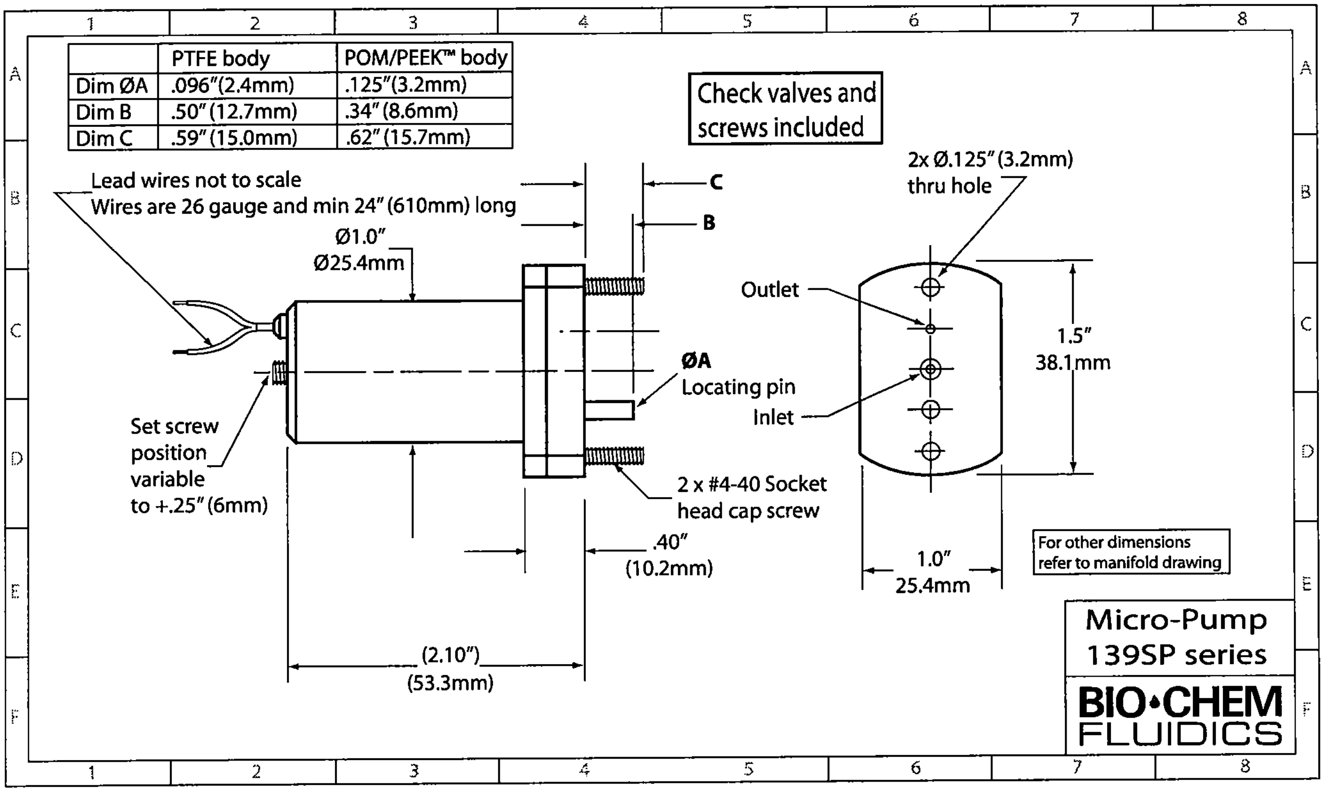

MANIFOLD INTERFACE DRAWING

	PTFE body	POM/PEEK™ body
Dim A	.280"(7.11mm)	.345"(8.76mm)
Dim B	.280"(7.11mm)	.350"(8.89mm)
Dim ØC	.106"(2.69mm)	.136"(3.45mm)
Dim D	.600"(15.2mm)	.380"(9.65mm)

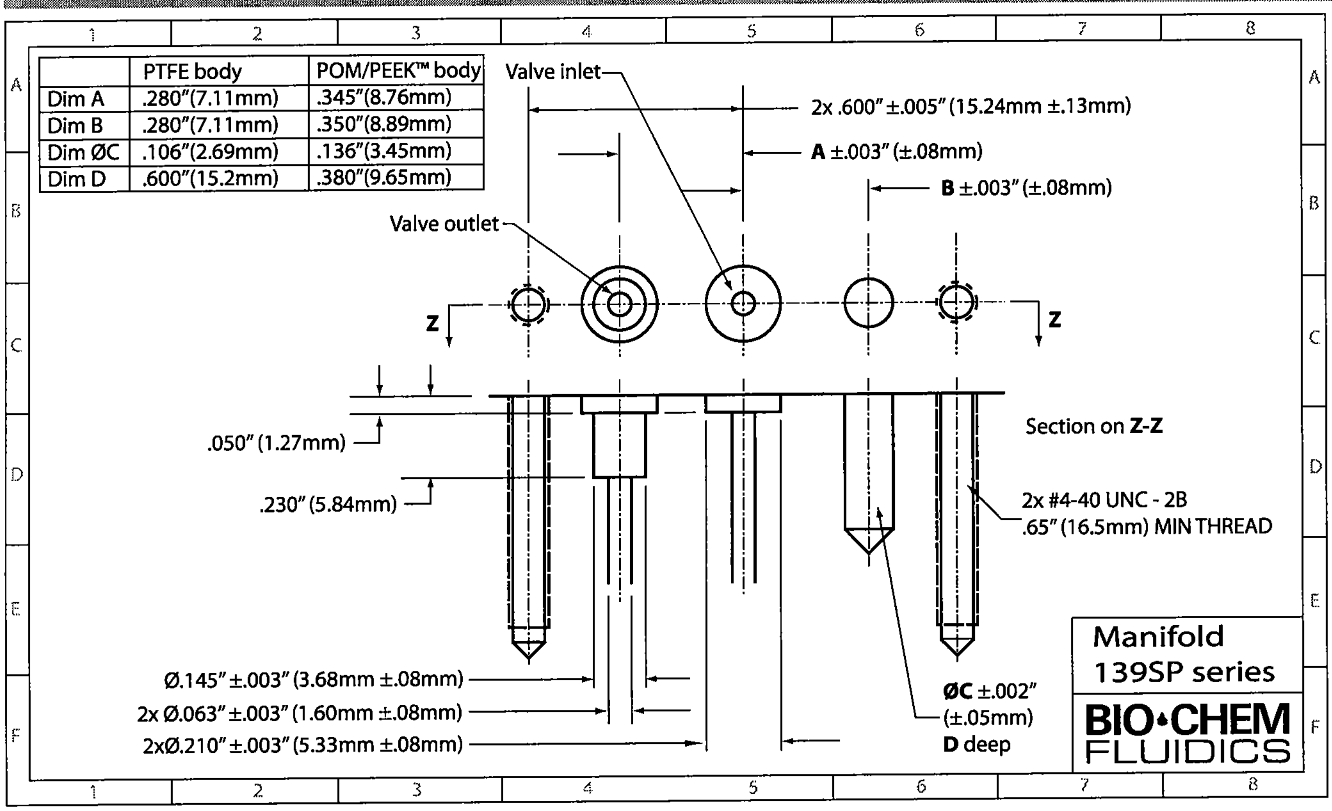

MANIFOLDS

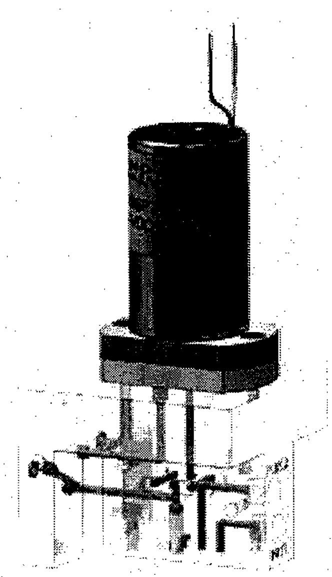

Custom-built manifolds are used to organize multiple Micro-Pumps and other Fluid Control Devices such as Isolation Valves into an efficient, pre-assembled, space-saving module that is designed to meet your specific flow needs. Manifolds can range from simple blocks for two devices to complex shapes with intricate flow paths for many devices. Bio-Chem Fluidics has produced complex manifolds for as many as 84 Micro-Pumps on a single block.

Features:

- Reduction of internal equipment space requirements.
- Allows for the combining of valves, tubing, pumps and connectors into a single, pre-assembled component.
- Elimination of unsightly and unmanageable wiring and tubing.
- Helps to reduce inventory.
- Reduces production time and costs associated with testing, handling and assembling multiple components.
- Materials of construction to suit fluid characteristics including, but not limited to; PTFE, POM, PEEK™, acrylic and PPS.

Please contact your local Bio-Chem Fluidics facility to discuss your manifold requirements with one of our engineers.

Custom manifold for (1) 139SP Micro-Pump (shown) and (3) isolation valves (not shown). Blue lines indicate the fluid path; the red dots are ruby balls used as plugs.

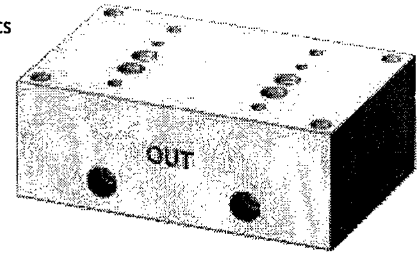

Custom manifold for (2) 139SP Micro-Pumps (not shown).

MOUNTING OPTIONS

Bio-Chem Valve™ Solenoid Operated Micro-Pumps can be installed into your equipment with a variety of mounting options including mounting clips, rings and flanges. Some of the pumps can be mounted directly via mounting holes that are drilled into the pump body. For more details refer to the "Mounting Accessories & Options" spec sheet.

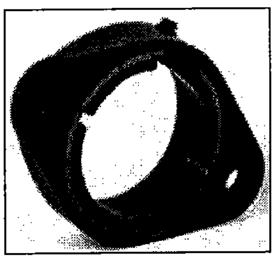

MU-Series Mounting Flange

- Constructed from sturdy, glass-filled Polypropylene
- Spring steel retainer ring and set screw ensure a secure fit
- Surface withstands alcohol, bleaches and other common cleaning agents
- Can be bulkhead mounted, inside or outside
- Screw hole orientation relative to tubing can be adjusted to fit available system space

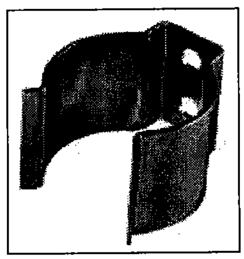

MC-Series Mounting Clip

- Constructed from Spring Steel
- Simple construction - no tools required to secure pump into position
- Holds pump securely inside instrument

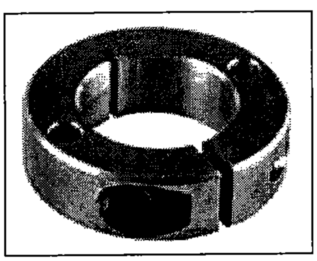

MR-Series Mounting Ring

- Constructed from Aluminum
- Tightening screw secures ring firmly to pump but can be loosened for re-positioning
- Can be bulkhead mounted, inside or outside
- Screw hole orientation relative to tubing can be adjusted to fit available system space

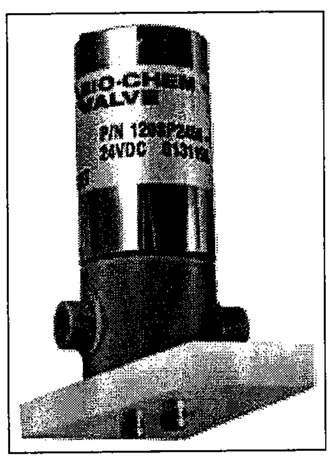

Integral Mounting Holes

- Threaded mounting holes in the base of the pump provide a more permanent way to mount directly to a plate or base
- Mounting holes are standard on 120SP and 150SP Micro-Pumps

EXHIBIT H

Application Note

Micropumps for Infusion Therapy

In medical applications, such as infusion therapy, micropumps can be an attractive alternative to standard pumps due to their size, weight and low energy demand. The micropump mp6-psense with its double actuator configuration offers the possibility of an intrinsic flow control. Therefore it can fulfill higher requirements on safety and accuracy under varying conditions as the standard pump mp6. By the controlled loop function the flow can run constantly under varying conditions as pressure, viscosity or temperature changes.

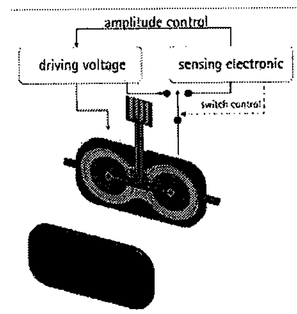

Fig. 1: Flow-sensing schematic of micropump mp6

Infusion therapies like for example the continuous dosing of nutrient solution in parenteral diets have high demands on the flow accuracy. Important is the starting behavior and the stable flow during the course of infusion with a minimum of short time fluctuations. The micropump mp6-psense from Bartels Mikrotechnik with intrinsic flow control has been tested for such applications. A clear and simple picture of the general flow rate stability over time can be gained by a trumpet curve analysis. The trumpet curve shows the variations of the mean flow accuracy over specific observation periods. The variations are presented only as maximum and minimum deviations from the overall mean flow within the observation window. The flow performance of the pumps is measured over a time period of 25 hours after a 24 hour stabilizing phase or emptying of half the reservoir according to the definitions of the standard DIN EN 60601-2-24.

Since the flow controlled micropump mp6-psense has a very dynamic behavior stable flow conditions can already be achieved after 10 minutes. Therefore the stabilization phase could be considerably shortened. The trumpet curve analysis over defined time intervals then shows the maximum positive and negative errors, occurring in the time interval. Achievable flow rates of the mp6-psense are 0,5 – 5 ml/min with a flow accuracy of 10%. For a flow rate of 125 ml/h the exemplarily trumpet curve of mp6-psense is shown below. In short observation windows the error of flow is already below 5 %. With increasing intervals it decreases below 1 %. The absolute error is below 2 %.

Bartels mikrotechnik

Bartels Mikrotechnik GmbH, Emil-Figge-Str. 76a, 44227 Dortmund, Germany
www.bartels-mikrotechnik.de, microComponents@bartels-mikrotechnik.de
Tel: +49-231-9742-500, Fax: +49-231-9742-501

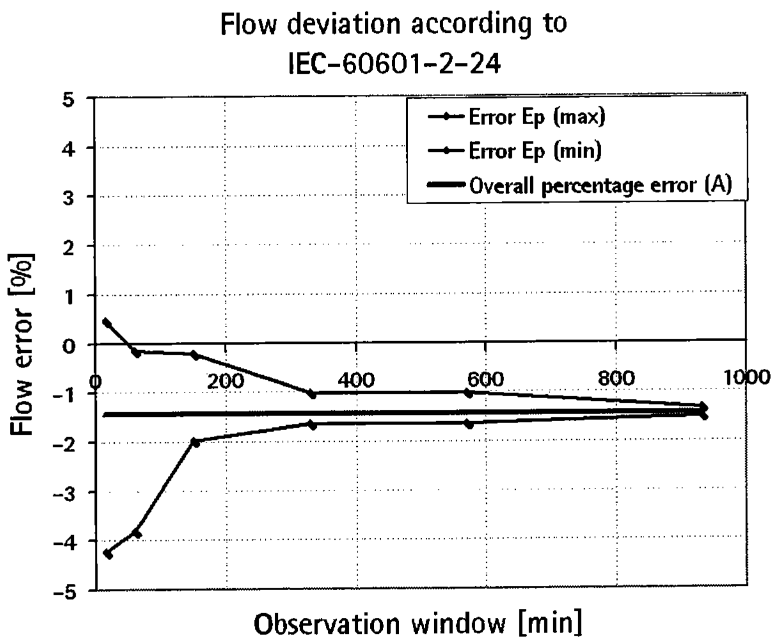

Looking at the overall complexity, from the pump side, this solution is fully based on a proven, mass produced component. Additional effort is required for the driving electronics but as the signal processing is straightforward the unit keeps its portability and capability of being driven with batteries. Especially in applications where the micropump should be used as a disposable unit while the electronics is being reused, the full potential of this solution comes into play.

Infusion therapies with flow rates below 0,5 ml/min can either be achieved by quasi-continuous pumping, for which small volumes are dosed in defined time intervals. Or a flow controlled micropump with an integrated flow sensor is used which can achieve lower flow rates with higher accuracies. The flow range of such a system is from 60 µl/min to 5 ml/min with 5 % accuracy.

Take benefit of the innovative potential of this pump for your products! Be one step ahead compared to your competitors and get in contact with us concerning your application. Besides the standard components, Bartels Mikrotechnik is also specialized in the development of customer specific adaptations.

Bartels Mikrotechnik GmbH, Emil-Figge-Str. 76a, 44227 Dortmund, Germany
www.bartels-mikrotechnik.de, microComponents@bartels-mikrotechnik.de
Tel: +49-231-9742-500, Fax: +49-231-9742-501

EXHIBIT I

Turnkey Design
SERVICES LLC

Micro Pump Technology &
Advanced Engineering Services

Flow On Demand Technology *12757 S. Western Ave. Suite 229, Blue Island, IL 708-293-1120*

Turnkey Design Services
Micro Pump Technology

Turnkey Design
SERVICES LLC

Flow On Demand Technology

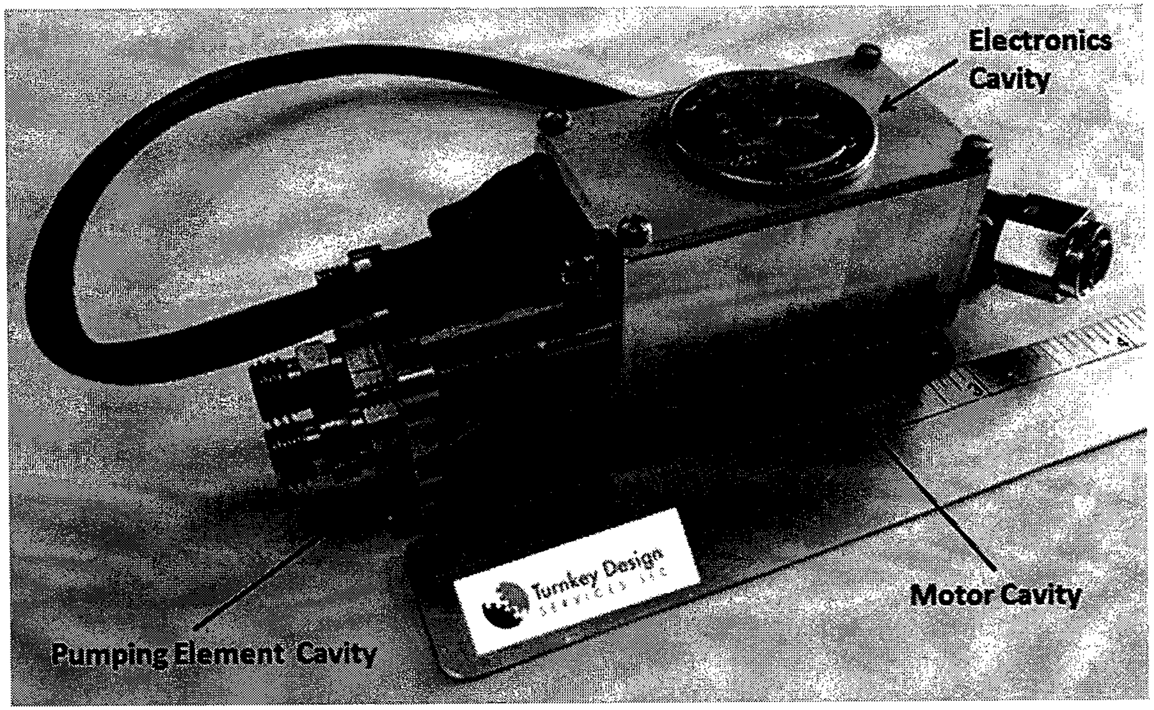

Turnkey Design Services MFP30-1 Pump

Turnkey Design
SERVICES LLC

Technology Description

Flow On Demand Technology

- Baseline and Smart Configurations
  - Input voltage range: 24-32 Vdc, 28 Vdc nominal regulated
  - Flow set by 4 to 20 mA or 0-5 V command input
  - Fuel inlet temperature: -40°F to 160°F
  - Flow metering accuracy ±1.5%
  - Over a 12 inch dry lift and self-priming capability
  - Can operate with an interrupted fuel/oil supply for 5 minutes with no performance degradation
  - Can handling fluid viscosities up to 5500 cSt
  - 1s rise and fall transient response time

Turnkey Design
SERVICES LLC

Flow On Demand Technology

Smart Pump Configuration

- Capable of delivering the commanded flow independent of temperature
  - Measure fluid temperature
  - Look up required motor speed for set flow command
  - Closed loop control on speed
- Communicate with engine controller
  - Transmit and receive signals
    - Status signal
    - Fault
    - Health status
  - Uses flow sensor to monitor flow at set motor speed and compare to baseline for health status (internal wear/life)
  - Monitor current and compare to baseline for health status (bearing wear/life)

Turnkey Design
SERVICES LLC

Flow On Demand Technology

Advantages over Competitors

- Smaller and Lighter
  - Fully integrated pump, motor and controller
    - All components are designed in-house
  - Capability to operate at higher motor speeds
    - Patent pending technology
  - Higher hydraulic efficiency and suction performance
    - Less leak paths and easier to control mfg. tolerances
- Better Performance
  - Metering accuracy
  - Transient response
  - Lower power consumption

Turnkey Design SERVICES LLC

Flow On Demand Technology

Advantages over Competitors

- V/L Capability
  - Better filling capabilities
    - Lower required charging pressure
    - Less prone to cavitation
  - Break up bubbles
    - When vapor enters pump it is broken up to smaller manageable pieces
  - Accumulator
    - Pump inlet is feed thru a filled accumulator so that inlet remains charged
- Higher Resistance to Contamination
  - Torturous path before entering pump inlet (bubble masher)
    - Metal particles are attracted to the motor permanent magnets
    - Heavier dirt particles are slung to the outside and flow to inlet is inside

Turnkey Design
SERVICES LLC

Flow On Demand Technology

Advantages over Competitors

- Lower Cost
  - Many flow/pressure variations using common generic hardware
    - Microprocessor, cam eccentricity and rotor
  - High cost materials/coatings not required to meet life requirement
  - Easier to machine hardware (simple shapes)
  - No hall effect sensors, bonding and wiring

Turnkey Design SERVICES LLC

Transient Response

Flow On Demand Technology

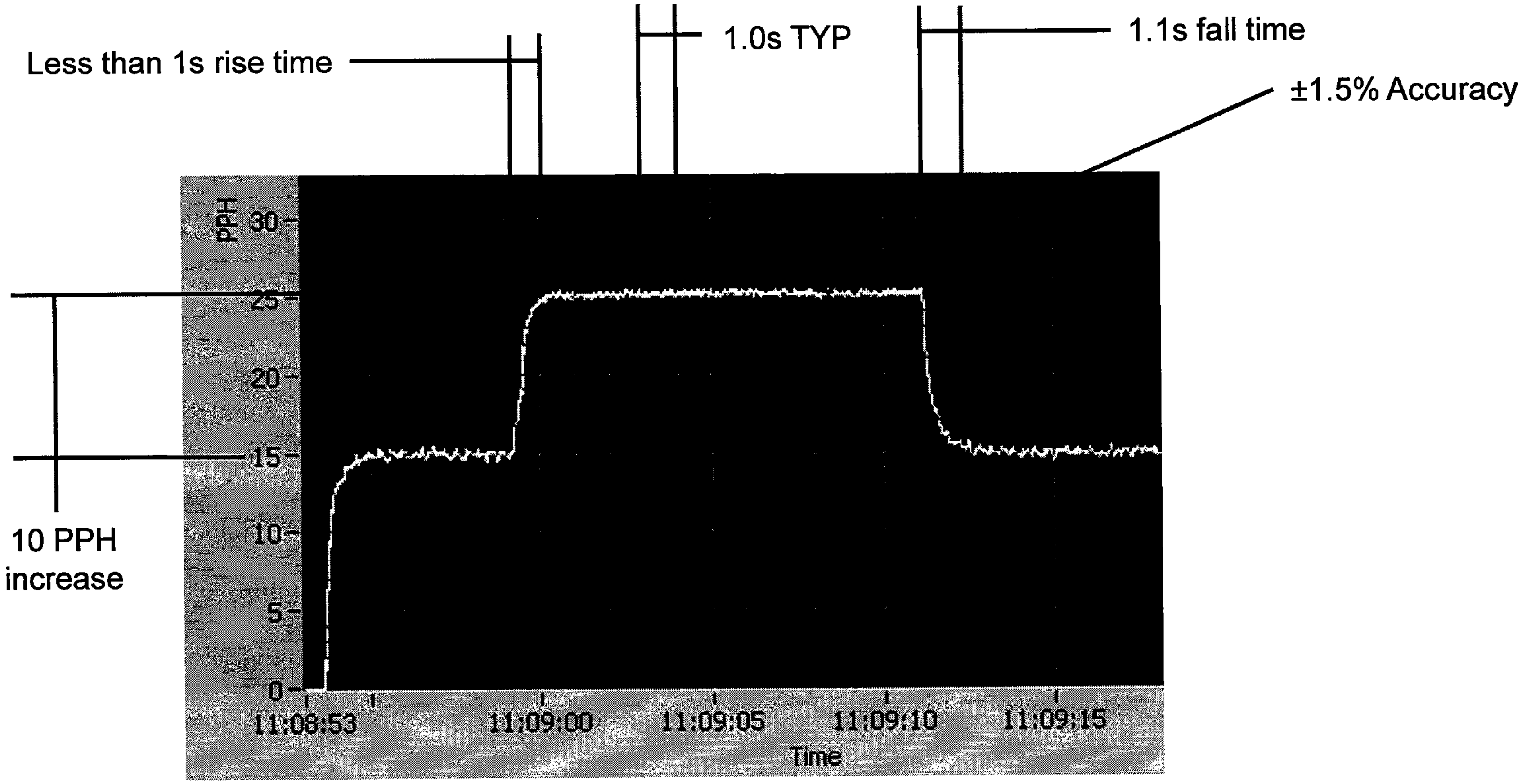

Turnkey Design SERVICES LLC

Typical Flow Data

Flow On Demand Technology

Test Data Viscor Calibration Fluid 1487 at Room (SG=.79) with .035 Orifice

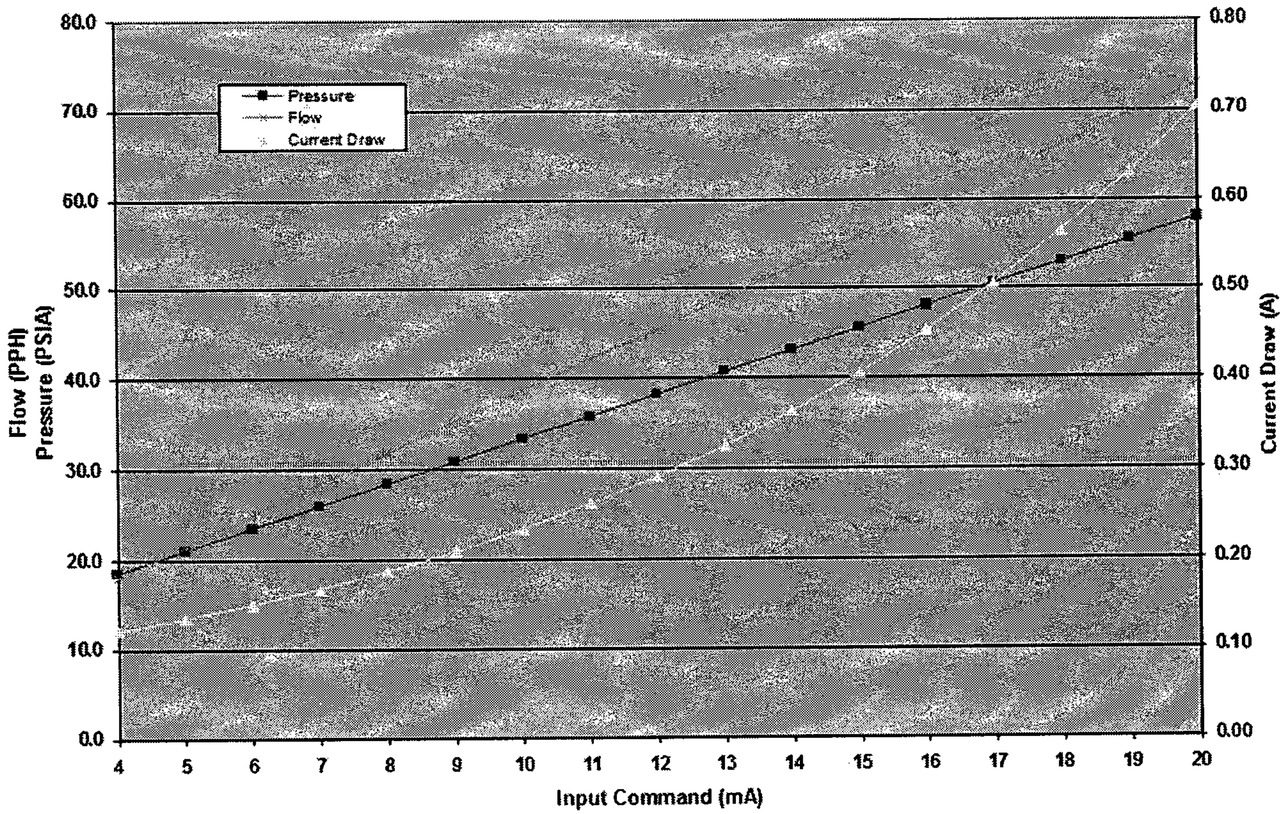

Turnkey Design
SERVICES LLC

Typical Flow Data

Flow On Demand Technology

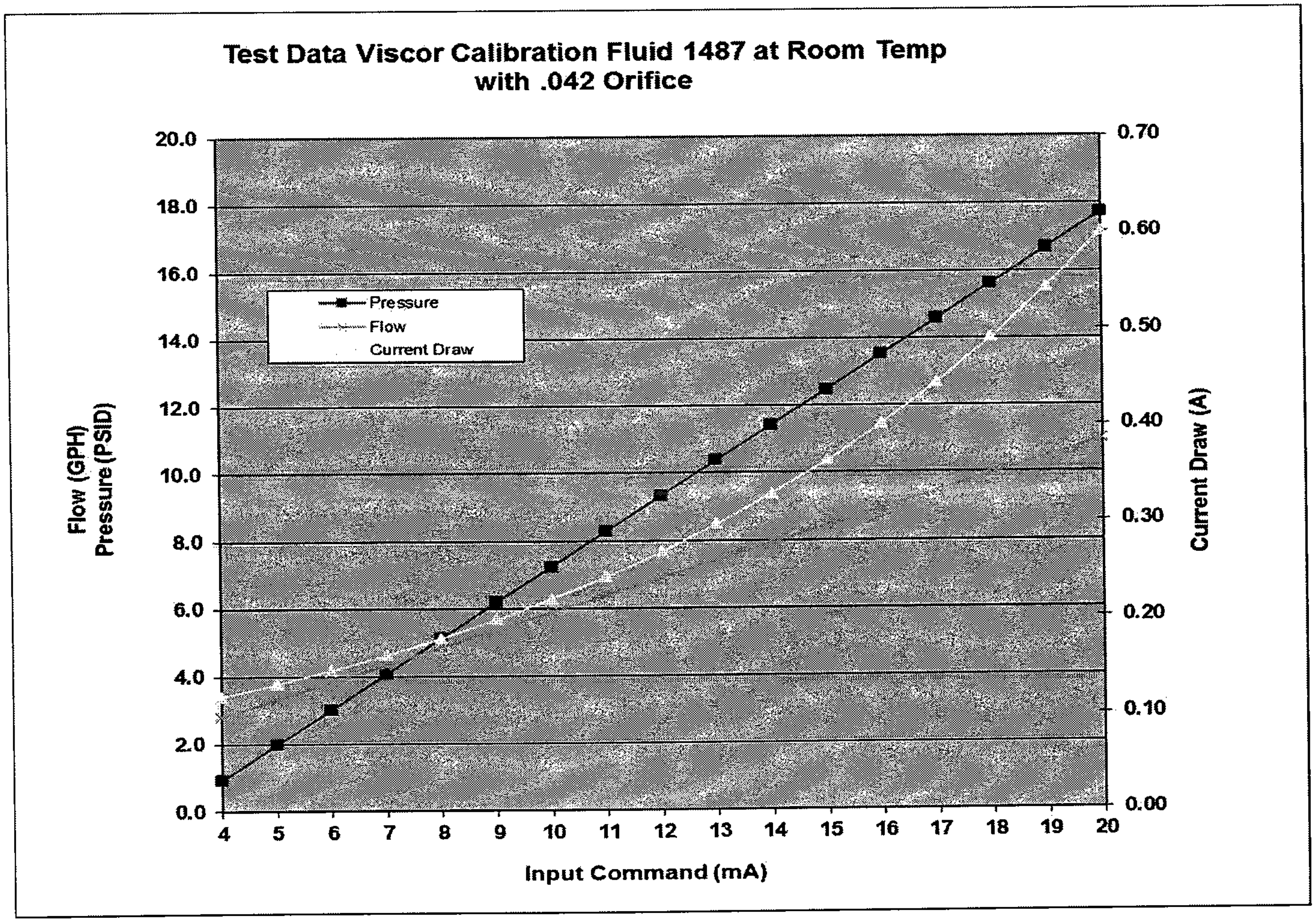

EXHIBIT J

Did you know: f borborygmus sounds like it means something impolite, you're right.

micropump

mi·cro·pump [**mahy**-kr*uh*-puhmp] Show IPA

noun

a tiny pump implanted under the skin for the timed administration of medication.

Compare solion.

Origin:

micro- + pump[1]

Word Dynamo Rating For Micropump

People who can define **Micropump** may know **11,290** words.

How many words do you know?

Micropump is always a great word to know. So is **flibbertigibbet**. Does it mean: 00:09

a chattering or flighty, light-headed person.

a scrap or morsel of food left at a meal.

Related Words

implantable solion

MORE

Quote Of The Day

..e terrible thing about terrorism is ..t ultimately it destroys those who ..actise it. Slowly but surely, as they try to extinguish life in others, the light within them dies."

-Terry Waite

MORE

search dictionary

Example Sentences

Valve-less thermally-driven moving-phase-change **micropump**.
Pumping mechanism of thermally driven phase transition **micropump**.

EXHIBIT K

Text Size: A A A

Home About Us Our Technology Leadership Team Press Careers Contact Us

Innovating Vision

The Replenish, Inc. MicroPump™ provides an innovative treatment method by precisely automating the delivery of drugs.

- Product Description
- MicroPump™ System
- Patent Protection

PRODUCT DESCRIPTION AND DEVICE DEVELOPMENT

Replenish, Inc.™ has developed a small, refillable, implantable ocular drug pump. The MicroPump™ implant is a “smart device” that is programmable to dispense nanoliter-sized doses (a volume sensor gives closed-feedback) of drugs every hour, day or month as needed before refills. The tiny MicroPump™ can be ‘replenished’ using a disposable, proprietary 31-gauge needle tubing kit.

Some of the pump’s features include the following:

- One-way check valve (prevents backflow leakage)
- Fluidic flow sensor
- Bi-directional telemetry system for wireless programming and battery recharges
- Programmable state-of-the-art microcontroller with calendar to ‘wake up’ when it’s time for medication
- Optional cannula with pars plana clip directs medication in the same location as intravitreal injections

Home About Us Our Technology Leadership Team Press Careers Contact Us

Disclaimer: The Replenish MicroPump™ System is for investigational use only and is not yet approved for commercial distribution.